Dissertation

submitted to the
Combined Faculties for the Natural Sciences and for Mathematics
of the Ruperto-Carola University of Heidelberg, Germany
for the degree of
Doctor of Natural Sciences

presented by
Master of Science – Molecular Bioengineering Minh T. N. Nguyen
born in: Long An (Viet Nam)

Oral-examination: .09.2014

Influence of Post-translational Modifications on Hsp90 Activity and Function

Referees: Prof. Dr. Matthias P. Mayer

Prof. Dr. Oliver Gruss

Table of Contents

Table of figures

List of Tables

List of Appendices

SUMMARY

The 90 kDa heat shock proteins constitute a family of highly conserved molecular chaperones that are essential in all eukaryotic cells. Assisted by an increasing number of cochaperones, Hsp90 forms highly dynamic complexes with numerous client proteins, many of which are signaling molecules controlling cell homeostasis, proliferation, differentiation, cell death, etc. Therefore, Hsp90 sits at one of the center positions in the protein quality control system and requires delicate regulation by the combination of different mechanisms. It is already well established in the field that the multiple conformations of Hsp90 are driven by association/dissociation with nucleotide and ATP hydrolysis together with binding and release of cochaperones as well as client proteins. On the other hand, post-translational modifications are becoming increasingly recognized as another layer of regulation that adds up to the complexity of the whole machinery. Hsp90 is a phospho-protein: approximately 40 sites have been detected in proteomics reports; nonetheless, individual phospho-sites seem to have different impact on the chaperone function of Hsp90.

In the first part of this work, I aimed to analyze the global phosphorylation status of human cytosolic Hsp90 proteins in cancer versus non-cancer cells in a quantitative way and to examine whether the phosphorylation status relates to tumor selectivity characteristics of Hsp90 inhibitors. Due to technical issues, not all previously reported phosphorylation sites were detected. Thus, my data did not provide a clear conclusion about the global phosphorylation status of the Hsp90 proteins in cell lysates. My data also did not provide evidence for a correlation between detected phosphorylation sites and malignancy. Instead, I found indications for novel phosphorylation sites that were not covered in proteomics studies so far. The exploration of Multiple Reaction Monitoring Mass spectrometry (MRM-MS) rather than normal liquid chromatography coupled with tandem mass spectrometry (LC-MS/MS) also confirmed that such a specific approach could be utilized for further applications in quantification of target proteins and modifications in complex samples without the risk of losing target material in isolation steps or altering the relative abundance of modifications due to enrichment steps prior to MS.

In the second part of this work, I focused on characterzing a novel serine phosphorylation that was first detected in the previous part and recently has been confirmed by other proteomics studies. Using *S. cerevisiae* as the model system in which both endogenous Hsp90 can be conditionally deleted, I was able to resolve the difference in chaperone function of human Hsp90β wild-type and phospho-mutants when being the sole source of Hsp90 proteins in yeast cells. From general yeast viability and cell morphology as well as specific chaperone activation capacity for well-defined client proteins, my data suggested that the human Hsp90β wild-type was indeed phosphorylated *in vivo* and demonstrated strongly a correlation between S365 phosphorylation and chaperone activity of Hsp90β. S365 phosphorylation mimicking status was proven to be favorable for chaperoning glucocorticoid receptor (GR), heat shock factor (HSF-1) and the MAPKK Ste11 to response stronger and/or faster to each corresponding stimulus while showing no effect on transactivation activity of the transcription factor HAP1 (Heme activator protein), another known Hsp90 client. My results supported a hypothesis in which a single modification on the molecular chaperone would be sufficient to provide a certain level of client specificity and modulate cellular responses upon environmental stimuli.

To resolve further the mechanism of how S365 phosphorylation exerts its impact on Hsp90 function, I utilized *in vitro* minimal GR-activation system consisting of purified Hsp70, Hsp40, HOP, p23 and different Hsp90 wild-type or phospho-variant proteins. The profitable effect of S365E phospho-mimetic variant as compared with non-phosphorylatable variants was confirmed while that of wild-type protein was abolished due to the lack of post-translational modifications from *E. coli* expression and purification. Given the *in vivo* results of not only GR but also of a few other client proteins, I also examined the interaction of the Hsp90β wild-type protein and S365 phosphomutants with cochaperones by size-exclusive chromatography coupled with fluorescence detector using labeled proteins and isothermal titration calorimetry. The results showed that S365 phosphorylation impairs the binding of Hsp90β protein to both cochaperones Aha1 and Cdc37.

Altogether, the data provided evidence for phosphorylation at serine 365 on human Hsp90β that contributes to regulation of Hsp90 function via direct impacts on client and indirect effects via cochaperones involved in the chaperone cycle. As expected, the regulation of this molecular chaperone is the result of a delicate combination between several mechanisms rather than a single one, which would be more flexible to adapt to the variety of macro- and micro-environmental fluctuations that higher eukaryotes always must cope with.

ZUSAMMENFASSUNG

Die 90kDa Hitzeschockproteine bilden eine Familie hoch konservierter molekularer Chaperone, die in allen eukaryotischen Zellen essentiell sind. Unterstützt von einer steigenden Anzahl von Cochaperonen bildet Hsp90 hochdynamische Komplexe mit zahlreichen Proteinen, Kliente genannt. Bei vielen handelt es sich dabei um Signalmoleküle, die die Zellhomöostase, -proliferation, -differenzierung, wie auch den Zelltod etc. steuern. Daher nimmt Hsp90 eine zentrale Rolle im Proteinqualitätskontrollsystem ein und erfordert eine sorgfältige Regulation durch eine Kombination verschiedener Mechanismen. Es wird angenommen, dass die mannigfaltigen Konformationen von Hsp90 durch die Assoziation/ Dissoziation von Nukleotiden, ATP Hydrolyse wie auch durch die Bindung und Freisetzung von Cochaperonen und Klientproteinen bestimmt werden. Daneben wird immer deutliche, dass posttranslationale Modifikationen eine weitere Ebene der Regulation bilden, die zusätzlich zur Komplexität dieser Maschinerie beitragen. Hsp90 ist ein Phospho-Protein: Ca. 40 Phosphorylierungstellen wurden bereits in Proteom-Studien identifiziert. Nichtsdestotrotz scheinen einzelne Phosphorylierungsstellen die Chaperonfunktion von Hsp90 unterschiedlich zu beeinflussen.

Das Ziel des ersten Teils dieser Arbeit war es, den globalen Phosphorylierungszustand der humanen, cytosolischen Hsp90-Proteine in Krebszellen im Vergleich zu nicht malignen Zellen quantitativ zu analysieren und zu prüfen, ob der Phorphorylierungsstatus mit Tumorselektivitätseigenschaften von Hsp90-Inhibitoren in Zusammenhang steht. Aufgrund von technischen Komplikationen konnten nicht alle zuvor bekannten Phosphorylierungsstellen nachgewiesen werden. Daher konnte mit diesen Daten keine eindeutige Aussage über den globalen Phosphorylierungsstatus von Hsp90-Proteinen in Zelllysaten gemacht werden. Meine Daten lieferten ebenfalls keinen Beleg für eine Korrelation zwischen den nachgewiesenen Phosphorylierungsstellen und Malignität. Stattdessen fand ich Hinweise auf neue Phosphorylierungsstellen, die bis dahin noch nicht von Proteom-Studien worden waren. Die Untersuchung mittels „Multiple Reaction Monitoring“ - Massenspektrometrie anstatt normaler Flüssig-chromatographie verbunden mit Tandem-Massenspektrometrie bestätigte auch, dass eine solch spezifische Vorgehensweise für weitere Anwendungen in Quantifizierung von Targetproteinen und Modifikationen in komplexen Proben benutzt werden könnte. Dabei gäbe es nicht das Risiko das Targetmaterial in Isolationsschritten zu verlieren oder die relative Häufigkeit von Modifikationen aufgrund von Anreicherungsschritten, die vor MS notwendig sind, zu verändern.

In dem zweiten Abschnitt dieser Arbeit konzentrierte ich mich auf die Charakterisierung einer neuen Serinphosphorylierung, die erstmals im vorherigen Teil beschrieben und kürzlich auch durch andere Proteom-studien bestätigt wurde. Mit *S. cerevisiae* als Modellsystem, in dem beide endogene Hsp90 codierende Gene durch ein Hsp90 Gen des Menschen ersetzt wurde, war ich in der Lage, Unterschiede in der Chaperonfunktion vom humanen Hsp90β-Wildtyp und den Phospho-Mutanten festzustellen. Vom allgemeinen Hefewachstumsverhalten und der Zellmorphologie wie auch der spezifischen Chaperonaktivierungskapazität für gut beschriebene Klientproteine, wiesen meine Daten darauf hin, dass der Hsp90β-Wildtyp *in vivo* tatsächlich phosphoryliert war. Zudem zeigte sich eine starke Korrelation zwischen der S365-Phosphorylierung und der Chaperonaktivität von Hsp90β. Es wurde gezeigt, dass sich der S365-Phosphorylierungs-imitierende Zustand günstig auf das Chaperonieren des Glucocorticoid-Rezeptors (GR), Hitzeschock-Faktors (HSF-1) und MAPKK Ste11 auswirkt, sodass diese stärker und/ oder schneller auf jeden

entsprechenden Stimulus reagieren, während sich kein Effekt auf die Transaktivationsaktivität des Transkriptionsfaktors HAP1 (Heme Aktivator Protein) zeigte, bei dem es sich um einen weiteren bekannten Hsp90-Klienten handelt. Meine Ergebnisse unterstützen die Hypothese, dass eine einzige Modifikation der molekularen Chaperone ausreichen würde, um einen bestimmten Grad an Klientenspezifität zu bestimmen und zelluläre Antworten auf Umweltreize modulieren zu können.

Um weiterhin die Mechanismen aufzuklären, wie die S365-Phosphorylierung sich auf die Hsp90-Funktion auswirkt, verwendete ich ein *in vitro* Minimal-GR-Aktivationssystem bestehend aus aufgereinigtem Hsp70, Hsp40, HOP, p23 und Hsp90-Wildtyp oder verschiedene Hsp90-Phospho-Varianten. Es wurde bestätigt, dass die S365E-Phospho-mimetische Variante einen günstigen Effekt im Vergleich zu den nicht phosphorylierbaren Varianten hat, während dies für das Wildtyp-Protein aufgrund der fehlenden posttranslationalen Modifikationen infolge der *E.coli* Expression und Aufreinigung nicht der Fall war. Angesichts dieser *in vitro* Resultate für GR, aber auch für einige andere Klientproteine, untersuchte ich auch die Interaktion von Hsp90-Wildtyp und den S365-Phosphomutanten mit Cochaperonen mittels Größenausschluss-chromatographie und isothermer Titrationskalorimetrie. Die Ergebnisse zeigten, dass die S365-Phosphorylierung die Bindung von Hsp90β-Proteinen an die Cochaperone Aha1 und Cdc37 beeinträchtigt.

Alles in allem bieten diese Daten einen Beleg dafür, dass die Phosphorylierung des Serins 365 im Hsp90β des Menschen zur Regulation der Hsp90-Funktion beiträgt, einerseits über direkte Auswirkungen auf Protein Klienten und anderseits indirekt durch Effekte auf Cochaperone, die in diesem Chaperonzyklus beteiligt sind. Wie erwartet, ist die Regulation dieses molekularen Chaperons eher das Resultat einer feinabgestimmten Kombination aus verschiedenen Mechanismen, als das Ergebnis eines einzelnen Mechanismus. Ersteres System wäre flexibler in der Adaption an große und kleinste Umweltschwankungen, welche höhere Eukaryoten immer bewältigen müssen.

1 INTRODUCTION

1.1 PROTEIN FOLDING AND MOLECULAR CHAPERONES

A single cell contains thousands of different proteins that fulfill a large variety of essential functions in metabolism, regulation and development. Proteins, after being synthesized as linear chains of amino acids, have to adopt defined three dimensional structures to fulfill their corresponding function. The process of structure acquisition (termed folding) is not the same for every protein: While many of them attain the appropriate structure and conformation very rapidly after synthesis, some remain in one or a few intermediate state(s) for an extended period and/or only fully transform into the native state when triggered by specific substrates or signals. Even though the process of folding is principally spontaneous without any cost of energy and determined only by the amino acid sequence of the protein and thermodynamics, protein folding inside a cell is more complicated. There are numerous intracellular factors that drive against the appropriate folding of a protein from its nascent polypeptide chain. Those factors include the vectorial release mode of nascent polypeptide chain, the rate of translation that is orders of magnitude slower than that of folding, the existence of many ribosomes translating on one mRNA and molecular crowding in the cytosol. Even when proteins have attained their native state, they are constantly in danger of misfolding due to colliding with other macromolecules in the cytosol, a threat which is enhanced by environmental factors such as thermal, heavy metals, or oxidative stress. Those situations render proteins to be trapped in malfunctioning and potentially toxic conformations which eventually cause severe diseases such as Alzheimer's, Parkinson's, Huntington's, type II diabetes, cystic fibrosis, many types of cancer, etc. Therefore, most proteins need help from molecules called "molecular chaperones" to achieve and maintain their functional conformation (Frydman 2001).

Molecular chaperones are so called because they guide proteins through these folding pathways without interfering or associating in the final folded product. The term molecular chaperone was first used in literature by Ron Laskey (1978) to describe nucleoplasmin, a nuclear protein that binds to histones and mediates nucleosome assembly and then extended by John Ellis (1987) to describe proteins that mediated the post-translational assembly of protein complexes. The proteins that are now known as molecular chaperones actually have been discovered in several independent scientific works.

Many molecular chaperones are strongly produced under heat stress conditions. They are therefore named **H**eat **s**hock **p**roteins (Hsp) plus their apparent molecular weight (40, 70, 90, etc …) on SDS polyacrylamide gels. Later, their close homologues (which are constitutively expressed) were called **H**eat **s**hock **c**ognate proteins (Hsc), also with the number indicated approximately molecular weight. Those heat shock proteins are greatly up-regulated in response to the higher tendency of aggregation of cellular proteins in thermal stress. They prevent nonproductive intermolecular interactions between either nascent polypeptides or stressed-damaged proteins and restore their native structures, as well as promote degradation when these attempts fail. Thus, molecular chaperones do not only play a critical role in protein folding but also participate significantly in anti-aggregation including protein disaggregating, refolding and degradation in order to maintain protein homeostasis and response to stresses (Frydman 2001; Höhfeld et al. 2001; Young et al. 2004).

Among the major chaperone systems, the highly abundant and in all eukaryotic cells, essential 90kDa heat shock protein (Hsp90) is unique due to its several intriguing characteristics (Young 2001; Pearl & Prodromou 2006; Wandinger et al. 2008; Dezwaan & Freeman 2008). In recent years, many onco-proteins were discovered to be Hsp90´s clients, making this protein a prime target for anti-tumor therapy. Understanding the molecular mechanism of Hsp90 is therefore not only scientifically interesting and challenging but also of high medical relevance.

1.2 HEAT SHOCK PROTEIN 90

1.2.1 HSP90 GENERAL CHARACTERISTICS

Hsp90 is a highly conserved member of the heat shock protein family with 60% sequence identity between yeast and human homologues and 40% between *E. coli* HtpG and human Hsp90β. Making up 1-2% of total cellular protein and even more when induced by stress, Hsp90 proteins are essential for viability of eukaryote cell, while dispensable in prokaryotes (Mayer & Bukau 1999; Pearl & Prodromou 2006). Surprisingly, the level of Hsp90 can be significantly reduced without affecting cell viability, at least in normal conditions (Nathan et al. 1997; Picard 2002).

In most cells, Hsp90 proteins have several homologues not only in the cytosol but also in organelles such as mitochondria, endoplasmic reticulum and chloroplast. In the cytosol, there are mostly two isoforms of Hsp90 such as Hsp90α and Hsp90β in human (*Homo sapiens*), or Hsc82 and Hsp82 in budding yeast (*S. cerevisiae*). Isoforms are most known to differ in the regulation of their expression: either constitutively (like Hsp90β, Hsc82…) or inducible by stress (like Hsp90α, Hsp82 …)

1.2.2 HSP90 STRUCTURE

The Hsp90 proteins throughout evolution share high structural homology with similar domain organizations. The protein forms dimer with each protomer consisting of 3 main domains, linked flexibly to each other: N-terminal, middle, and C-terminal domain. In higher eukaryotes, an extended and highly charged linker region with variable lengths connects the N- domain to the rest of the protein (Figure 1-1).

The N-terminal domain of Hsp90 contains the nucleotide binding pocket of the molecule, in a structure known as the “Bergerat” fold which Hsp90 shares with the members of the gyrase–Hsp90–histidine kinase–MutL (GHKL) family. It is composed of a two-layer α/β sandwich in which eight β-sheet strands building the bottom of the ligand pocket, whereas surrounding and on-top α-helices make up a cleft (Pearl & Prodromou 2006). Many well-known Hsp90–specific inhibitors such as geldanamycin (GA) and radicicol also bind to this pocket, and hence severely affect Hsp90 activity. Another unique feature of the ATP binding region in Hsp90 as well as in proteins of GHKL family is a flexible structural element, the ATP ‘lid’, a conserved loop consisting of two α-helices that claps over the nucleotide-binding pocket when ATP is bound and forms a closed conformation. This lid seems to be one important conformational switch for the ATP hydrolysis function of Hsp90 and is also part of binding sites for co-chaperones like p23/Sba1 and Cdc37 (Roe et al. 2004; Ali et al. 2006).

The middle domain (M domain) consists of 2 α-β-α sandwiches connected to one another by an α3 helical coil, with the larger one near to the N-terminal domain and the charged linker. Compared to the structures of other GHKL family members, the Hsp90 M domain shows higher divergence of corresponding regions, and in particular the second smaller α-β-α motif represents an independent fold not found in other GHKL proteins. Amino acids 375 to 388 in the yeast homologue make up the conserved catalytic loop within the Hsp90 M domain, harbouring the arginine 380 residue that is essential for ATP hydrolysis as it contacts the γ-phosphate of ATP (Meyer et al. 2003). Moreover, ATP trapping (being locked in the nucleotide binding pocket to be hydrolyzed before it is released) occurs only in Hsp90 fragments containing the middle domain, suggesting that the middle domain of Hsp90 is important for the trapping of the ATP molecule (Wegele et al. 2003).

The Hsp90 M domain also has a large surface that was implicated in several publications to be involved in the binding of client proteins (Sato et al. 2000; Meyer et al. 2003; Müller et al. 2004; Street et al. 2011). An exposed hydrophobic patch surrounding Trp300 and an amphipathic loop (residues 329–339) when being mutated showed severe effect in the maturation of v-src kinase (Meyer et al. 2003). In a very recent study using NMR

to investigate complex of Tau and human Hsp90, it is confirmed that Hsp90, in contrast with Hsp70 and Hsp60, uses this large surface (in combination with surfaces stretching over N-terminal domain) as a permanently open and accessible docking region that accumulate otherwise low-affinity contacts into a strong interaction (Karagöz et al. 2014).

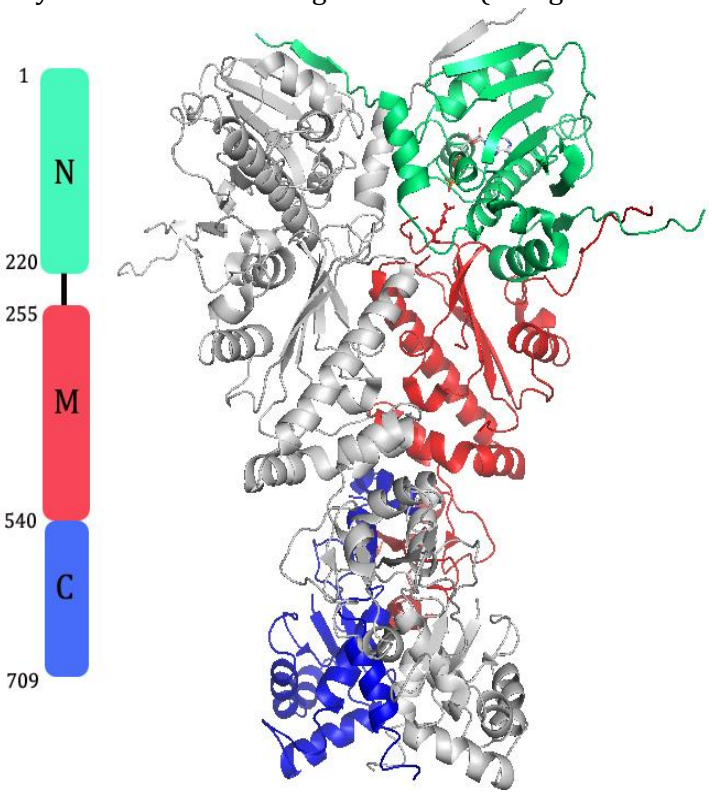

FIGURE 1-1: DOMAIN ORGANIZATION OF THE YEAST HSP90.

Left: Schematic domain organization of the yeast hsp90: N domain (N) (residue 1-220, green), middle domain (M) (255-540, red) and c domain (C) (540-709, blue). Right: Full-length yeast hsp90 dimer (pdb: 2cg9) in complex with AMPPNP and p23/sba1.

As mentioned, Hsp90 is a constitutive dimer and the C-terminal domain is essential for the dimerization of a functional Hsp90 molecule (Minami et al. 1994). It consists of a curved α-helix, a three-stranded β-sheet, a three-helix coil and an extended disordered arm (Ali et al. 2006; Pearl & Prodromou 2006). A helix-strand segment (residues 587-610 in yeast Hsp82) packs tightly with the respective counterpart from the other protomer, creating a helix bundle that forms the dimer interface. The association between the Hsp90 protomers is on the order of Kd ~60nM and thus comparatively strong (Richter et al. 2001). Since only dimer form of Hsp90 is fully active (Chadli et al. 2000), the C-terminal domain is also indispensable. The C domain is not involved directly in the ATP hydrolysis reaction of Hsp90 but it essentially contributes to this function by mediating the dimeric state: Cysteine bridged NM mutants of Hsp90 comprising only the N and M domain had ATPase activity similar to the wild - type protein whereas the monomeric NM variants had barely detectable ATP hydrolysis (Wegele et al. 2003).

At the very end of this domain, there is a MEEVD motif, binding site for proteins with tetratricopeptide repeat (TPR). In fact, many of Hsp90´s cochaperones such as Cpr6, Cpr7, Hop, Tom70, Ppt1, Dpit47, CHIP … have TPR domain, which makes a solid confirmation for the second important role of C-terminal domain as domain for cochaperone interactions (Prodromou et al. 1999). This is also the missing part of HtpG in comparison to eukaryotic Hsp90 proteins, nevertheless, the overall fold of all Hsp90 proteins seem to be highly similar. It is noteworthy that even though Hsp90 is constitutively dimer, C-terminal domains of two protomers in the dimer do not always stably dimerized. In fact, in single molecule FRET, it

was shown that C-termini open and close with fast kinetics. Moreover, C-terminal dimerization is anti-correlated with N-terminal dimerziation and is also modulated by the nucleotide binding state of Hsp90 (Ratzke et al. 2010).

1.2.3 HSP90 CHAPERONE ACTIVITY AND CLIENT PROTEINS

1.2.3.1 HSP90 CHAPERONE ACTIVITY

Hsp90 clearly has functions as a classical chaperone: its ability to suppress the aggregation process of model proteins under elevated temperatures without the need of ATP or other proteins were confirmed by *in vitro* experiments (Miyata & Yahara 1992; Jakob et al. 1995). However, this seems to be only one aspect among Hsp90 functions. As mentioned previously, Hsp90 is found in high concentrations even in unstressed cells and is indispensable in most organisms also under physiological conditions (see section 1.2.1 (page 11)). This indicates that Hsp90 is required in fundamental biological processes both in normal and stress conditions. However, among the heat shock protein, Hsp90 is unique because it is not required for the *de novo* folding of polypeptides. Instead, Hsp90 exerts its activity on later stage of folding, namely maturation, maintenance and activation of client proteins (Nathan et al. 1997; Wegele et al. 2004; Lindquist et al. 2010). In certain conditions, Hsp90 also have active roles in degradation of "hopeless" misfolded proteins (Murata et al. 2001; Xu et al. 2002; Morishima et al. 2008; Stankiewicz et al. 2010).

Although Hsp90 is frequently described as a ''molecular chaperone machinery,'' evidence showed that the Hsp90 machinery does not exist as one large complex containing Hsp90 and all co-chaperones but instead, Hsp90 and co-chaperone proteins interact with client proteins in a sequential order making several distinct complexes during the whole process (Smith 1993; Smith et al. 1993; Johnson et al. 1994; Smith et al. 1995; Johnson & Toft 1995; Dittmar et al. 1996; Barent et al. 1998; Kosano 1998; Y Morishima et al. 2000; Yoshihiro Morishima et al. 2000; Kanelakis et al. 2002).

Much of the current knowledge about the Hsp90 chaperone cycle was gained from research on steroid hormone receptors (SHRs), one of the earliest identified Hsp90 client families by Pratt and coworkers. According to reconstitution experiments, the assembly of SHRs is a chronological progression through three major complexes with different cochaperone compositions. The cycle starts with the nascent polypeptide or the pre-existing SHR without its ligand being recognized and bound by Hsp70/Hsp40 system to form the so called "early complex". The substrate-Hsp70 complex interacts with Hsp90 and they further form the "intermediate complex" whereby Hsp70 and Hsp90 is bridged by the organizing protein HOP (Smith et al. 1993; Dittmar & Pratt 1997; Chen & Smith 1998; Wegele et al. 2004). The substrate is then transferred completely to Hsp90, making the "late complex" in which Hsp70 and HOP are replaced by p23 and immunophillins (Cyp40, FKBP52, etc) which stabilize the complex by arresting Hsp90 in its close and substrate-binding conformation (Smith et al. 1993; Smith 1993; Johnson et al. 1994; Forafonov et al. 2008; Freeman et al. 2000). Further conformational changes in the late complex facilitate the maturation of SHR (mostly its hormone binding domain) so that it binds ligand with high affinity (Figure 1-2).

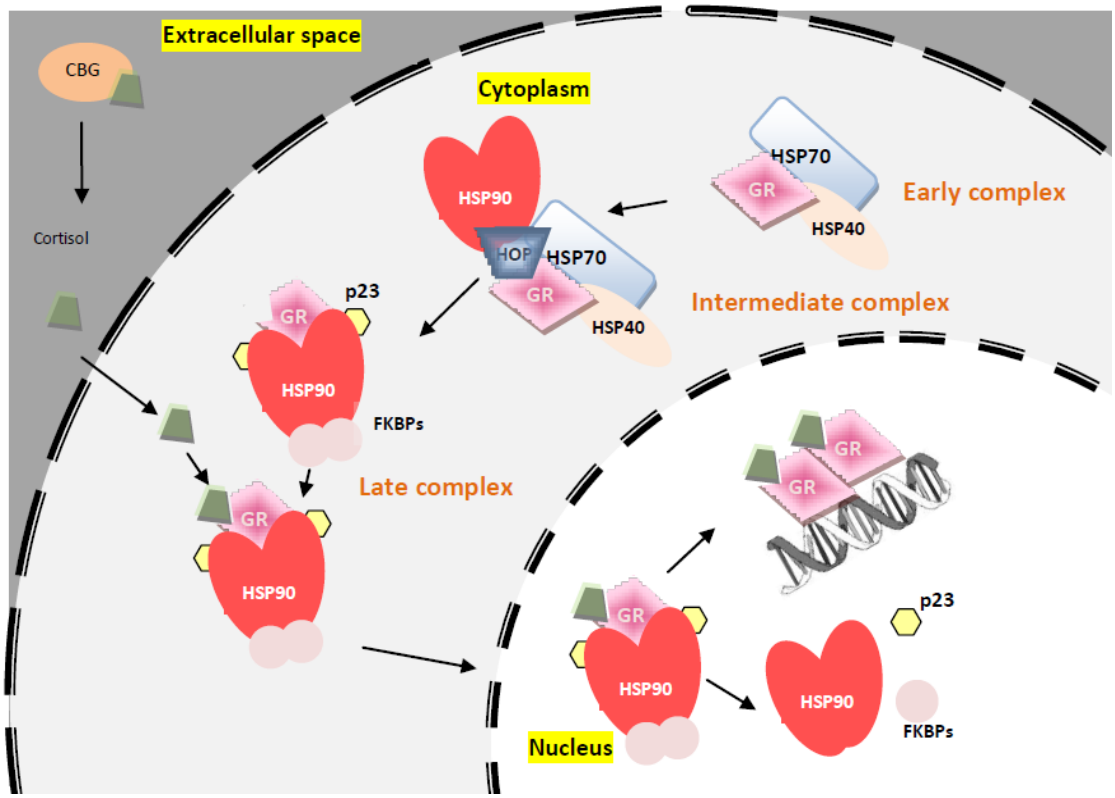

FIGURE 1-2: CHAPERONE CYCLE OF HSP90 FOR STEROID HORMONE RECEPTORS.

Hsp70/Hsp40 forms an **early complex** with the client protein. HOP can interact with both Hsp70 and Hsp90, bridging the two chaperones to facilitate client transfer to Hsp90 system in the **intermediate complex**. Next, Hsp70 and HOP dissociate from Hsp90-client complex and are replaced by p23 and immunophillins (FKBP proteins) forming the **late complex**, in which the client protein is activated by ligand binding or upstream signal.

For some of the receptors, such as progesterone (PR), they have nuclear localization signals that are functional in the absence of hormone, and these receptors move into the nucleus where they exist in the same multiprotein heterocomplex with Hsp90. Other receptors, such as the glucocorticoid receptor, are localized predominantly in the cytoplasm in the absence of hormone and move into the nucleus in a hormone-dependent fashion. For those of the latter type, the dissociation of ligand-bound SHRs from Hsp90 complex was initially assumed to be a cytoplasmic event which happened before the ligand-bound SHRs enter the nucleus and act as transcription regulator. However, studies from the last three decades have convincingly demonstrated that efficient transport of ligand-bound SHRs into the nucleus (half-life approximately 5min) requires Hsp90 complex including hsp90 and cochaperones such as TPR immunophillins FKBP51 and FKBP52 (Czar et al. 1997; Galigniana 1998; Galigniana et al. 2001; Galigniana et al. 2002; Davies et al. 2002; Galigniana et al. 2004; Harrell et al. 2004; Piwien Pilipuk et al. 2007; Echeverría et al. 2009; Galigniana et al. 2010). The alternative Hsp90-independent retrograde translocation of these receptors is much slower (40-60min half-life), allowing for degradasome formation and subsequent targeting of the receptor to proteasome (Galigniana et al. 2004).

This model provides us with a first picture of how Hsp90 cooperates with different co-chaperones sequentially to assist the folding of its client proteins. However, the detailed mechanism for individual client or client family remains to be further elucidated. For example, many co-chaperones have been identified to regulate Hsp90 functions but only a few of them has been described in the current model of the chaperone cycle. Other cochaperones, such as Cdc37 and Aha1, have been demonstrated to be indispensible for

certain client or client class or beneficial under critical conditions. Their integration into the chaperone cycle would also be of great interest to the field.

While early studies focused on protein folding, Hsp90's integration into the overall quality control system was not really appreciated until the benzoquinone ansamycin, geldanamycin (GA), was shown to be a specific inhibitor of the chaperone (Whitesell et al. 1994). Numerous subsequent studies revealed that upon GA treatment, client protein kinases and transcription factors were rapidly destroyed via the ubiquitin/proteasome pathway (Uehara et al. 1986; Schulte et al. 1996; Hartmann et al. 1997; Whitesell et al. 1998; Nimmanapalli et al. 2001; Katschinski et al. 2002; Basso et al. 2002; Grbovic et al. 2006; Lu et al. 2010) and in the meantime, the Hsp70 system was induced (McLean et al. 2004; Davenport et al. 2007; McCollum et al. 2009). These events lead to remarkable results in oncogenic transformation as several of Hsp90 cellular substrates are conformational labile signal transducers that play key roles in all hallmarks of cancer development such as cell proliferation and survival (Raf-1, HER2, etc.), cell cycle progression and apoptosis evasion (p53, Akt, Cdk4, Cdk6, telomerase, etc.), tumor angiogenesis (HIF-1α, VEGF, etc.), invasion and metastasis (MMP2, urokinase, etc.). On top of that, it's worth noting that many oncogenic variants of these same client proteins display unusual stable association with Hsp90 chaperone complexes, which results in impairing the normal proteolytic turnover of these molecules and in the end, providing an overall promoting of oncogenic transformation. This was observed with v-Src, an unstable protein kinase, which has a greater requirement for Hsp90 than its cellular counterpart c-Src (Xu & Lindquist 1993). Similarly, mutant forms of p53 and B-Raf protein kinase have stronger interactions with molecular chaperones than their wild type counterparts do (Sepehrnia et al. 1996; Whitesell et al. 1998; Esser et al. 2005; Müller et al. 2005; Grbovic et al. 2006). These observations may partly explain the higher sensitivity of tumor in contrast to normal, untransformed cells to Hsp90 inhibitors that are currently in clinical development. These findings can also refer to another pivotal but previously unrecognized role of Hsp90 in evolution in which this unique chaperone acts as a capacitor by helping to fold polymorphic variants of the same protein (Rutherford & Lindquist 1998; Queitsch et al. 2002). Upon intense selection pressure within the particular host environment, these otherwise hidden variants may gain certain advantages over their wild type counterparts and take over normal cellular homeostasis control. In the case of cancer development, under extreme selection pressure such as hypoxia, high interstitial pressure, constant apoptosis signaling and nutrient deprivation, it is likely that those variants are the key determining proteins that shaping the ability of tumor cells to adapt and evolve. Hsp90, therefore, sits at a very critical position of the cellular quality control system: the nexus of final folding and degradation pathways, in addition to regulating expression of other quality control components.

On the one hand, these critical roles of Hsp90 allow the potential of small molecule Hsp90 inhibitors to disrupt multiple oncogenic clients simultaneously which makes up a unique and therapeutically attractive feature of these compounds. On the other hand, it becomes very difficult to predict which patients are likely to benefit from such drugs if response is dictated by the constellation of molecular genetic defects present in their particular tumor.

1.2.3.2 HSP90 CLIENT PROTEINS

Hsp90 is a "selective" chaperone, whose principles for client selection are still poorly understood. The list of its clients consists of more than 200 proteins and is still enlarging.

Transcription factors	Kinases	Others
- Steroid hormone	- Raf family (Raf-1, B-Raf)	- Telomerase

receptors (GR, ER, PR, AR, etc.) - Heat shock factor-1 (HSF-1) - P53 - Hypoxia-induced factor 1α (HIF-1α) - Heme-activated protein (Hap1) - Stat2, Stat3, Stat5 - Oct4 and Nanog - Etc.	- Src family (v-src, Lck, Fyn, etc.) - Akt - Cyclin-dependent kinases (Cdk2, Cdk4, Cdk6, Cdk9, Cdk11, etc.) - ErbB2 - Bcr-Abl - eEF-2 kinase - MAPK6 - JAK1 - VEGFR-1, VEGFR-2 - Aurora-B - Etc.	- Apaf-1 - Calmodulin - Mdm2 - DNA polymerase α - Hepatis B virus reverse transcriptase - Tau - Proteosome - Myosin - Urokinase - Matrix metalloproteinase-2 (MMP2) - Etc.

TABLE 1-1: HSP90 CLIENT PROTEINS.

The list consists of more than 200 proteins and can be categorized into 3 classes: transcription factors, kinases and others. A full list of updated Hsp90 clients can be found in: http://www.picard.ch/downloads/Hsp90interactors.pdf

Via its numerous clients, Hsp90 seems to influence many aspects of cell biology such as cell signaling, protein trafficking, innate immune response, cell motility, viral infection or even evolution. Currently, it is estimated that Hsp90 from *S. cerevisiae* physically or genetically interacts with more than 1000 different proteins, which accounts for ~20% of the yeast proteins, making it the most highly connected protein in the yeast genome (the BioGRID Interaction database and Lindquist et al. 2010). However, it is not clear to which extent all proteins found to physically interact with Hsp90 are really dependent on its action for adopting their functional states, or their requirement of Hsp90 are cell-type and/or environmental specific.

In general, Hsp90 client proteins are diverse in sequence as well as in structure. Among these, transcription factors and kinases represent two major groups, indicating that Hsp90 has large impact on cellular regulatory processes (Table 1-1) (Wegele et al. 2004).

Client recognition

How Hsp90 recognizes specifically its client proteins despite high diversity in structures has remained one of the biggest questions in the field. In contrast to many other chaperone systems like Hsp70 that recognize exposed hydrophobic parts on partially unfolded proteins, Hsp90 seems to preferentially act on highly structured nearly native-like substrate proteins (Jakob et al. 1995). This finding was confirmed by several other studies lately. A recent study for example could show that Hsp90 specifically bound only to the structured region of a staphylococcal nuclease fragment that was otherwise largely unfolded (Street et al. 2011). Also, in case of the steroid hormone receptors that are essentially depend on Hsp90 to acquire hormone binding activity *in vivo*, Hsp90 does likely not promote the folding of a newly translated polypeptide of the receptor. Instead, Hsp90 is involved in the late step of client maturation: reactivating the receptor for ligand binding after its being partially unfolded by Hsp70 (Kirschke et al. 2014). In general, the role of Hsp90 seems to be likely stabilization of a specific labile conformation of the client but not to promote its de novo folding. The conformational state of a protein might be a more important determinant for rendering it a candidate suited for Hsp90 binding than a particular well defined binding motif.

This proposed hypothesis is further supported by a high throughput interaction system from study of (Taipale et al. 2012). In this work, the authors have illustrated evidence that determinants for Hsp90 binding in client proteins are both widely distributed and highly

localized depending on the client family itself. The client selectivity of Hsp90 for kinases, a major class of its client classes, is further mediated by the cochaperone Cdc37.

From the Hsp90 side, according to the most recent results from an NMR study on Hsp90-Tau complex, client binding sites also seem to occupy a large sureface of approximately 106Å length that runs over two domains (N-terminal and M-domain) with many low affinity contacts including both hydrophobic and hydrophilic binding sites. These low-affinity contacts, however, can build up to a high-affinity binding energy. This allows recognition of scattered hydrophobic residues in late folding intermediates that remain after early burial of the Hsp70 and other "early" chaperone sites (Karagöz et al. 2014). This large client binding interface of Hsp90 is also quite unique among the chaperones: it is rather an exposed surface than a cleft, pocket or chamber, more extended than that of any protomer of known chaperones (Hsp70s, Hsp60s or Hsp100s). Remarkably, although no longer continuously connected, most of the substrate-binding hotspots in Hsp90 N and M domains remain accessible upon dimerization of N-terminal domains. These binding sites on Hsp90 also do not interfere with interaction regions of many cochaperones, including Aha1 and p23. Interaction sites for Cdc37 are partially overlapping, however, since the specific client in this study is not a kinase (Tau) and Cdc37 is likely to bind to on the other protomer of the Hsp90 dimer than the client protein (Vaughan et al. 2006), ternary complex should still be possible.

1.2.4 HSP90 REGULATION MECHANISMS

Given the numerous client proteins that are dependent on Hsp90 function, it is not surprised that Hsp90 has to be tightly and sophisticatedly regulated. Indeed, Hsp90 is a conformationally flexible protein that mostly associates with a subset of approximately 20 proteins (termed "cochaperones") to perform its function. Besides, binding and hydrolysis of ATP is essential and also known to contribute to driving the Hsp90 machinery through distinct conformations. These conformations in turn interact, assist the client protein to achieve or maintain a certain conformation and release it: Each of these steps is also coupled with dynamic association and dissociation of cochaperones. Moreover, evidence is emerging that post-translational modifications of Hsp90 itself are involved significantly as well in regulating this complex chaperone machinery. In the following sections, each of these regulating factors of Hsp90 will be discussed in more details.

1.2.4.1 ATPASE ACTIVITY OF HSP90

Hsp90 proteins possess ATPase activity that is absolutely essential for its function (Obermann et al. 1998; Panaretou et al. 1998a). In general, the ATP hydrolysis by Hsp90 is slow, with a turnover number of ~0.5-1 min^{-1} for yeast Hsp90 (Panaretou et al. 1998b; Weikl et al. 2000; Richter et al. 2001) and only 0.09 min^{-1} for human Hsp90 (McLaughlin et al. 2002; Stankiewicz et al. 2010). The affinity of Hsp90 for nucleotide is rather weak with Kd (dissociation constant) on the order of ~100μM (Prodromou et al. 1997; Panaretou et al. 1998b; Weikl et al. 2000; Wegele et al. 2003) . The ATPase-coupled conformational changes in Hsp90 have been studied intensively with much success provided from structural studies.

In its ATPase cycle, Hsp90 adopts a number of structurally distinct conformations, which are induced by nucleotide (Graf et al. 2009). In the apo state, Hsp90 adopts a V shape conformation, termed "open conformation". ATP binding trigger a series of conformation changes including the closure of the lid segment in N domain, transient dimerization of the two N domains in the dimer and the docking of the catalytic loop from M domain into the nucleotide-binding pocket of the N domain (Pearl & Prodromou 2006; Ali et al. 2006). Finally Hsp90 reaches a more compact conformation, termed "closed conformation" in which the N domains are dimerized, locked by swapping of β-strands between two protomers and M domains twisted along the molecule axis forming a "clamp" structure. Then Hsp90 reaches a fully closed state in which ATP hydrolysis occurs. After ATP is hydrolyzed, the N- domains disassociate, release ADP, Pi and Hsp90 returns to the open

conformation again. A region at the very beginning of the N-terminal (first 24 amino acids) was supposed to be an instrinsic regulator of Hsp90 ATPase activity because removal of this part on the one hand confers flexibility to the lid region but on the other hand, results in loss of productive N-terminal dimerization and hence, also loss of ATPase activity (Richter et al. 2002; Richter et al. 2006).

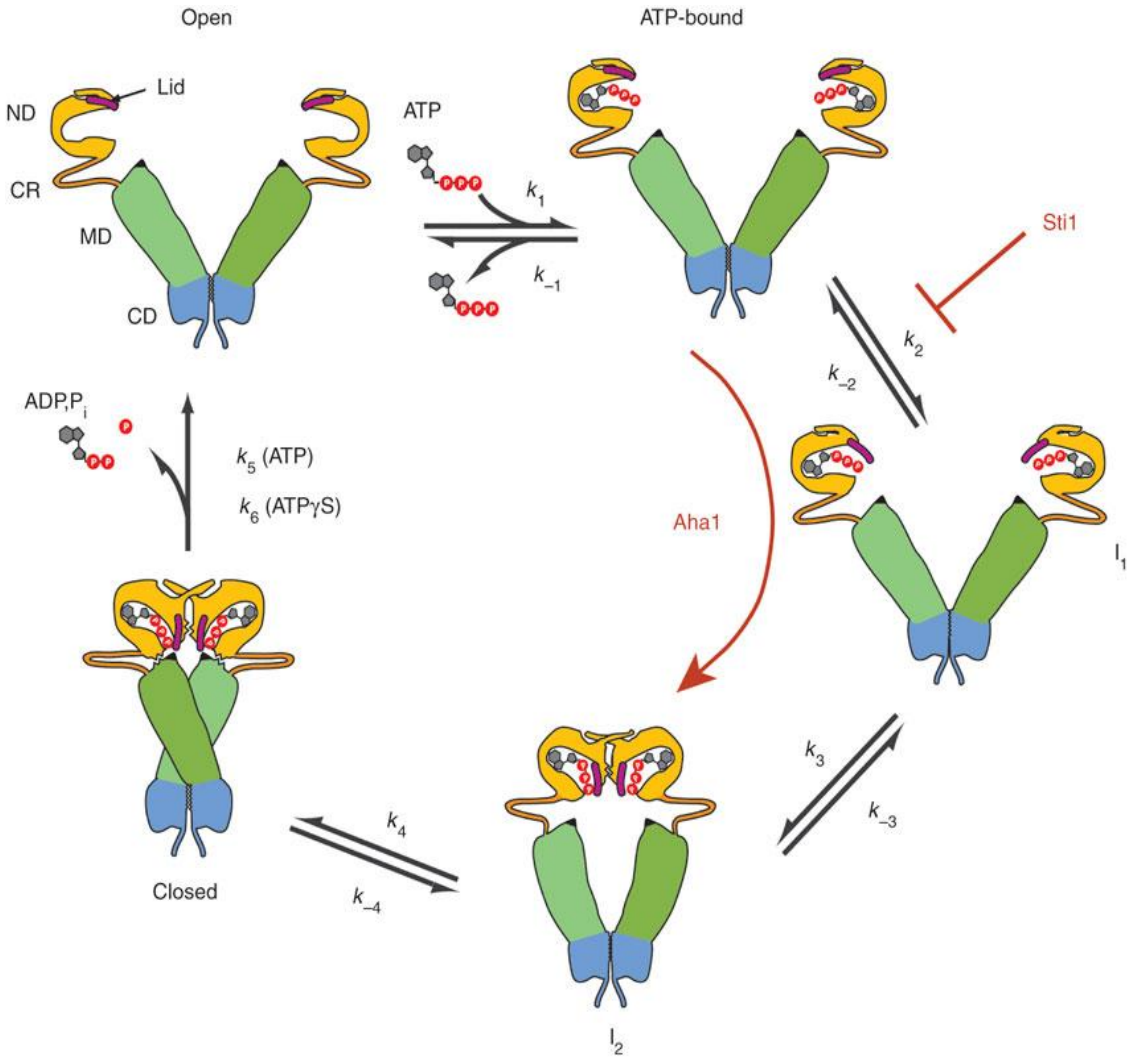

FIGURE 1-3: MODEL OF THE HSP90 ATPASE CYCLE.

The cylcle starts with Hsp90 in open conformation (top, left). After fast ATP binding, conformational changes in N-terminal domain resulted in repositioning of lid segment (I_1). Then N-terminal domains from two protomers dimerize (I_2) and rearrangement of N-M domains leads to the fully closed state in which atp hydrolysis occurs. Cochaperones such as Sti1 or Aha1 regulate Hsp90 ATPase cycle by inducing structural changes that either blocks or facilitates formation of intermediate conformations. Reproduced from (Hessling et al. 2009)

The first view of "closed conformation" of a full-length Hsp90 came from the crystal structure of yeast Hsp82 bound with the co-chaperone p23/Sba and the non-hydrolysable ATP analogue AMPPNP (Ali et al. 2006) (Figure 1-1). Recent biophysical studies using single molecule FRET assays allowed further dissecting of the ATP-induced conformational changes (Mickler et al. 2009; Hessling et al. 2009). In principle, there are two important intermediates between the open and closed conformation. The first intermediate (I_1) has ATP bound and lid region closed over the nucleotide binding pocket but N domains of two protomers are still apart. Then the N-terminal dimerization leads to the formation of the second intermediate state (I_2), in which the M domain repositions and interacts with the N

domain. The transitions between open conformation to I_1 and from I_1 to I_2 are rate-limiting steps of the ATPase cycle rather than the hydrolysis reaction itself (Hessling et al. 2009) (Figure 1-3).

The dynamics of Hsp90 conformations were, however, shown to be only weakly coupled with the ATPase cycle in single molecule FRET (Mickler et al. 2009). This finding is also in agreement with a previous observation using ensembles from electron microscopy data (Southworth & Agard 2008), indicating that Hsp90, independence of nucleotide, has many conformational states and the binding of nucleotide would only shift the equilibrium more in favor of one or another state rather than locking all Hsp90 molecules in a single conformation.

1.2.4.2 COCHAPERONES

Hsp90 alone exhibits limited chaperone activity towards a wide range of subtrates. Hsp90 acts in a multiple-chaperone complex, including other chaperones, adaptors, modulators, etc. termed in general "cochaperones", on client proteins. More than 20 of such cochaperones have been identified in eukaryotic cells and were shown to regulate Hsp90 in different ways such as via ATPase cycle as well as recruitment or release of specific client proteins to and out of the complex (Young & Hartl 2000; Richter et al. 2004; Pearl & Prodromou 2006; McLaughlin et al. 2006; Wandinger et al. 2008; Vaughan et al. 2009; Retzlaff et al. 2009; Retzlaff et al. 2010; Gaiser et al. 2010a; Li et al. 2011; Li et al. 2013). Some representative cochaperones will be discussed further in more details.

HOP (Hsp70/Hsp90 Organizing Protein)

HOP belongs to a class of proteins called TPR-containing proteins (TPR: tetratricopeptide repeat), which share the presence of a TPR domain in their structures. This TPR domain recognizes the C-terminal MEEVD motif in Hsp90 through a highly conserved clamp domain. Structurally, TPR domain consists of generally three degenerated 34-amino acid repeats forming two anti-parallels α helices separated by a turn. The helix-turn-helix motifs stack upon each other to form a superhelical groove, which interacts with TPR acceptor modules (Scheufler et al. 2000).

Together with HOP, many other TPR proteins are also cohaperones of Hsp90 such as members of PPIase family: Cyp40 (yeast homologous Cpr6/Cpr7), FKBP51, FKBP52, and phosphatase PP5 (yeast homologue Ppt1), etc (Barent et al. 1998; Wandinger et al. 2006).

Early experiments on steroid hormone receptors have identified Hsp90, Hsp70 and HOP in a large 9S complex (Smith 1993; Wegele et al. 2004). Hsp70 is known to be a chaperone by itself, involved in folding nascent polypeptide and refolding misfolded proteins. HOP doesn't have chaperoning activity but can bind to both Hsp90 and Hsp70, forming an intermediate complex in which the substrate is transferred from Hsp70 to Hsp90 for the final stage of folding (Wegele et al. 2004; Wegele et al. 2006). When deleted, its yeast homologue (Sti1) was shown to be important for GR maturation and also for an unrelated Hsp90 client protein, v-src kinase, confirming its role as Hsp90 cochaperone for clients in general (Chang et al. 1997).

HOP contains three TPR domains: TPR1, TPR2a and TPR2b which allows it to interact simultaneously with Hsp70 and Hsp90 (both have EEVD motif at the C-terminus). It also inhibits the ATPase activity of Hsp90 non-competitively (Richter et al. 2003). Several studies have identified TPR1 and TPR2a being responsible for binding to Hsp70 and Hsp90, respectively (Scheufler et al. 2000; Brinker et al. 2002). However, further evidence using truncation constructs of HOP in ATPase assays, pulldown, crosslinking experiments and hydrogen deuterium exchange mass spectroscopy (HD-MS) have revealed that interaction between Hsp90 and HOP involves also TPR2b and also provided more insights into the molecular mechanism of how HOP inhibits Hsp90's ATPase activity (Flom et al. 2007; Johnson et al. 2007; Lee et al. 2012). Taken from the Hsp90 side, there is an overall reduction of conformational flexibility of Hsp90 when bound to HOP. In more details, HOP utilizes both TPR2a and TPR2b to stabilize Hsp90 in an open conformation preventing N-

terminal dimerization and docking of the NBD with the MD (Richter et al. 2003; Lee et al. 2012). These findings explain why HOP can facilitate client transfer from Hsp70 to Hsp90 system and provide more proofs that HOP may be required by most Hsp90 clients to interact with Hsp90.

p23

p23 is the smallest protein in the Hsp90 machinery (molecular weight 18-25 kDa) which was first characterized in the Hsp90-steroid hormone receptor complex (Johnson et al. 1994). Together with HOP, Hsp70, Hsp40 and Hsp90, p23 make up a minimal *in vitro* system that is capable of chaperoning Hsp90 client proteins such as steroid hormone receptors or hepatitis B virus polymerase (Hu et al. 1997). Similar to HOP, p23 was also reported as a part in Hsp90 complexes with several other clients such as estrogen receptor, human Fes protein-tyrosine kinase, human heat shock transcription factor Hsf1, human aryl hydrocarbon receptor (Nair et al. 1996), telomerase (Holt et al. 1999) and hepadnavirus reverse transcriptase (Hu et al. 1997), etc. Whether p23 directly binds to those client proteins or via Hsp90 is not clear, since unlike most of other Hsp90 cochaperones, p23 itself has a chaperone activity to passively prevent aggregation of denatured proteins (Bose et al. 1996; Freeman et al. 1996).

This protein is also a well conserved component of the Hsp90 machinery, composed of 2 domains: N-terminal mainly formed by β-sheets and an unstructured C-terminal tail. p23's own chaperone activity (but not its binding to Hsp90) is dependent on this unstructured part (Weikl et al. 1999). Interestingly, this region was also reported to be important for activation of progesterone receptor (Weaver et al. 2000) and regulation of telomerase (Woo et al. 2009) via the Hsp90 system.

Binding of p23 to Hsp90 is direct and enhanced significantly by ATP as well as decreased by ADP (Johnson & Toft 1995; Sullivan et al. 1997). A crystal structure of yeast p23/Sba1 and full length yeast Hsp90 (Hsp82) has given even more interesting insights into the mechanism of p23 interacts with Hsp90: p23/Sba1 has several contacts with the backside of the ATP-lid in the N-terminal domain of Hsp90 which is only presented in the correct three-dimensional configuration when Hsp90 is in the ATP-bound state; moreover and unexpectedly, p23 stabilizes the catalytic loop in an active conformation (Ali et al. 2006). In contrast to p23/Sba1 positioning in the crystal structure that favors a ATP-hydrolysis-promoting conformation of yeast Hsp90, biochemical evidence in several publications demonstrate that similar to HOP, p23 inhibits Hsp90's ATPase activity (McLaughlin et al. 2002; Panaretou et al. 2002; Richter et al. 2004; McLaughlin et al. 2006). Recently, work from our group by hydrogen-deuterium exchange mass spectroscopy and single turnover ATPase assay have demonstrated that p23/Sba1 reduces the conformational flexibility of the ATP lid and thus, preventing product release which resulting in inhibiting ATPase activity (ref: from Frontiers paper: Graf).

p23 can form ternary complexes with Hsp90 and Cpr6 or PP5 (Harst et al. 2005; Woo et al. 2009; Li et al. 2011), but competes with HOP/Sti1 (Li et al. 2011) and Aha1 (Harst et al. 2005; Li et al. 2013) for binding, indicating clearly that p23 enters at a late stage of Hsp90 chaperone cycle. It is reasonable to postulate that after the client is transferred from Hsp70 to Hsp90 via HOP, p23 joins the complex, traps Hsp90 in a closed state with extensive inter-dimer contact and sustains this conformation for the completion of client activation before the release of the ATP hydrolysis product.

Aha1

One interesting cochaperone of Hsp90 is Aha1 ("**A**ctivator of **H**sp90 **A**TPase **1**). Aha1 is first identified by homology searches with Hch1, ("**h**igh-**c**opy **H**sp90 supressor 1), which rescues the phenotype of a Hsp90 ts-mutation (E381K) (Nathan et al. 1999; Panaretou et al. 2002). Both, Hch1 and Aha1, were found to directly interact with Hsp90, *in vivo* and *in vitro* (Panaretou et al. 2002). Hch1 and Aha1 have a stimulatory effect on the Hsp90 ATPase activity, however, to different extents. The isolated Aha1 N- terminal fragment, which corresponds to the Hch1 full-length protein, also stimulates Hsp90's ATPase but only to approximately 25% that of full length protein, whereas its C-terminal fragment had no effect.

Hch1 was shown to stimulate Hsp90 ATPase activity to a similar extent as Aha1-N, but only at higher concentrations of the cochaperone required (Panaretou et al. 2002). Given their overlapping functions with respect to Hsp90 ATPase activation, it is surprising that yeast cells contain both Hch1 and Aha1 at the same time while in higher organisms only Aha1 homologues can be found. A knockout of either Hch1 or Aha1 in yeast cells did not result in any obvious growth defect, suggesting that their function might be intimately connected only with rather specific Hsp90 clients. However, when Hsp90 levels were depleted in cells or under other stress conditions, a double knockout of Hch1 and Aha1 led to a reduced thermotolerance (Panaretou et al. 2002; Lotz et al. 2003). Results from v-src maturation which is Hsp90-dependent in *Saccharomyces cerevisiae* also indicates that Hch1 can to some extent compensate for Aha1 functions and that both cochaperones obviously impact on Hsp90 client protein activation (Panaretou et al. 2002; Lotz et al. 2003). The concentration of Aha1 in cells seems to be critical. Overexpression of Aha1 can have deleterious effects as shown for CFTR (Mollapour et al. 2014) . The folding and maturation of CFTR is so inefficient that it requires prolonged association with molecular chaperones (Loo et al. 1998; Youker et al. 2004), while by accelerating ATPase cycle of Hsp90, Aha1 reduces dwell time of client in the chaperone complex. Thus, for the Hch1/Aha1 cochaperones, unique property of accelerating Hsp90 ATPase activity seems to be connected with the activation of certain Hsp90 client proteins, supporting the hypothesis that cochaperones might importantly contribute to the client specificity of the Hsp90 machinery.

Details on interactions between the N- terminal domain of Aha1 bound the Hsp90 M-domain were discovered from crystallography study (PDB: 1USV), revealing possible mechanism of Aha1 effects on the Hsp90 cycle (Meyer et al. 2004). The N domain of Aha1, with its elongated cylindrical structure orienting along the long axis of Hsp90´s M domain, interacts extensively with all three subdomains of this segment (Figure 1-4). Most interactions are polar, between those basic residues exposed on M domain´s surface and acidic residues from Aha1. There is one notably non-polar contact (since it involves the catalytic residue Arg380 of Hsp90), in which a hydrophobic patch on Aha1 packs against a similar patch on Hsp90. By comparing the structures of Hsp90´s M domain in free and Aha1-bound crystals, it is hypothesized that Aha1 interactions causes some movements in the catalytic loop of Hsp90´s M domain, which release the catalytic Arg380 from its retracted and inactive interaction with nearby residues, enabling its insertion into the nucleotide-binding pocket in the N-terminal domain. FRET measurements also support this hypothesis: The presence of Aha1 was shown to enable Hsp90 bypassing the I_1 state (ATP-bound and lid closed) to directly reach the I_2 state (N-terminal dimerized and M-domain repositioned towards ATP-binding pocket) in the ATPase cycle (Hessling et al. 2009) (Figure 1-3).

The C-domain of Aha1 was shown to further contribute to the ATPase stimulation by providing additional binding contacts with the N domain of the opposing Hsp90 protomer or a hydrophobic groove formed by transient, ATP-dependent dimerization of both Hsp90 N domains which stabilizes its closed dimerized conformation capable of ATP hydrolysis (Retzlaff et al. 2010; Koulov et al. 2010). Interestingly, Aha1 binds in an asymmetric fashion to Hsp90, one molecule of the cochaperone per Hsp90 dimer is sufficient for full ATPase stimulation, leaving the possibility of a simultaneous client protein binding to an Hsp90 - Aha1 complex (Retzlaff et al. 2010).

In size-exclusion chromatography, Aha1 competes with HOP/Sti1, Cdc37 and p23 for binding to Hsp90 (Harst et al. 2005). Recently, using analytical ultracentrifugation, it was further resolved that Aha1 together with Cpr6 and nucleotide dissociates HOP/Sti1 from Hsp90-client complex to accelerate the progression of the chaperone cycle to fully-closed state of Hsp90 in which Aha1 is then replaced by p23 (Li et al. 2013).

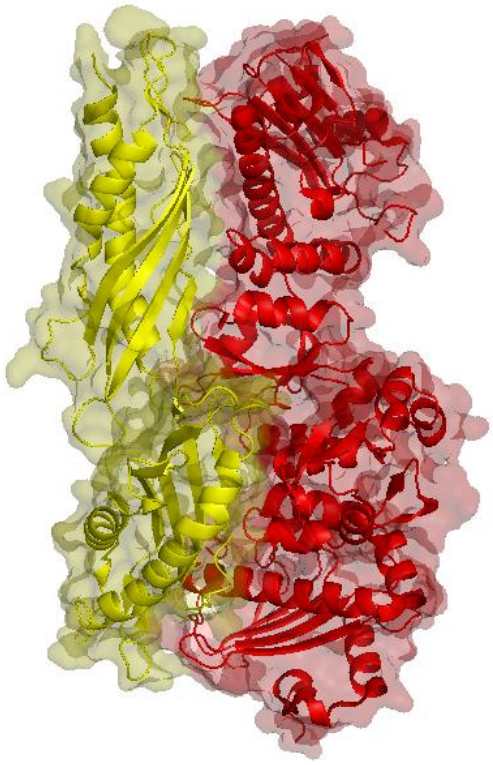

FIGURE 1-4: CRYSTAL STRUCTURE OF YEAST AHA1 IN COMPLEX WITH YEAST HSP90
(Aha1: N-terminal domain, Residue 1-156, colored yellow) (Hsp90: M-domain, residue 272-530, colored red) (Pdb 1usv).

Aha1/Hsp90 interaction is considered to be important for the chaperoning of many Hsp90 clients, including ErbB2, v-src, Cdk4, c-raf, etc (Holmes et al. 2008; Lotz et al. 2003; Panaretou et al. 2002). However, the significant decreased Aha1 interaction with certain Hsp90 variants provoked observable effects only with a selected number of clients (Mollapour, Tsutsumi, et al. 2011; Mollapour et al. 2014) indicating that Aha1 is critical only for selective clients in the Hsp90 client set and like the cochaperones p23 and Cdc37 (Felts & Toft 2003; MacLean & Picard 2003; Kimura et al. 1997), may have additional activities in cells that are independent of its role in modulating Hsp90 activity (Sun et al. 2012).

Cdc37

Cdc37 is another co-chaperone which inhibits the ATPase activity of Hsp90 (Siligardi et al. 2002; Gaiser et al. 2010b). This interference is mediated by the insertion of the Cdc37 R167 side chain into the nucleotide binding pocket of Hsp90, which directly inhibits the binding of ATP (Roe et al. 2004). Furthermore, the packing of C-terminal helixes of Cdc37 onto Hsp90's lid segment prevents its closing over the nucleotide-binding pocket and blocks the access of catalytic residue(s) from Hsp90's M-domain to the pocket. Finally, Cdc37 positions itself between the two N domains of Hsp90 dimer, impeding their dimerization and thus, arrests Hsp90 ATPase cycle in a conformation responsive for client loading (Roe et al. 2004; Siligardi et al. 2002) (Figure 1-5). These structural findings are in agreement with studies in yeast which exhibited interaction between Cdc37 and Sti1/HOP - the cochaperone that also acts in client transfering to Hsp90 - either in cell extract or in purified system. The biological significance of this interaction also has been shown genetically. Combinations of *cdc37* and *sti1* mutations are synthetically lethal (Abbas-Terki et al. 2002), and strains lacking Sti1 are defective in maturation of the Ste11 kinase, a defect that can be suppressed by overexpression of Cdc37 (Lee et al. 2004).

Cdc37 was originally identified by genetics study in *S. cerevisiae* as a gene essential for cell cycle progression (hence the ***cdc*** designation for **c**ell **d**ivision **c**ycle), which is in agreement with biochemical evidence of its association and critical role for important cyclin-dependent kinases such as Cdc28 (Reed 1980; Gerber et al. 1995). It has been proven to be essential for viability in many eukaryotic model organisms even though poorly consevered (MacLean & Picard 2003). It is also found in the complex of Hsp90 and the tyrosine kinase v-src and later, in the complex of Hsp90 and many other kinase clients (Stepanova et al. 1996; Grammatikakis et al. 1999; Shao et al. 2001; Abbas-Terki et al. 2000; H. Wang et al. 2002; Mort-Bontemps-Soret et al. 2002; Vaughan et al. 2006; Taipale et al. 2012). Therefore, it has been long thought that Cdc37's primary function is an Hsp90 specific cochaperone for protein kinases. Kinases in general have diverse structures, however, all contain a conserved catalytic domain, especially the glycine-rich (Gly-X-Gly-X- X-Gly) motif, which Cdc37 recognizes and binds with its N-terminal domain (Shao et al. 2003; Prince & Matts 2005; Terasawa et al. 2006; Vaughan et al. 2006; Polier et al. 2013). Similar to p23, Cdc37 has its own intrinsic chaperone activity which was shown by stabilizing purified unfolded β-galactosidase in an activation competent state (without refolding it) and also the

inherently unstable casein kinase II *in vitro* (Kimura et al. 1997). More interestingly, *in vivo*, Cdc37 can even partially compensate for decreased Hsp90 function, for e.g in maintaining v-Src (an Hsp90 kinase client) activity. An Hsp90-binding deficient Cdc37 variant when over-expressed can replace the essential full-length protein as well (Kimura et al. 1997; P. Lee et al. 2002). Cdc37 is also not entirely dedicated to kinases as substrates, although they dominate the currently known list of Cdc37 clients. It was shown to interact with and together with Hsp90, is required for androgen receptor (Rao et al. 2001) and hepadnavirus reverse transcriptase activation (X. Wang et al. 2002).

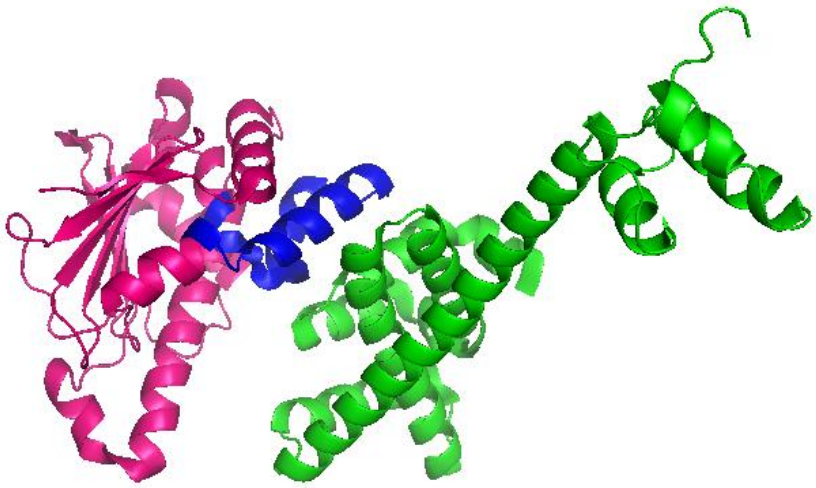

FIGURE 1-5: CRYSTAL STRUCTURE OF HUMAN CDC37 IN COMPLEX WITH YEAST HSP90

(Cdc37: C-Terminal, residues 125-378, colored green) (Hsp90: N-Terminal domain, residues 1-214, colored pink – the lid region is highlighted in blue) (Pdb 1us7).

Taken together, the data suggests that Cdc37 may act on client proteins independently of Hsp90 and that the function of Cdc37 on kinase and not-kinase client proteins of Hsp90 is rather more than just introducing the clients to Hsp90 or stabilizing their complex with Hsp90.

As mentioned, the list of Hsp90 cochaperones consists of many more components including Hsp70, FKBP51/FKBP52, CHIP, PP5, Ppt1, Cyp40, Sgt1, Tah1, Pih1, Cns1, VCP, etc. Most of the Hsp90 co-chaperones were first identified by virtue of their co-purification with Hsp90 complexes isolated from cell extracts; or were identified by virtue of physical or genetic interactions with Hsp90 proteins. These cochaperones regulate the ATPase activity of Hsp70 or Hsp90 and/or have specific *in vivo* functions, such as localization or trafficking. They also may affect Hsp90 function in a client-specific manner. The overall composition of the Hsp90 molecular chaperone machine appears to vary in diverse eukaryotic organisms, and genes encoding co-chaperones that stimulate (Aha1) or inhibit (Hop/Sti1 and Cdc37) the essential ATPase activity of Hsp90 are not absolutely conserved (Johnson & Brown 2009).

Recently, proteomic data also showed that all known cytoplasmic Hsp90 cochaperones were by far sub-stoichiometric to the total cytosolic pool of Hsp90 proteins (Finka & Goloubinoff 2013). A substoichiometric molar ratio 1:7 was found for the p23 (which inhibits Hsp90 ATPase), 1:16 for the Hsp70/Hsp90-organizing protein (STIP1, HOP), 1:34 for Aha1 (activator of the Hsp90 ATPase (AHSA1), 1:41 for the ubiquitin ligase CHIP, and 1:46 for the oncogenic cochaperone adaptor CDC37. Such substoichiometric ratios indicate that none of the cochaperones form intrinsic subunits of core Hsp90 dimers and rather associate dynamically to regulate the numerous cellular activities of Hsp90 (Finka & Goloubinoff 2013). Thus, the function of most co-chaperones may be restricted to subsets of client proteins either species-specific or in response to certain cellular conditions. Furthermore, these findings also indicate that in cells, there are further regulation

mechanisms that modulate distinct cochaperone recruitment to Hsp90 complexes at different stage of the chaperone cycle.

1.2.4.3 POST-TRANSLATIONAL MODIFICATIONS

Another level of regulation that has gained increasing attention is post-translational modifications of Hsp90.

Hsp90s are known to be heavily post-translational modified, including phosphorylation at several sites (serines, threonines and tyrosines), S-nitrosylation, acetylation, lysine methylation, ubiquitination and most recently SUMOylation with effects observed on client and/or cochaperones interaction, client maturation and subsequent, degradation (Figure 1-6) (S P Lees-Miller & Anderson 1989; Bali et al. 2005; Kovacs et al. 2005; Martínez-Ruiz et al. 2005; Dote et al. 2006; Duval et al. 2007; Scroggins et al. 2007; Yang et al. 2008; Kurokawa et al. 2008; Kekatpure et al. 2009; Mollapour, Shinji Tsutsumi, et al. 2010; Mollapour, Tsutsumi, et al. 2011; Franco et al. 2013; Mollapour et al. 2014). Although some of the modified amino acid positions have already been identified (mostly by incorporation of the corresponding radio-labeled groups and/or mass spectrometry), it is still a challenging task to obtain a global qualitative or quantitative picture of the modifications.

S-nitrosylation is a reversible modification in which a nitrogen monoxide group is attached to the thiol side chain of cysteine. For this modification, a feedback loop between human Hsp90 and its substrate endothelial nitric oxide synthase (eNOS) was discovered (García-Cardeña et al. 1998; Martínez-Ruiz et al. 2005). eNOS activity depends on the chaperone activity of Hsp90; whereas the nitrosylating agent NO modifies human Hsp90 at Cys597 (in the C-terminal domain) and this modification inhibits the Hsp90 ATPase activity, which in turn diminishes the up-regulation of eNOS activity by Hsp90. This might facilitate a tight regulation of cellular NO production in a negative feedback loop (Martínez-Ruiz et al. 2005). Further studies also showed that surprisingly both C-terminal as well as N-terminal association properties of C597-nitrosylated variant of Hsp90 were altered and thus, equilibrium between different conformations of Hsp90 is also shifted (Retzlaff et al. 2009).

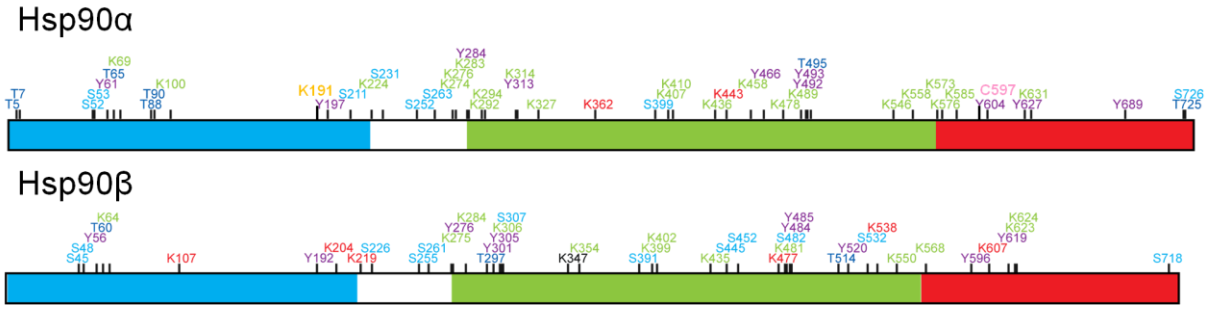

FIGURE 1-6: POST-TRANSLATIONAL MODIFICATION SITES ON HSP90.

Phosphorylation S (light blue) or T (Dark blue) or Y (purple); Methylation K (Black); Acetylation K (green); Ubiquitination K (red); S-Nitrosylation C (pink) and Sumoylation K (orange))

Acetylation is the post-translational modification that adds acetyl groups to proteins, typically on lysine residues. Histones are one of the first and major acetylation target and thus, historically acetylating enzymes were termed histone acetylases (HAT) and deacetylating enzymes histone deacetylases (HDAC). However, these enzymes act on more protein targets than histone, including Hsp90. For acetylation of Hsp90, a similar scenario to S-nitrosylation emerges. Histone deacetylase (HDACs) inhibitors, which result in the hyperacetylation of Hsp90, lead to a reduced interaction with and maturation of several of its substrate proteins, such as p53, Raf1, Bcl-Abl, and the glucocorticoid receptor (Yu et al. 2002;

Nimmanapalli et al. 2003; Murphy et al. 2005; Kovacs et al. 2005)(Kovacs et al. 2005; Murphy et al. 2005; Yu et al. 2002; Nimmanapalli et al. 2003). As a consequence, an increase in proteasomal degradation of some Hsp90 substrates was detected. Besides the ability to interact with its substrate proteins, the ATP binding properties of Hsp90 was also shown to be compromised upon acetylation of Hsp90 (Murphy et al. 2005; Rao et al. 2008). The enzymes deacetylating Hsp90 were identified to be mostly HDAC6, but also HDAC10 or HDAC1 (Kovacs et al. 2005; Zhou et al. 2008; Park et al. 2008). It is however not clear yet whether distinct HDACs alter Hsp90 acetylation state on individual site or they may work redundantly. *In vivo*, Hsp90 is acetylated at several sites; one was identified as Lys294 (in human Hsp90α) (Scroggins et al. 2007). Using acetylation-mimicking variant or a mutant that connot be acetylated of Hsp90, the authors have shown that acetylation at this lysine on Hsp90 leads to diverse effects on the chaperone interaction with different cochaperones while mostly weakens its interaction with client proteins (Scroggins et al. 2007). Acetylation of Hsp90 is also required for viability in *Saccharomyces cerevisiae* indicating its significant role to at least one important Hsp90 client in yeast (Scroggins et al. 2007).

SUMOylation in Hsp90 was already reported several times in proteomics studies in the last ten years (Panse et al. 2004; Zhou et al. 2004; Pountney et al. 2008). However, identification of individual SUMOylated lysine residues and their impact on Hsp90 function remained unexplored until a very recent publication by Neckers and colleagues, in which a SUMOylation of an N domain lysine conserved in both yeast and human Hsp90 were demonstrated to initiate recruitment of Aha1 to the chaperone complex in cells. Interestingly, the N-terminal SUMOylation of Hsp90 is asymmetric and it also unexpectedly facilitates binding of Hsp90 inhibitors and sensitizes yeast and mammalian cells to these drugs (Mollapour et al. 2014).

Phosphorylation is one of the most common post-translational modifications of proteins in general and has been extensively studied over decades. Phosphorylation of Hsp90 is not an exception: Hsp90 was detected as a phosphoprotein associated in immunoprecipitated v-src polypeptides from *in vitro* or *in vivo* synthesis in late 1970s (Sefton et al. 1978). Hsp90 phosphorylation level is quite high under physiological conditions: it is one of the major phosphorylated proteins in cells both under normal and heat shock conditions (Kelley & Schlesinger 1982; S P Lees-Miller & Anderson 1989). More interestingly, Hsp90 has several phosphorylated isoforms as could be observed in 2D gel (Welch et al. 1983). For mammalian Hsp90 proteins, the majority of Hsp90 molecules contain on average 5.8 mol of phosphate per mol of dimer (Iannotti et al. 1988).

Phosphorylation of Hsp90 was reported to occur on serine, threonine and tyrosine residues distributed along the proteins in all three domains (Iannotti et al. 1988; S P Lees-Miller & Anderson 1989; Smith 1993; Mimnaugh et al. 1995; Zhao et al. 2001; Adinolfi et al. 2003; Ecroyd et al. 2003; Ogiso et al. 2004; Duval et al. 2007; Kurokawa et al. 2008; Miyata 2009; Mollapour, S. Tsutsumi, et al. 2010; Mollapour, Tsutsumi, et al. 2011; Soroka et al. 2012; Muller et al. 2012; Solier et al. 2012; Barabutis et al. 2013). Kinases suggested to phosphorylate Hsp90 include casein kinase 2 (CK2), DNA-dependent protein kinase (DNA-PK), protein kinase A (PKA), GSK3-β, Akt and in yeast cells, Swe1/Wee1 and the Akt homolog Sch9 (S P Lees-Miller & Anderson 1989; Morano & Thiele 1999; Barati et al. 2006; Muller et al. 2012; Mollapour, Shinji Tsutsumi, et al. 2010; Mollapour, Tsutsumi, et al. 2011; Solier et al. 2012). Interestingly, one of the cofactors associating with Hsp90 via a TPR domain is PP5/Ppt1, a *bona fide* phosphatase which dephosphorylates Hsp90 in a specific manner only when bound to Hsp90 (Wandinger et al. 2006). Dephosphorylation of Hsp90 is important for its *in vivo* function, as in a PPT1 deletion strain, the maturation of several substrate proteins was found to be impaired (Wandinger et al. 2006).

On the other hand, influences of phosphorylation on Hsp90 activity are diverse and site-dependent. Some phosphorylation sites seem to be involved in client-specific manner, whereas others regulate more or less all studied client proteins with similar or

contradictory effects (S P Lees-Miller & Anderson 1989; Susan P Lees-Miller & Anderson 1989; Duval et al. 2007; Mollapour, S. Tsutsumi, et al. 2010; Mollapour, S. Tsutsumi, Truman, et al. 2011; Solier et al. 2012; Muller et al. 2012) . More details on regulation of Hsp90 by some well-characterized phosphorylation sites of Hsp90 will be discussed further in the following.

Thr5 and Thr7 (human Hsp90α) (Susan P Lees-Miller & Anderson 1989; Solier et al. 2012; Quanz et al. 2012)

Study in late 1980s by Lees-Miller *et al* has shown that double-stranded DNA-activated protein kinase isolated from HELA cells is able to phosphorylate Hsp90α at Thr5 and Thr7 (these residues are not conserved in the Hsp90β isoform) (Susan P Lees-Miller & Anderson 1989). More than 20 years later, both reports from Quanz *et al* and Solier *et al* have further gained insights into physiological significance of this phosphorylation event: Hsp90α phosphorylation by DNA-PK is linked to response to DNA-damage and critically involved in both DNA damage repair foci as well as apoptosis events (Quanz et al. 2012; Solier et al. 2012).

Thr36 (human Hsp90α) or Thr31 (human Hsp90β) or Thr22 (yeast Hsp82) (Mollapour, Tsutsumi, et al. 2011; Mollapour, S. Tsutsumi, Kim, et al. 2011)

Thr22 in yeast Hsp82 is a conserved threonine residue in the N domain of Hsp90 which corresponds to Thr36 in human Hsp90α or Thr31 in human Hsp90β. Work by Mollapour *et al* in 2011 has provided evidence that in yeast, Thr22 is the only site in the N-terminal domain of Hsp90 that gets phosphorylated by CK2 (which is not the case in human Hsp90α where CK2 phosphorylates numerous threonine residues in the N-terminal domain). This is an unexpected finding as Thr22 in yeast Hsp90 or Thr36 in human Hsp90α is not followed by series of acidic residues as commonly known for CK2's recognition motif.

Thr22 is among a group of residues that have been shown to form an interacting cluster in ATP-bound Hsp90. The hydrophobic interactions established by this cluster are essential for N-terminal dimerization and are necessary for active site formation and for ATPase activity (Cunningham et al. 2008). CK2-mediated phosphorylation of Thr22 requires ATP binding but not N-dimerization. *In vitro* and *in vivo* assays ultilizing nonphosphorylatable and phosphomimetic variants of Hsp90 at this residue reveals that CK2-dependent phosphorylation status at this position influences Hsp90 chaperone activity in a very complicated manner. Mutation of this residue to the nonphosphorylatable variant (T22A) did not significantly affect Hsp90 ATPase activity, while phosphomimetic mutation (T22E) reduced ATPase activity by more than half, although both mutants were able to support yeast growth when present as the sole Hsp90 *in vivo*. Consistent with its reduced ATPase activity, N domain dimerization of yHsp90-T22E in the presence of AMPPNP was less efficient than that of either wild-type yeast Hsp90 or yeast Hsp90-T22A. Neither T22 mutants were able to fully chaperone several kinase clients in yeast, including v-src, Ste11, and Mpk1/Slt2. In general, yeast Hsp90-T22E displayed the more severe chaperone defect. In mammalian cells, the situation is similar. Because neither nonphosphorylatable nor phosphomimetic Hsp90 mutants are competent to chaperone v-src, conformational changes provided by dynamic phosphorylation and dephosphorylation of T22/T36 are likely to be necessary for optimal Hsp90 chaperoning of this client while it is not clear which is optimal for the other clients. On the other hand, in yeast, Hsp90 T22E mutation supported greater than 4-fold more glucocorticoid receptor (GR) activity compared to wild-type Hsp90, while mutation to T22A resulted in less than half the GR chaperoning activity of wild-type Hsp90 despite their uniform binding to GR in immunoprecipitation (IP) assay. Like GR, stability and/or maturation of the highly dependent Hsp90 client CFTR was enhanced in both yeast and mammalian cells expressing T22E/T36E Hsp90 variant. Thus for some particular clients, including GR and CFTR, phosphorylation of Hsp90 at T22/T36 seem to be of great benefit.

Similar to chaperoning effect on kinase clients, interactions of Hsp90 with the cochaperones Aha1 and Cdc37 are severely weakened in both forms of Hsp90 phospho mutants. This effect on cochaperone interaction is likely part of the underlying mechanism for the chaperoning defects since Aha1 overexpression *in vivo* not only restored association

of Cdc37 and Aha1 itself with Hsp90 but also repaired fully or partly Hsp90 chaperone activity for kinase clients. Interestingly, Aha1 overexpression even reduced the chaperone activity of yeast Hsp90-T22E to the level of wild-type yHsp90, while increasing GR activity in the context of yeast Hsp90-T22A to twice that of wild-type yHsp90. Overall, CK2-dependent phosphorylation of T22/T36 in Hsp90's N domain significantly affects chaperone function in yeast and mammalian cells, allowing Hsp90 to discriminate among its extensive client set, in part by modulating interaction of the cochaperones Cdc37 and Aha1.

Another important characteristic of phosphorylation at Thr22/Thr36 is that phosphomimetic variant when expressed as sole source of Hsp90 in yeast exhibits increased sensitivity to wide range of Hsp90 inhibitors at high concentrations. This result identifies T22 as an important determinant of Hsp90 inhibitor sensitivity in yeast.

Tyr38 (human Hsp90α) or Tyr24 (yeast Hsp82) (Mollapour, Shinji Tsutsumi, et al. 2010)

Swe1/Wee1 tyrosine kinase is an Hsp90 client that regulates the G2/M cell cylcle transition by phosphorylating Cdc28 (Booher et al. 1993; McGowan & Russell 1993; Harvey & Kellogg 2003). Swe1 also directly phosphorylates a conserved tyrosine residue (Tyr24 in yeast Hsp82 and Tyr38 in human Hsp90α) in the N-terminal domain of Hsp90 proteins both *in vitro* and *in vivo* using yeast model. In yeast cells, Swe1-mediated phosphorylation of Hsp90 occurs in S phase of the cell cycle and causes Hsp90's translocation from nucleus to cytoplasm. There was no tyrosine phosphatase identified to be involved despite extensive search using phosphatase inhibitors by the authors, suggesting that this tyrosine phosphorylation may be switched off by degradation.

Similar to Thr22, Tyr24 belongs to the interface between two N-terminal domains in yeast Hsp82 dimer (Cunningham et al. 2008). Swe1/Wee1 targets Tyr24/Tyr38 when Hsp90 in an "open" conformation (N-terminal undimerized) because this residue is not accessible when Hsp90 is in the "closed" conformation. Mutation of this residue to a non-phosphorylatable amino acid (Y24F/Y38F) reduces Hsp90 binding to Aha1 and p23 cochaperones and negatively affects the ability of Hsp90 to chaperone selected set of client proteins including v-src, ErbB2, Raf-1, Cdk4, Ste11, etc, suggesting positive effect of Hsp90 phophorylation at this tyrosine residue on client activation. Notably, the phosphomimetic variant which represents constitutive phosphorylation at this residue cannot complement double deletions of Hsp90 in yeast and purified protein exhibits almost no ATPase activity despite the fact that it binds to to nucleotides with a similar affinity as wild type protein. It is intriguing to see how one phosphorylation site which in principle turns the protein into a better chaperone for clients instead causes harmful influences in general growth and finally leads to lethality. It is very likely that this phosphorylation is only crucial for maximized activation of certain client(s) in this very narrow time window (S-phase) and must be removed rapidly before it exerts harmful effects.

The authors also showed that inhibition of kinase activity on wild type protein or using non-phosphorylatable variant of both yeast and human Hsp90 result in increased binding to geldanamycin from yeast lysate. This finding is also in agreement with 17AAG-induced apoptosis assay in PC3 and HELA cells in which numbers of apoptotic cells is elevated when treated in addition with Wee1 kinase inhibitor. Given the fact that affinity to geldanamycin of purified wild type and non-phosphorylatable Hsp90 are comparable, these observations strongly indicate that phosphorylation status at this Tyr24/Tyr38 only mediates binding to geldanamycin indirectly via another layer of regulation inside cellular environment - which may be binding partners to Hsp90 in this particular phosphorylated form or even another modification primed by this phosphorylation on Hsp90 itself.

Thr-90 (human Hsp90α) (Wang et al. 2009; Wang et al. 2012)

Thr-90 phosphorylation was systematically investigated by work of Wang *et al.*, in which they presented evidence that protein kinase A (PKA) specifically phosphorylates Hsp90α at this site. This phosphorylation is significantly elevated in proliferating cells as compared with that in starved conditions in HELA cells that transiently overexpressed PKA. More importantly, this phosphorylation event was shown to regulate Hsp90α secretion and

subsequently, promote tumor invasiveness in MCF-7 cells. It's noteworthy that PKA, also known as cAMP-dependent protein kinase, has been implicated in a wide range of cellular processes and specially regulates cell proliferation in response to growth factors and/or nutrients. These results highlighted Thr-90 phosphorylation as a promising candidate for tumor progression diagnostic marker.

Ser231 and Ser263(human Hsp90α) or Ser225 and Ser255 (human Hsp90β)

(Dougherty et al. 1987; S P Lees-Miller & Anderson 1989; Ogiso et al. 2004; Degiorgis et al. 2005; Molina et al. 2007; Han et al. 2008; Dephoure et al. 2008; Kurokawa et al. 2008; Old et al. 2009; Xia et al. 2009; Woo et al. 2009; Iliuk et al. 2010; Bennetzen et al. 2010; Olsen et al. 2010; Herskowitz et al. 2011; Zhao et al. 2011; Hsu et al. 2011; Phanstiel et al. 2012; Weber et al. 2012; Kettenbach et al. 2013; Shiromizu et al. 2013; Zhou et al. 2013)

These are probably the two most common phosphorylation sites of Hsp90 which were detected in numerous proteomics (Degiorgis et al. 2005; Molina et al. 2007; Han et al. 2008; Dephoure et al. 2008; Old et al. 2009; Xia et al. 2009; Olsen et al. 2010; Iliuk et al. 2010; Hsu et al. 2011; Zhao et al. 2011; Herskowitz et al. 2011; Phanstiel et al. 2012; Weber et al. 2012; Kettenbach et al. 2013; Zhou et al. 2013; Shiromizu et al. 2013) and biochemical studies (Susan P Lees-Miller & Anderson 1989; Ogiso et al. 2004; Kurokawa et al. 2008; Woo et al. 2009). First identified in HELA cell extracts in 1989 for both Hsp90 isoforms (S P Lees-Miller & Anderson 1989), these serine phosphorylations could be confirmed by an *in-vitro* phosphorylation assay using CK2 from HELA cells, calf thymus or rabbit reticulocytes. Although Hsp90 is highly phosphorylated, Lees-Miller *et al* only determined 1.7mol phosphate per mole purified Hsp90 from HELA cells (which may be due to limited techniques at the time) which were corresponding to these two serine sites, indicating their high abundance or even constitutive phosphorylation status in cellular Hsp90 population.

Ser231 and Ser263 (human hsp90α) are two conserved residues in the Hsp90 charged linker region, which has not been resolved by crystallography and is thought to be flexible and largely unstructured. More importantly, this region is implicated to be critical in modulating Hsp90 (Tsutsumi et al. 2009; Hainzl et al. 2009). These two conserved serines on both human Hsp90 isoforms are followed by positive-charged residues which matches well to the recognition motif of CK2 and indeed, they are phosphorylated by this ubiquitous and constitutive kinase at least *in vitro* (S P Lees-Miller & Anderson 1989). However, CK2 also phosphorylates many other sites on Hsp90 proteins (Mollapour, Tsutsumi, et al. 2011; Mollapour, S. Tsutsumi, Kim, et al. 2011) and Ser263 on Hsp90α is also reported to be phosphorylated by another kinase (B-Raf) in rat mesangial cells (Old et al. 2009). So it is not clear yet whether CK2 is the relevant and only kinase *in vivo* that phosphorylates these sites in certain cell types or in redundance with B-Raf .

Up to now, several other studies detected this phosphorylated form of Hsp90s associated with Hsp90 client proteins such as aryl hydrocarbon receptor (AhR)(Ogiso et al. 2004), apoptotic peptidase activating factor 1 (Apaf-1)(Kurokawa et al. 2008), telomerase (Woo et al. 2009), etc. Effects of these phosphorylations are quite diversed and seem to be client-dependent.

Work by Ogiso *et al.* has demonstrated that in purified AhR complexes from cell extracts, Hsp90β was phosphorylated in both these serines while in Hsp90α, only Ser231. Mutation of Ser 226 and 255 to alanine, which cannot be phosphorylated, increased Hsp90 binding to AhR, whereas mutation to glutamic acid, which mimics phosphorylated Ser did not affect binding as compared with wild type protein in IP assay. AhR was also more active when coexpressed with the Ser 226/255Ala Hsp90β mutant. These data are consistent with a model in which phosphorylated Hsp90 interacts more weakly with client proteins, whereas unphosphorylated Hsp90 interacts more strongly. However, although important, it is likely that phosphorylation of Ser 226/255 is not the sole determinant of AhR association with Hsp90 because both residues were phosphorylated also in free (AhR-unbound) Hsp90 (Ogiso et al. 2004).

Surprisingly, although these serine phosphorylation seems to be abundant and very likely even constitutive in many cell types including cancer cell types such as HELA (S P

Lees-Miller & Anderson 1989), hepatocellular carcinoma (Han et al. 2008), melanoma (Old et al. 2009), invasive breast cancer MDA-MB-231 (Iliuk et al. 2010), etc, they were absent in Ba/F3 leukemia cells (Kurokawa et al. 2008). Hypophosphorylated Hsp90β bound strongly to Apaf-1, preventing cytochrome c-induced Apaf-1 oligomerization and caspase-9 recruitment while phosphorylated Hsp90β interacted weakly with the apoptosome in untransformed cells. Expression of mutant Hsp90β (S226A/S255A), which mimics the hypophosphorylated form in leukemic cells, conferred resistance to cytochrome c-induced apoptosome activation in normal cells, confirmed that phosphorylation of these residues on Hsp90β is linked to inhibition of apoptosome function. Moreover, inhibition of Hsp90b phosphorylation triggers some degree of chemoresistance in the leukemic cells, potentially because of apoptosome inhibition whereas expression of Hsp90b (S226A/S255A) *per se* is not sufficient to transform normal Ba/F3 cells or primary mouse hematopoietic cells suggesting that additional oncogenic signaling is necessary to drive tumorigenesis.

In this work (Kurokawa et al. 2008), the authors also reported that suppression of these abundant or constitutive phosphorylations of Hsp90β is mediated by leukemogenic tyrosine kinases Bcr-Abl, FLT3/D835Y and Tel-PDGFR although the detailed molecular mechanism is not yet uncovered. It could very likely be that these leukemogenic tyrosine kinases upregulate an Hsp90-directed phosphatase(s) or downregulate a kinase(s) targeting these sites. It is also interesting to note that little binding of the Hsp90α isoform to Apaf-1 was observed, indicating an isoform functional division.

The model in which unphosphorylated Hsp90 have stronger interactions with client proteins than phosphorylated protein and thus, chaperone those clients better is once again challenged in the case of telomerase, as reported in a study of (Woo et al. 2009). The authors have shown that full-length p23 enhances Hsp90 phosphorylation by facilitating interactions of the chaperone with CK2 and results in increased telomerase activity. In contrast, a capase-truncated p23 form supports binding of the phosphatase PP5 to Hsp90 or prevents PP5's dissociation from Hsp90 which boost dephosphorylation of the chaperone. The dephosphorylated Hsp90, in turn, negatively affects telomerase activity. The site-specific influences were confirmed by introducing phosphorylation-defective (S231A/ S263A) and phosphomimetic (S231E/S263E) constructs of human Hsp90α into HELA cells. The double mutant S231A/S263A displayed decreased Hsp90 serine phosphorylation, indicating that these residues are authentic targets for phosphorylation and more importantly, did not support telomerase activity; whereas the S231E/S263E phospho-mimetic mutant enhanced telomerase activity to an extent similar to that of the wild-type protein.

Tyr301 (human Hsp90β) (Duval et al. 2007; Kettenbach et al. 2013)

A study of Duval *et al* in 2007 characterized another tyrosine phosphorylation site of human Hsp90β, Tyr301, which has been detected recently in another proteomics report in 2013 (Kettenbach et al. 2013). Duval and coworkers have demonstrated that Vascular endothelial growth factor receptor 2 (VEGFR-2)–bound Hsp90β is phosphorylated in response to VEGF stimulation in a c-src–dependent manner on this tyrosine residue and that this event is necessary for VEGF-induced eNOS association to Hsp90 resulting in stimulated NO production. Tyrosine phosphorylation of Hsp90β is an early event in VEGF-mediated signal transduction in endothelial cells: It is increased after VEGF stimulation of endothelial cells and is present only when internalization of the VEGF -2 is allowed.

The Tyr-301 residue of Hsp90β is located at the beginning of the middle domain of Hsp90 which is implicated in client binding (Hawle et al. 2006a; Karagöz et al. 2014), and this region has previously been shown to mediate the interaction of Hsp90 with eNOS and Akt (Fontana 2002; Sato et al. 2000). In addition, this tyrosine residue is extremely conserved from yeast to human, supporting for the possibility that phosphorylation at this site may govern a wide variety of functions in multiple organisms.

Thr725 and Ser726 (human Hsp90α) or Ser718 (human Hsp90β) (Muller et al. 2012; Dephoure et al. 2008; Phanstiel et al. 2012)

Other interesting phosphorylation sites on human Hsp90α and β are at the extreme C-termini of the proteins, in proximity of the MEEVD motif which is the binding site

for TPR cochaperones. They were already detected in proteomics papers earlier (Dephoure et al. 2008; Phanstiel et al. 2012) but only recently characterized by Muller *et al*. The series of acidic residues in MEEVD motif makes this region perfectly match to CK2's recognition pattern. Nevertheless, in an *in vitro* assay using peptides, not only CK2, but CK1 and GSK3b kinases also could phosphorylate these sites. Given their specific positions, as expected, these phosphorylations have strong effects on the interactions between Hsp90 and TPR cochaperones such as CHIP and HOP. Both data result from an enzyme-linked immunosorbent assay and fluorescence polarization consistently showed that non-phosphorylated C-terminal peptides of Hsp90 interact more strongly with CHIP than the phosphorylated forms of these peptides. In contrast, HOP binds more strongly to the phosphorylated peptide of Hsp90α. These findings were once again confirmed in IP experiments from HEK293 cells using wild-type or phospho-mutants (phosphomimetic and nonphosphorylatable variants) of both Hsp90 isoforms. More significantly, the authors demonstrated that primary human cancer cells contain high levels of phosphorylated Hsp90s and show increased levels of HOP protein (Muller et al. 2012).

It is known that Hsp90 do not only chaperone client protein for maintenance, maturation or activation but also extend to regulate degradation of unfolded clients. In this protein triage decision to maintain protein homeostasis, the fate of client proteins is not decided solely by Hsp90 but rather by a concerted cooperation of Hsp70, Hsp90 and the specific adaptors HOP or CHIP. While HOP is important in coordination between Hsp70 and Hsp90 for protein folding, the E3-Ubiquitin Ligase CHIP targets Hsp90 client for ubiquitination and degradation (Chang et al. 1997; Chen & Smith 1998; Murata et al. 2001; Xu et al. 2002; Hernández et al. 2002; Song & Masison 2006; Stankiewicz et al. 2010; Lindquist et al. 2010). These data identify C-terminal phosphorylation of Hsp90 as a switch for regulating co-chaperone binding and indicate that cancer cells possess an elevated protein folding environment by the combination of co-chaperone expression and chaperone modifications.

Additionally, looking at the phosphorylation aspect of Hsp90 in a broader view, given that Hsp90 proteins are heavily phosphorylated, it is comprehensible to hypothesize that different phosphorylation events could happen in a sequential order and in combination during Hsp90 cycle. However, only recently a few studies addressed the phosphorylation events of Hsp90 from this angle.

A global approach by Buchner and colleagues provided evidence for regulation of Hsp90 by a series of phosphorylation sites (Soroka et al. 2012). Using a yeast strain deleted for Ppt1, which encodes a serine/threonine phosphatase, the yeast homolog of PP5, and SILAC (Stable isotope labeling with amino acid in cell culture), they identified 10 phosphorylation sites in middle domain and dimerization domain of Hsp82/Hsc82. In general, using all-A or all-E mutants that mimics either non-phosphorylatable or phosphoylated status of all corresponding sites, the authors could show that phosphorylation decelerates the Hsp90 machinery, reduces chaperone function *in vivo*, sensitizes yeast cells to Hsp90 inhibition and affects DNA repair processes.

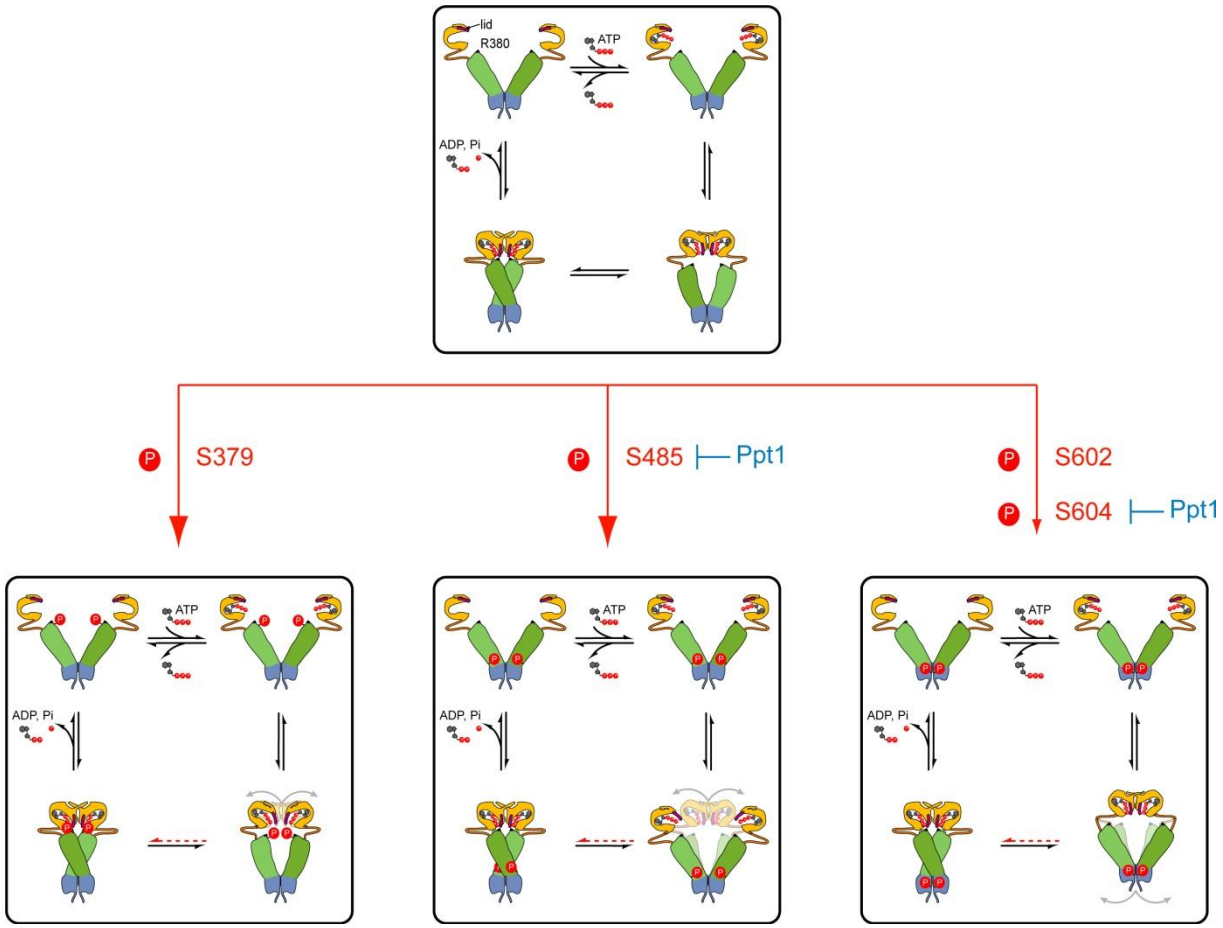

FIGURE 1-7: PROPOSED MECHANISM OF HSP90 PHOSPHO-REGULATION.

Four phosphorylation sites influences the conformational dynamics of Hsp90 by employing different mechanisms. Phosphorylation at S379, located right next to ATPase catalytic-critical residues, interferes directly with structural rearrangements within the catalytic region. Modification at S485 which is positioned in the hinge region between middle domain and C-terminal domain modulates conformational flexibility within dimeric Hsp90. Phosphorylation of S602 and S604 in the C-terminal domain impairs intersubunit communication required for activation of ATP hydrolysis that can be induced by Aha1 (Soroka et al. 2012).

Particularly, among these sites, four serine phosphorylation sites (S379, S485, S602 and S604) were proven to influence several aspect of the conformational cycle of Hsp90. Individually, they share the common property of decreasing the ATPase activity of the chaperone and the first two serines phosphorylation in the middle domain also impair general chaperone activity of Hsp90. These properties are not surprising for modification at S379 in the middle domain because this site is situated in the catalytic loop next to R380, a key residue required for ATP hydrolysis, and therefore, it is very likely that modification at the adjacent S379 disrupts the essential interactions within the catalytic region. The second active phospho-site, S485, is positioned at the lower part of middle domain, close to the junction with the C-terminal domain. Phosphorylation at S485 not only interferes with the ATP hydrolysis cycle but also the association with co-chaperones by reducing the conformational flexibility of Hsp90. Modifications at S602/S604 in the dimerization domain are dispensable for yeast viability and activation of specific set of client, nevertheless, still impairs both basal ATPase activity and activation by Aha1. The binding of the phosphomimetic mutants at these sites to Aha1 as characterized in analytical ultracentrifugation also indicates that phosphorylation at S602 and S604 interferes with cochaperone-induced structural rearrangements across subunits. The mechanistic analyses of the active phospho-sites showed that each site has a unique mode of action, including an influence on the formation of the catalytic site, the conformational flexibility of the protein

and intersubunit communication (Figure 1-7). They can be seen as switch points for the conformational communication within distant domains of Hsp90.

Another profound investigation by Neckers and colleagues on the Hsp90 and Cdc37-mediated chaperone cycle for protein kinase clients set light on a series of important tyrosine phosphorylation events (Xu et al. 2012) (Figure 1-8). In fact, the posttranslational modification status of both Hsp90 and Cdc37 enables the cycle to proceed unidirectionally.

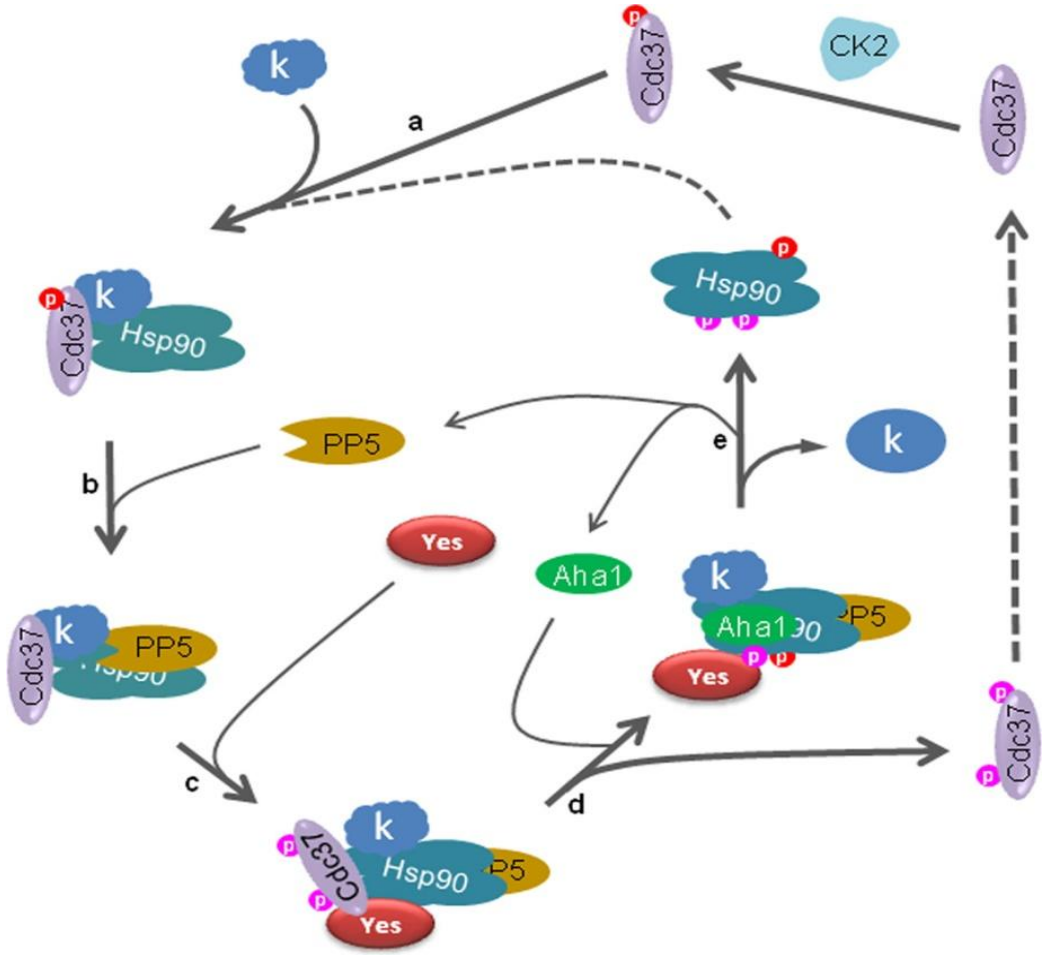

FIGURE 1-8: PROPOSED MODEL FOR THE SEQUENTIAL TYROSINE PHOSPHORYLATION EVENTS THAT DRIVE THE HSP90 AND CDC37-MEDIATED CHAPERONE CYCLE FOR PROTEIN KINASE CLIENTS

The cycle starts with (a) the Ck2-phosphorylated Cdc37 interacting with protein kinase (k) client and bringing it to Hsp90. The co-existence of Cdc37 and PP5 in the Hsp90-client complex as shown in (b) allows dephosphorylation of Cdc37 and prepares for other phosphorylation events on Cdc37 that reduces binding between Cdc37 and protein kinase (c). Y197 on Hsp90 further disrupts interaction between Hsp90 and Cdc37 leading to dissociation of the cochaperone from the complex while another phosphorylation Y313 promotes binding of Aha1 to Hsp90 (d). Aha1 accelerates the chaperone cycle of Hsp90 resulting in release of the protein kinase client and Aha1 in turn also dissociates from the Y627-phosphorylated Hsp90 (e). Cdc37 and Hsp90 then both can be dephosphorylated to enter a new cycle (Xu et al. 2012).

S13-phosphorylated Cdc37 binds to a protein kinase client of Hsp90 and both interact with Hsp90 forming a ternary complex. The additional association of this complex with PP5 phosphatase allows dephosphorylation of Cdc37 at S13 and priming for access of Yes kinase, which results in Y4 and/or Y298-phosphorylated Cdc37. This phosphorylation form of Cdc37 has weaker interaction with kinase clients (individual clients are affected to different degrees by phosphorylation at either one or both tyrosines). Interestingly, this modification does not disturb association with Hsp90. Nevertheless, Cdc37-bound Hsp90 is so restrained in its conformation that it cannot advance to other conformations that are

required for ATP hydrolysis, i.e. dissociation of Cdc37 is essential for the chaperone cycle to procceed. It would be even more beneficial if dissociation of Cdc37 could in the meantime facilitate association of other cochaperones that are critical for later steps in the chaperone cycle such as Aha1 or p23. Such coupled-effect should be mediated via modification on the main player, Hsp90 itself. Indeed, further phosphorylation of Hsp90 on Y197 (possibly by Yes kinase but not limited to it) promotes dissociation of Cdc37 from the chaperone complex, while Hsp90 phosphorylation on Y313 induces conformational changes favoring recruitment of Aha1, which stimulates Hsp90's ATPase activity and drives maturation of the client kinase. Finally, Hsp90 phosphorylation on Y627 leads to dissociation of Aha1, PP5, and client kinase to complete the cycle. Assumingly, dephosphorylation of both Hsp90 and Cdc37 later would then enable them to enter a new cycle.

Post-translational modifications of Hsp90 certainly have added another layer of regulation to the complexity of Hsp90 system. The enrichment of PTMs of Hsp90 in metazoans as compared to that in prokaryotes and single cell eukaryote indicates that through evolution, in these multi-cellular species, Hsp90 has gained more clients and/or had to adapt with more diverse conditions which require additional fine-tuning of the system. Therefore, understanding the influences of individual post-translational modifications as well as the simultaneous or sequential combination among them will undoubtedly be highly rewarding as they complement our knowledge of the multilayered system that eukaryotes in general and human cells in particular have developed to precisely control Hsp90 functions.

1.2.5 TUMOR SELECTIVITY OF HSP90 INHIBITORS

The most particular characteristics of Hsp90 as a molecular cheprone is its client set comprising more than 200 proteins (Pearl & Prodromou 2006), many of which are key components for the formation, growth and survival of cancer cells (Xu & Neckers 2007). This client set renders Hsp90 a promising target for cancer treatment since inhibiting Hsp90 should affect several essential regulatory circuits in cancer cells at once. Initially, Hsp90 was not considered a suitable target since this molecular chaperone is essential in all eukaryotic cells tested. Nevertheless, it was shown by several studies that tumor, but not normal cells, accumulate Hsp90 inhibitors and are much more sensitive to those compounds (Whitesell et al. 1992; Nguyen et al. 2001; Solit et al. 2002; Chiosis & Neckers 2006; Breinig et al. 2009). These observations on the tumor selectivity of Hsp90 inhibitors had encouraged the entrance of two GA analogues (17-AAG and 17-DMAG) into clinical trial and several other screening or synthesis for new small molecule that inhibits Hsp90 specifically. However, the molecular mechanism of this tumor selectivity remains elusive.

In vitro, using different approaches, several research groups have reported different aspects and even contradictory results on Hsp90-inhibitors affinity and sensitivity (Kamal et al. 2003; Llauger-Bufi et al. 2003; Gooljarsingh et al. 2006). Using co-IP and competitive binding assays, Kamal *et al*. have measured an approximately 100-fold higher binding affinity of 17-AAG to tumor cell derived Hsp90 as compared to Hsp90 from normal cells. They also detected that in tumor cells, unlike in normal cells, almost the entire Hsp90 population is in complex with cochaperones. *In vitro* reconstituted Hsp90 complexes also exhibit higher ATPase activity, suggesting that they are in an active form. From these findings, Kamal *et al*. has proposed that due to its more-than-normal busy roles in cancer cells, a bigger fraction of Hsp90 proteins is in complexes in an activated, high-affinity conformation (Kamal et al. 2003). However, these results have been challenged by Llauger-Bufi *et al.* and Gooljarsingh *et al.* who reported the same high affinity for purified recombinant human Hsp90 (Llauger-Bufi et al. 2003; Gooljarsingh et al. 2006).

Despite different binding affinities determined for Hsp90-inhibitor complexes *in vitro*, the tumor selectivity of the inhibitors *in vivo* for both cell culture and animal xenograft models is found to be consistent in many studies by assessing cell viability, oncoproteins'

degradation, accumulation etc (Whitesell et al. 1992; Nguyen et al. 2001; Solit et al. 2002; Eiseman et al. 2005; Biamonte et al. 2006; He et al. 2006; Breinig et al. 2009) (Figure 1-9).

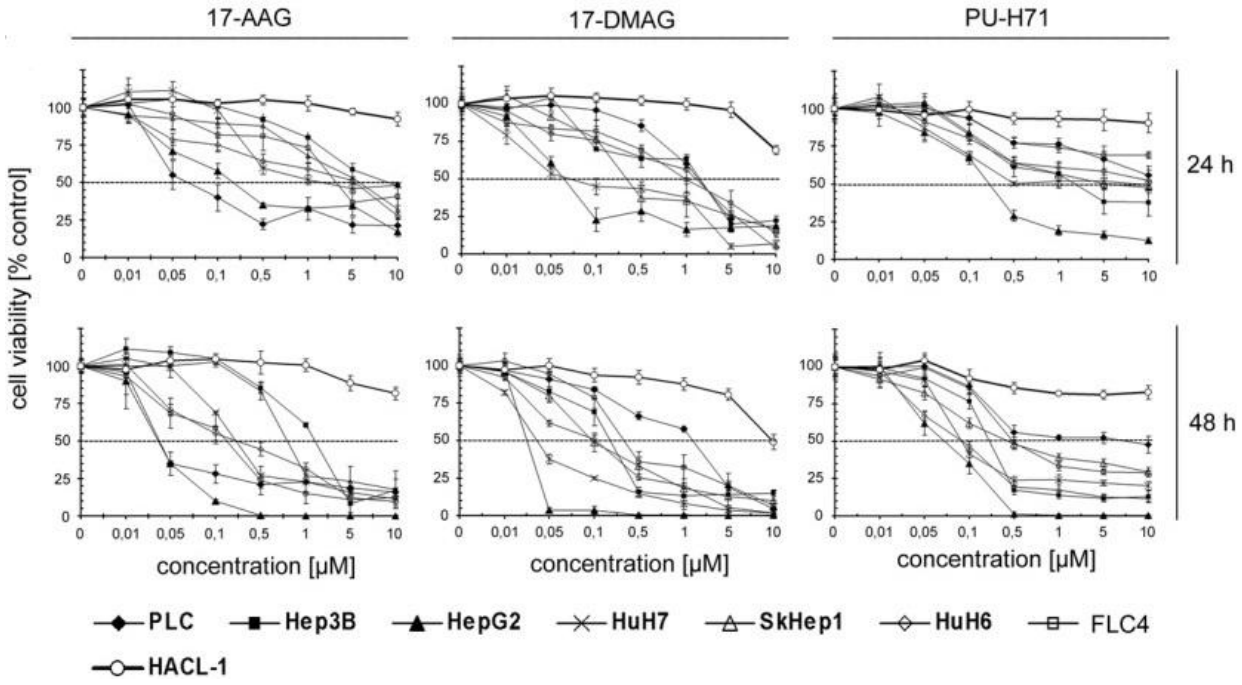

FIGURE 1-9: HSP90 INHIBITION REDUCES HEPATOCELLULAR CARCINOMA (HCC) CELL GROWTH

HCC cell lines and the nontumorigenic hepatocyte cell line HACL-1 were treated with increasing concentrations of Hsp90 inhibitors, and cell viability was analyzed after 24 and 48 hours with MTT assays to assess cell viability. Assays were performed in sextuplicate, and data are expressed as the mean ± standard deviation (n >=3) (Breinig et al. 2009).

Therefore, identification and characterization of tumor-specific properties responsible for the tumor selectivity of Hsp90 inhibitors can contribute significantly to our understanding of the molecular mechanism of Hsp90 and the development of advanced anticancer drugs that specifically target to the most prevalent form of Hsp90 in cancer cells.

1.3 DETECTION OF PHOSPHORYLATION MODIFICATIONS BY MASS SPECTROMETRY (MS)

Direct analysis of modifications requires isolation of the correctly processed protein in a sufficiently large amount for biochemical study - a feat that has only been possible in very few cases. The introduction of MS methods has offered an opportunity to detect PTMs in general and phosphorylation in particular with high sensitivity and resolution. MS measures mass-to-charge ratio (m/z), yielding the molecular weight and the fragmentation pattern of peptides derived from proteins. It therefore can be applied as a general method for all modifications that change the molecular weight.

1.3.1 STANDARD TANDEM MASS SPECTROMETRY (MS/MS) ANALYSIS

A standard workflow for the identification of PTM include the following steps: isolation or purification of the protein of interest; enzymatically digestion, normally by trypsin; separation of the digestion products by liquid chromatography (LC); analysis of the eluting peptides by tandem mass spectrometry (MS/MS); and data evaluation by a database search engine. In these MS/MS experiments, peptide ions (precursor ions) are isolated in a first stage of the mass spectrometer and then activated by collision with inert gas leading to fragmentation, usually at the peptide bonds. The fragmentation pattern of PTM containing

peptides is similar to that of the unmodified peptide with the mass difference of precursor ion and differences at those fragments that contain the modified amino acid, if the modified amino acid remains inact during the fragmentation process. These differences are their mass increment and thus, ideally the peptide sequence, the mass and location of the modification can be determined.

In practice, there are several inherent difficulties for the analysis of phospho-proteins. Even though MS proteomics has been very successful in identifying proteins in complex samples, these investigations typically mapped only a few peptides per protein, which is sufficient for identification but not for the determination of PTMs across the full-length sequence of a protein. First of all, obtaining full-sequence coverage for the unmodified protein already demands much more material than mere identification of it by MS sequencing. Moreover, protein modifications are typically not homogeneous and the possible combinations of different modification types on a certain protein are simply too large. The amount of protein in a single modification state can thus be a very small fraction in the total amount of the target protein. For these reasons, a central consideration in the characterization of global modifications of a specific protein is the need for as large an amount of the protein as possible. A general recommendation for PTM study is to start with amounts in the microgram range. A number of enrichment strategies in order to increase the relative abundance of the phosphopeptides or proteins of interest to that of unmodified counterparts has been developed, including immobilized metal affinity chromatography (IMAC), phospho-specific antibody enrichment, beta-elimination of phospho-serine and –threonine and replacement of phosphate group by biotinylated moieties, etc.

In most of the cases, the protein of interest is enzymatically digested into peptide level and the peptides are further fragmented by MS/MS. Even though the starting amount of peptides from a given protein is the same, it results very often in very different signal intensities for each of these peptides detected in MS. Thus, some of the peptides will be clearly visible and others not at all. This is particularly the case for complex samples and for modified peptides that often do not ionize as well as unmodified peptides. To avoid signal suppression which is commonly observed when highly complex peptide mixtures are injected into the mass spectrometer, peptides are typically separated before injection by reversed-phase chromatography to gain subsequent fractionation. Even so, it does not necessarily result in complete sequence coverage because it is still limited by the binding to the reversed phase column or by the optimal m/z range that most mass spectrometers can detect. For example, very short peptides of only a few amino acids or very long peptides of >30 amino acids are often not detected. This limitation can be alleviated by a combination of enzymatic digestion using enzymes with different specificity. The first choice of enzyme is usually trypsin, which cleaves C-terminal to arginine and lysine, therefore resulting in peptides with basic amino acids at the C terminus, which are most easily sequenced by MS. A second enzyme can then be endoproteinase Asp-N or Glu-C, which are also very specific. A example of such combinational approach was reported in work of Mohammed *et al* in which the authors have employed 4 proteases to reach 88% sequence coverage and identified novel phosphorylation sites of component proteins from purified yeast RNA polymerase II and III (Mohammed et al. 2008).

However, there is still no assurance that every part of the protein is covered and even if that were the case, a minor, modified form of a peptide may still escape detection. One possible reason is the lability of the modification itself: it can be lost even before the peptide itself fragments. The phosphogroup (+80 Da) can be stable (in the case of phospho-Tyrosine) or relatively labile (in the case of phospho-Threonine and especially phospho-Serine). It is still possible, however, to detect these modifications using "neutral loss scanning" for the loss of a phosphate moiety (98Da (H_3PO_4)) from the parent ion and "precursor-ion scanning" either for an ion at m/z 79 (PO_3^-) in negative ion mode for Ser/Thr phosphorylation or an ion at m/z 216.043 for Tyr phosphorylation in positive ion mode (Figure 1-10) (Mann & Jensen 2003).

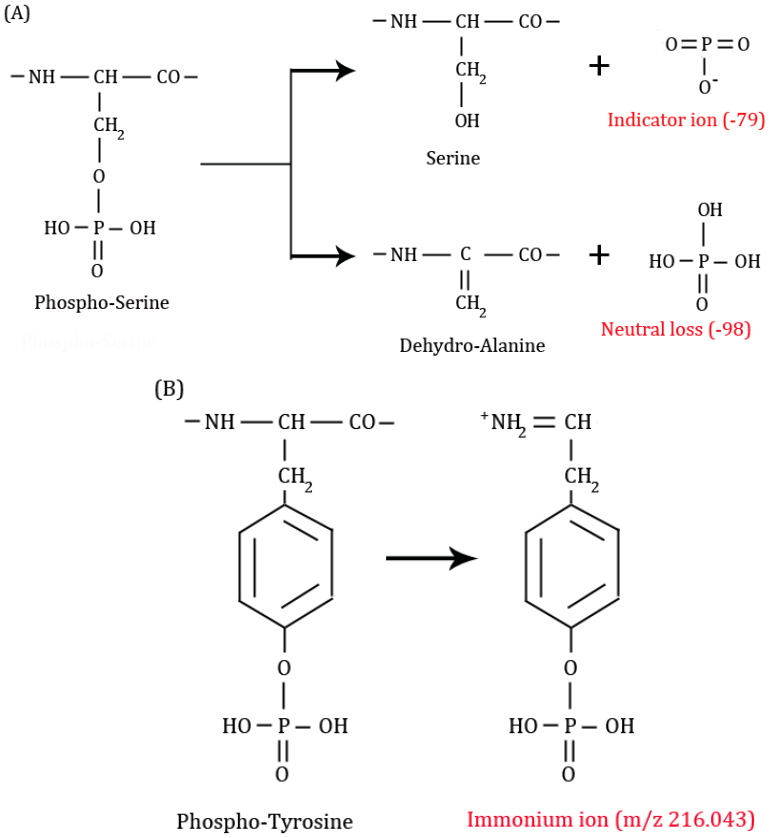

FIGURE 1-10: THE GENERATION OF NEUTRAL LOSS OR PRECURSOR IONS FROM PHOSPHORYLATED RESIDUES

In (A): phospho-Serine with neutral loss (H_3PO_4 (-98)) or generation of an indicator ion (PO_3^- (-79)) (similar for phospho-Threonine).
In (B): The phospho-Tyrosine immonium ion is generated by a combination of a- and y-type cleavage of a phospho-Tyrosine containing peptide, producing a diagnostic immonium ion having m/z 216.

Another risk that could cause the failure of detection of post-translational modifications happens in the final step: the database search. The experimentally determined peptide masses are matched against the list of peptide masses expected from the protein sequence. The nonmatching masses can arise as a result of contaminating proteins, unexpected or incomplete cleavage, or common chemical modifications (e.g., methionine oxidation). The remaining masses are inspected for mass differences compared with the expected peptides that correspond to a modification. On the one hand, one would like to include all the parameters as flexible as possible so that every detected precursor m/z and MS/MS spectra peaks can be assigned; on the other hand, the combination of all possible parameters, as mentioned, would significantly increases the false positive rate and duration of database search, some even to a degree that is technically limited. The correct selection of parameters for database search to tolerate best for both extremes is therefore critical.

1.3.2 MULTIPLE REACTION MONITORING MASS SPECTROMETRY (MRM-MS)

As mentioned, the identification of global phosphorylation status of a protein remains technically challenging due to both the low occurrence of these phosphopeptides and their intrinsic physicochemical nature, resulting in generally poor ionization and detection using standard MS techniques. Any step of isolation and enrichment prior to MS analysis may accidentally lead to counter-selection for the target modification. A better approach, obviously, is a direct selection based on pre-existing knowledge about the modifications of interest; nevertheless, it should involve as few processing steps prior to MS as possible. A relatively new MS approach, which meets such requirements, is named Multiple Reaction Monitoring (MRM) MS (also known as Selected Reaction Monitoring (SRM)).

Introduction

MRM exploits the unique capabilities of triple quadrupole (QQQ) MS for quantitative analysis. In MRM, the mass-resolving Q1 isolates the precursor, Q2 acts as a collision cell, and mass-resolving Q3 brings selected fragmented ions from the precursor to the detector (Figure 1-11). A precursor/product pair is often referred to as a transition. Several such transitions (precursor/fragment ion pairs) are monitored during the elution of the sample from the reversed-phase LC, yielding a set of chromatographic traces with the retention time and signal intensity for a specific transition as coordinates. The two levels of mass selection with narrow mass windows result in a high selectivity, as co-eluting background ions are filtered out very effectively. Unlike in other MS-based proteomic techniques, no full mass spectra are recorded in QQQ-based SRM analysis. The non-scanning nature of this mode of operation translates into an increased sensitivity by one or two orders of magnitude compared with conventional "full scan" techniques. In addition, it results in a linear response over a wide dynamic range up to five orders of magnitude. This enables the detection of low-abundance proteins in highly complex mixtures, which is crucial for systematic quantitative studies.

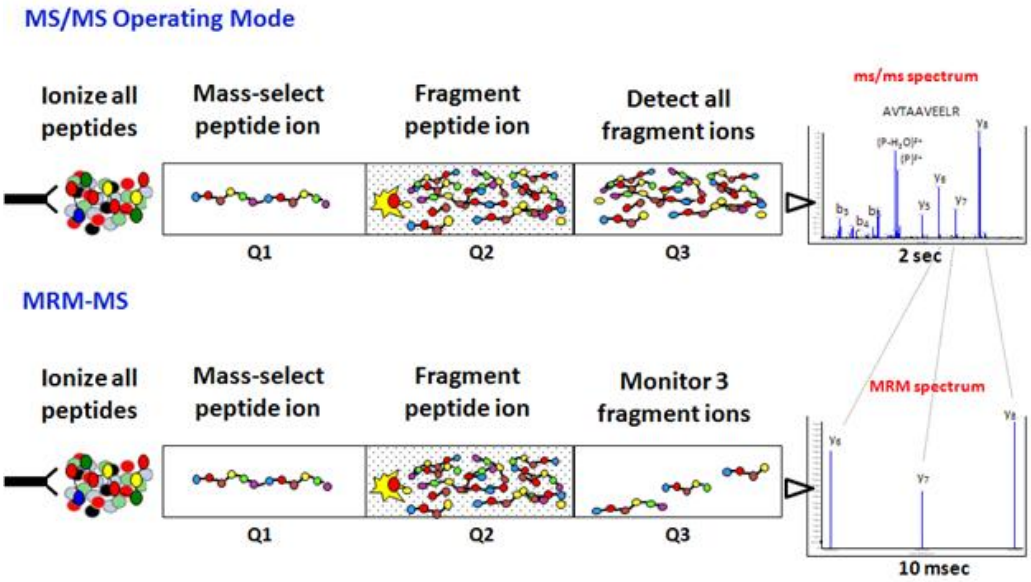

FIGURE 1-11: MASS SPECTROMETRY IN MS/MS OPERATING MODE AS COMPARED WITH MULTIPLE REACTION MONITORING (MRM) MODE.
(HTTP://WWW.BROADINSTITUTE.ORG/SCIENTIFIC-COMMUNITY/SCIENCE/PLATFORMS/PROTEOMICS/MRM-MULTIPLE-REACTION-MONITORING)

MRM is an information-dependent method, specially designed to analyze a single target protein rather than a general phosphorylation screening tool. MRM measurements are quantitative analyses that are strictly targeted to a predetermined set of peptides and depend on specific transitions for each selected peptide. Therefore, prior knowledge about the protein of interest is required to define those transitions. First, for each targeted protein, those peptides that present good MS responses and uniquely identify the targeted protein, or a specific isoform thereof, have to be identified. This can be achieved by manual calculation, available software or characterization from digestion mixture of purified proteins and synthetic peptides. Recently, a proteomic database called ProteomicsDB has been made available at https://www.proteomicsdb.org/ which assembled 92% of the human proteome using data from thousands of LC MS/MS experiments. A Windows appplication called Skyline (MacCoss Lab) also uses MS/MS spectral libraries to predict and choose suitable precursor ions to establish MRM methods. Such databases and programs provide enormous amount of information and a very convenient interface for the design and interpretation of MRM experiments that can be used initially for this step. Second, for each of those peptides, those

fragment ions that provide optimal signal intensity and discriminate the targeted peptide from other species present in the sample have to be determined. These optimized transitions are the essence of an MRM assay as they provide enough specificity to allow confident identification and quantification of targeted protein in complex samples. The time and effort required to establish these conditions is the price to pay for the excellent quantitative performance of MRM-based experiments. However, once established, such assays can be used indefinitely in any study that involves the particular targeted protein, for e.g., a study across several cell lines.

MRM applications in phosphorylation quantification analysis, on the one hand, are very promising since many biological effects are often due to changes in the level of modification rather than the total presence or absence of it. On the other hand, they are further limited by the fact that the precursor ion must contain the corresponding modified residue of interest regardless of whether such a peptide has good MS responses (i.e. to be well-ionized, has optimal mass range, unique for the protein or isoform of interested, etc).

1.4 AIMS & APPROACH

We were interested in tumor selectivity of Hsp90 inhibitors and hypothesized that this difference in affinity for Hsp90 inhibitors is due to different post-translational modifications in the two cytosolic human Hsp90 proteins Hsp90α and Hsp90β in malignant vs non-malignant cells. Therefore, we planned to characterize post-translational modification patterns in these cytosolic Hsp90s from a range of malignant and non-malignant hepatocyte carcinoma (HCC) cell lines. Starting with phosphorylation – the most prevalent post-translational modifications in eukaryotic cells, we utilized Mass Spectrometry (MS) to perform a global and relatively quantitative analysis of phosphorylation status of Hsp90s from hepatocytes. Our goal was to detect major phosphorylation site(s) of cytosolic human Hsp90s that contribute to the strong preference effect on inhibitors binding. It is generally accepted in the field that human cytosolic Hsp90s exists in the cells with different conformations, presumably also different post-translational modification states. For that reason, first of all, to avoid distortion of the natural steady-state levels of phosphorylation in cells, we used phosphatase inhibitors only at the time point of extract preparation and not for some hours during culturing of the cells before harvest, as generally done in phosphoproteomics projects to enrich *in vivo* the phosphorylation abundance. Secondly, the divergent inhibitor-binding effect is very unlikely to originate from phosphorylation of a minor part but rather from the major portion of the human Hsp90 population. This specific aim led to another important difference in our subsequent approach as compared with general proteomics analysis: in our experiments, no selective phosphopeptide enrichment steps were included. We were therefore dependent on exhaustive identification of peptides and furthermore, would have to reach full sequence coverage to conclude on the phosphorylation map of Hsp90.

For this global and relatively quantitative analysis, I planned to isolate Hsp90 from cell lysates, digest by different proteases and finally analyze by MS/MS for Hsp90 identification and phosphorylation detection. I employed two strategies to isolate Hsp90 from cancer cells, (1) affinity chromatography using a biotinylated variant of the Hsp90 inhibitor geldanamycin and streptavidin coupled to magnetic beads (GA-beads), and (2) IP with a specific antibody. At the beginning, in-solution digestion was more preferred than in-gel digestion to avoid introducing artificial modifications and limitation of final elution volume. However, in later analyses, I used in-gel digestion to enhance sequence coverage.

In parallel, we planned to analyze selected known phosphorylation sites using MRM-MS (Unwin et al. 2005). MRM-MS approach allows to monitor peptides of interest (in our case, phospho-peptides) directly from cell lysate samples without any

isolation/enrichment step, ensuring that no bias is introduced prior to MS, and hence, suitable for quantitative analysis.

As mentioned briefly in the previous section, there have been several proteomics analyses in which phosphopeptides from cytosolic human Hsp90s were detected. Nevertheless, only a few phosphorylation variants have been characterized further by biochemical assays and were reported to be related to or responsible for specific effects on Hsp90 such as T36, Y38, T90 (of the α isoform) and Y301(of the β isoform) (Duval et al. 2007; Wang et al. 2009; Mollapour, Shinji Tsutsumi, et al. 2010; Mollapour, Tsutsumi, et al. 2011; Wang et al. 2012). In all cases, individual kinases responsible for the specific phosphorylation site were identified. They were important kinases that are intimately involved in processes leading to tumor development, for e.g. CK2 or PKA. Discussions in more details about each individual phosphorylation site have been mentioned previously (see section 1.2.4.3). Moreover, even though the influence of these sites on Hsp90 conformational and ATPase cycle has been characterized, none of the phosphorylation sites was studied for their natural cellular abundance. Based on these reasons, we selected them as targets to monitor in complex samples their degree of phosphorylation and whether their status correlates with tumor development conditions and drug binding feature of Hsp90 in cancer versus non-cancer cells (Table 2-4). Novel phosphorylation site(s) from our MS data should also be included.

The results from both MS approaches were considered for further characterization of novel and/or interesting phosphorylation site(s). For this section, I planned to utilize a range of *in vivo* and *in vitro* assays that have been established in the group, including the use of yeast as a model system and purified wild-type and phosphomutants Hsp90 proteins together with cofactors such as clients and cochaperones for interaction and activation experiments.

2 RESULTS & DISCUSSIONS

2.1 ANALYSIS OF PHOSPHORYLATION OF HUMAN HSP90 IN CANCER CELL LINES

2.1.1 ISOLATION OF HSP90 PROTEINS FROM CELL LYSATES

This part was initially planned to be performed by our partner in M. Kern's group, Pathology Institute of University Heidelberg. We started with the HCC cell line HepG2, which displayed the strongest response to Hsp90 inhibitors (Breinig et al. 2009). As the control for a non-tumorigenic human liver epithelial cell line, we had planned to use HACL-1. However, we encountered two problems.

First, the IP did not work with all the antibodies tested by our partner. We didn't get specific precipitation of Hsp90 as well as enough material for further analysis. So at the beginning, we only got Hsp90 proteins from pulldown experiments using biotinylated-GA.

Second, the control non-tumorigenic human liver epithelial cell line HACL-1 didn't grow well in culture, and hence, we could not get enough cells as well as Hsp90 proteins extracted from it in both isolation methods. We decided to use another HCC cell line, Snu182 instead of HACL-1. Snu182 displayed much less response to Hsp90 inhibitors as compared to HepG2 (unpublished data, personal communication of M. Breinig).

(A)

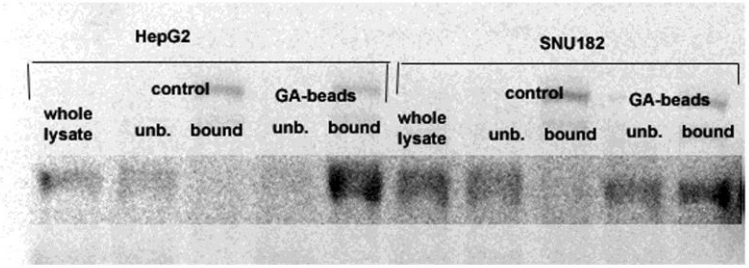

(B)

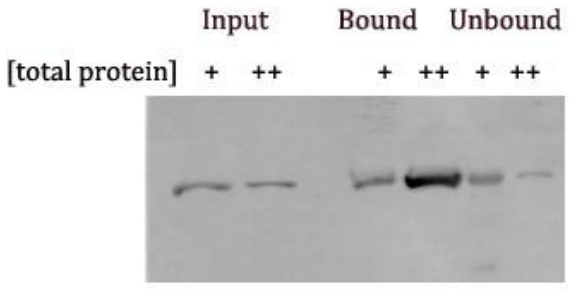

FIGURE 2-1: GA-BIOTIN PULL-DOWN OF HSP90 FROM CELL EXTRACTS.

Shown are Western blots against Hsp90 of different fractions from a GA-biotin pulldown assay of (A) HepG2 or Snu182 (data from cooperation partner, M. Breinig) or (B) HELA lysates. In (B), either 200µg (+) or 500 µg (++) of total lysate were used. A volume of the input material corresponding to 20 µg was loaded on the gel. In Bound and Unbound fractions, identical volumes were loaded for all samples.

In addition, I myself performed GA-biotin pulldown from HELA cells, a cervical cancer cell line, for MS analysis using a modified GA-pulldown protocol from M. Breinig. HELA cells were included in our analysis to compare the results with those from HepG2 and Snu182

so that liver-specific features could be distinguished from general cancer specific modifications.

From these three different cell lines: HepG2, Snu182 and HELA, Hsp90 proteins could be pulled-down using GA-Biotin beads (Figure 2-1). Moreover, using the same amount of GA-beads while increasing the total protein amount, I could isolate more Hsp90 proteins from HELA lysates without saturating the beads. I assumed that the population of Hsp90 bound on GA-beads should mainly contain the fraction of interest which has high affinity to the Hsp90 inhibitor GA.

Later, using an antibody specific for Hsp90α, I was also able to immunoprecipitate Hsp90 proteins from both HELA and HepG2 (Figure 2-2). Snu182 was not included due to discontinued supply from Pathology Institute. Unlike the case of GA-pulldown experiments, an elution step in the IP is mandatory to separate Hsp90 from IgG which stays bound on the beads so that I could use it in subsequent in-solution digestion. Of note, the elution step was not required in later analyses, in which I applied in-gel digestion prior to MS.

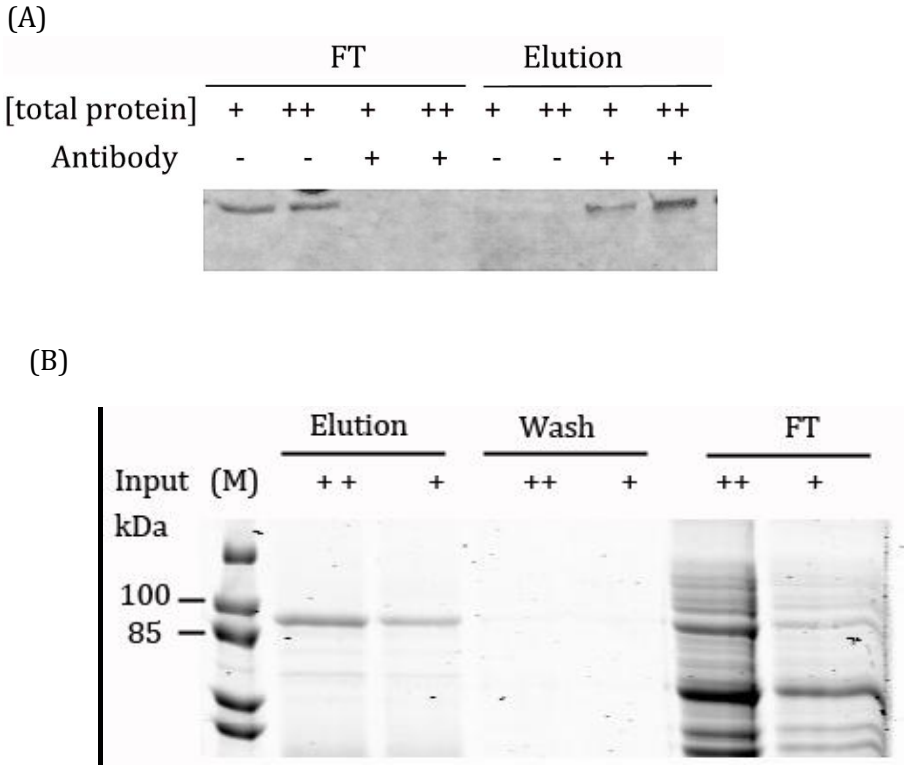

FIGURE 2-2: IMMUNOPRECIPITATION (IP) OF HSP90 FROM CELL EXTRACTS USING HSP90α-ANTIBODY (SPA-840).

Shown in (A) is a Western blot against Hsp90 of Flowthrough (FT) and Elution fraction from IP of HepG2. Either total protein amount of 50 µg (+) or 100 µg (++) was used; the larger sample was concentrated so that both samples had identical starting volume.

Shown in (B) is SDS-PAGE of Flowthrough (FT), Wash and Elution fractions from IP of HELA. Either total protein amount of 30 µg (+) or 60 µg (++) was used, the larger sample was concentrated so that both samples had identical starting volume.

In these IP, Hsp90 proteins in HELA and HepG2 extracts were successfully immunoprecipitated, suggesting that this antibody can effectively pull-down both isoforms or that the isoforms in cell extracts form heterodimers and thus, can be pulled-down using the antibody specific for Hsp90α.

To ensure that most of Hsp90 proteins in cell extracts were immunoprecipitated and I did not only analyze a fraction of Hsp90 (which may not be representative for overall cellular Hsp90), I also made several attempts to immunoprecipitate Hsp90 using antibodies against the β-isoform or Hsp90 in general (without specificity to either isoform). However,

the IP using these antibodies were in general much less efficient as can be shown in Figure 2-3 (elution fractions). Western blotting to evaluate IP efficiency showed that very little amount of both Hsp90 isoforms were detected in the elution fractions. Most of Hsp90 proteins seemed to stay unbound in the Flowthrough fractions or bound on protein A-beads. As stated previously, I could not use the Bead fraction for the subsequent in-solution digestion because the signal from IgG coupled on beads would dominate and interfere with the detection of Hsp90 proteins in the same fraction.

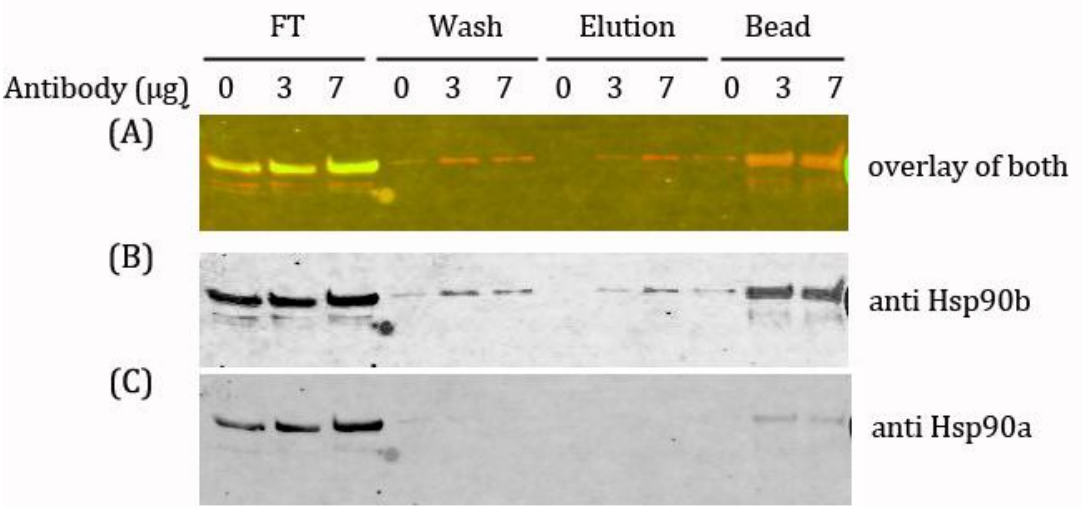

FIGURE 2-3: IMMUNOPRECIPITATION (IP) OF PURIFIED HSP90 (MIXTURE OF EQUAL AMOUNT OF BOTH ISOFORMS) USING HSP90β-ANTIBODY (CAYMAN-K41220A)

Western blots against Hsp90 of different fractions. (A): Overlay of Western blot against human Hsp90 both isoforms (In red: anti-human hsp90β; in green: anti- human Hsp90α); (B) & (C): Western blot against human hsp90 β and α, respectively.

In the end we decided to continue GA-pulldown and IP experiments with the α-specific antibody (SPA-840) for MS analysis.

2.1.2 GLOBAL MS ANALYSIS OF ISOLATED HSP90 FROM CELL LYSATES

2.1.2.1 DETECTION AND SEQUENCE COVERAGE OF HSP90 IN CELL LYSATES

MS analysis by the MaXis mass spectrometer

In these MaXis MS analyses, I received the HepG2/Snu182 GA-pulldown samples from our partner in the Pathology Institute and prepared similar pulldown experiments from HELA cells. The samples were digested using in-solution digestion protocol and subjected to the MaXis mass spectrometer. Due to limited sample amount, only in-solution digestion of the bead-bound fractions of GA pulldown by Trypsin were applied, and in a few batches, also by Glu-C or Asp-N.

In the pulldown experiments, we utilized biotinylated-GA and Streptavidin-beads to capture Hsp90 from lysates. The interaction of the biotin and streptavidin is the strongest noncovalent biological interaction known, which has a dissociation constant, Kd, in the order of 10^{-14}M. For that reason, I did not attempt to break this biotin-streptavidin interaction to elute Hsp90 but directly used the Bead fraction (will be reffered to as "Bound" fraction in GA-pulldown experiments). The Bound fractions in a Tris-base buffer were applied to SpeedVac in order to concentrate to the smallest volume possible. The dried Bound fractions were then resuspended in an ammonium bicarbonate buffer with 8M Urea to denature the proteins. Further denaturation steps include addition of DTT and iodoacetamide to fully reduce and modify cysteine residues. The denatured protein mixtures were diluted to lower than 4M

Urea which allowed digestion by LysC. An additional dilution to less than 2M Urea enabled further digestion of the proteins by Trypsin. The overall digestion mixtures were then injected into the LC-MS/MS system for analysis.

In general, cytosolic Hsp90 isoforms (Hsp90α and Hsp90β) were detected as the first and second hits in most GA pull-down MS runs. In control runs (pulldown cell lysates using beads without Biotinylated-GA), Hsp90 proteins were either not detected or could sometimes be detected with sequence coverage less than 5%. However, the sequence coverage of Hsp90 proteins in these analyses were also far below required values. From HepG2 cell extracts, Hsp90α and Hsp90β were detected with an average 26% and 42% sequence coverage, respectively. The situation is similar for samples from HELA and from Snu182 extracts (Table 2-1).

Due to insufficient sequence coverage, a conclusion about the phosphorylation status of Hsp90 in these cell extracts was not possible. Of notes, the set of peptides detected in the 3 different cell lines was highly overlapping, implying that they were peptides with good MS reponses. The missing part of the sequence could contain less-well ionized peptides; peptides that did not bind to reversed-phase column or those that had m/z values outside the MS optimal range of detection. The Mascot database search gave indications that the in-solution digestion was not complete: there were peptide ions with larger m/z values than the range of the database search. Even when I increased the digestion duration for both enzymes, the results were not much improved. The denatured proteins in the presence of bead matrices might form aggregates on the beads that reduced accessibility for proteases. Therefore, for later MS analyses, I applied GA pull-down or IP samples onto SDS-polyacrylamide gels to separate beads from the denatured proteins. In-gel trypsin digestion was applied and MS analysis was carried out using an Orbitrap mass spectrometer, which has a greater sensitivity in MS/MS as compared to the MaXis mass spectrometer.

Sequence coverage (%)	**Hsp90α**	**Hsp90β**
HepG2	26.00 ± 6.51	42.00 ± 2.00
Snu182	24.00 ± 2.83	40.50 ± 2.12
HELA	25.20 ± 5.17	46.00 ± 1.2

TABLE 2-1: SEQUENCE COVERAGE OF HSP90 ISOFORMS IN ANALYSIS BY THE MAXIS MS
The data are presented in average ± standard deviation from 2-4 experiments.

There was also an interesting feature in those MS analyses: Human Hsp90β isoform was always the first hit and detected with sequence coverage two-fold higher than that of Hsp90α in most of these runs (Table 2-1).

This observation suggested that Hsp90β was always enriched more in our samples than Hsp90α. There could be three potential explanations for it:

(1) Binding of Hsp90β to GA-beads is stronger than that of Hsp90α; or

(2) Under non-heat shock conditions, Hsp90β is higher expressed than Hsp90α; or

(3) Different post-translational modifications on each isoform in lysates diverge their binding to GA-beads.

(4) Downstream processing steps after isolation from cell extracts such as in-solution digestion and MS analysis provide preference for detection of one isoform over the other.

To test whether the first possibility is the case, a GA-pull down assay using purified Hsp90α and Hsp90β was performed. Under similar conditions including the incubation duration and the amount of GA-beads, the binding of both purified proteins to GA-beads was similar but much weaker as compared with Hsp90 proteins from lysates (see Figure 2-15, page 67). The second possibility could be examined by relative quantification of Hsp90 isoforms in cell lysates using quantitative Western blotting and isoform-specific

antibodies. However, it is unlikely that this possibility is the case because in later IP and GA-pulldown experiments followed by in-gel digestion and Orbitrap MS analysis this difference in sequence coverage between two isoforms decreased significantly (Table 2-2). The findings from the next part also ruled out the third hypothesis that difference originated from post-translational modifications and pinpointed to downstream processing steps in these initial GA-pulldown experiments as reasons for this Hsp90β-preferred detection.

MS analysis by the Orbitrap mass spectrometer

In these Orbitrap MS analyses, I prepared the HepG2/HELA samples myself using either GA-pull down experiments or IP assays and loaded the elution and/or beads fractions on gel. The in-gel digestion and MS analysis were performed in cooperation with MS facility, ZMBH.

Isolation method	Sequence coverage (%)	Hsp90α	Hsp90β
IP	HepG2	55.5 ± 10.6	59 ± 11.3
	HELA	53 ± 14.1	63 ± 11.3
GA-pulldown	HepG2	53 ± 10.7	56 ± 12.6
	HELA	49.4 ± 16.4	60.2 ± 13.9

TABLE 2-2: SEQUENCE COVERAGE OF HSP90 ISOFORMS IN ANALYSES BY THE ORBITRAP MS USING EITHER IMMUNOPRECIPITATION (IP) OR GA-PULLDOWN AS HSP90 ISOLATION METHOD.

The data are presented as average ± standard deviations from 2-4 experiments.

Similar to the MaXis MS analyses, in all runs, cytosolic Hsp90 proteins were detected as first hits. The sequence coverage of both Hsp90 isoform were increased significantly to the average of 50-65% and 55-70% for Hsp90α and Hsp90β respectively (Table 2-2). This enhanced efficiency was gained from the utilizing of in-gel digestion and the Orbitrap MS instead of in-solution digestion and QTOF MS, respectively. Nevertheless, there were higher fluctuations in the sequence coverage from similar IP or GA-pulldown experiments suggesting instability of instrument performance. Of note, in contrast to the MaXis MS results, the data from Orbitrap MS analyses showed no significant difference between two cytosolic Hsp90 isoforms.

A comparison plot between the sequence coverage of human Hsp90 proteins from MS analyses from the Maxis and the Orbitrap mass spectrometer showed that they were mostly overlapped (Figure 2-4). As mentioned, the peptides in those regions might be those that have good MS responses regardless of the digestion method and the mass spectrometer. A few peptides such as the very N-terminal peptide (2-41 of Hsp90α or 2-36 of Hsp90β) or the charge linker peptide (227-245 of Hsp90α or 222-234 of Hsp90β) were preferentially detected in one or the other analyses, suggesting that their abundance, stability, digestion and ionization behaviors might be at critical levels. Moreover, among the detected peptides in both MS analyses, many of them contained miss-cleavage site(s), indicating that both of the in-solution and in-gel digestion could have been further improved for higher efficiency.

(A)

(B)

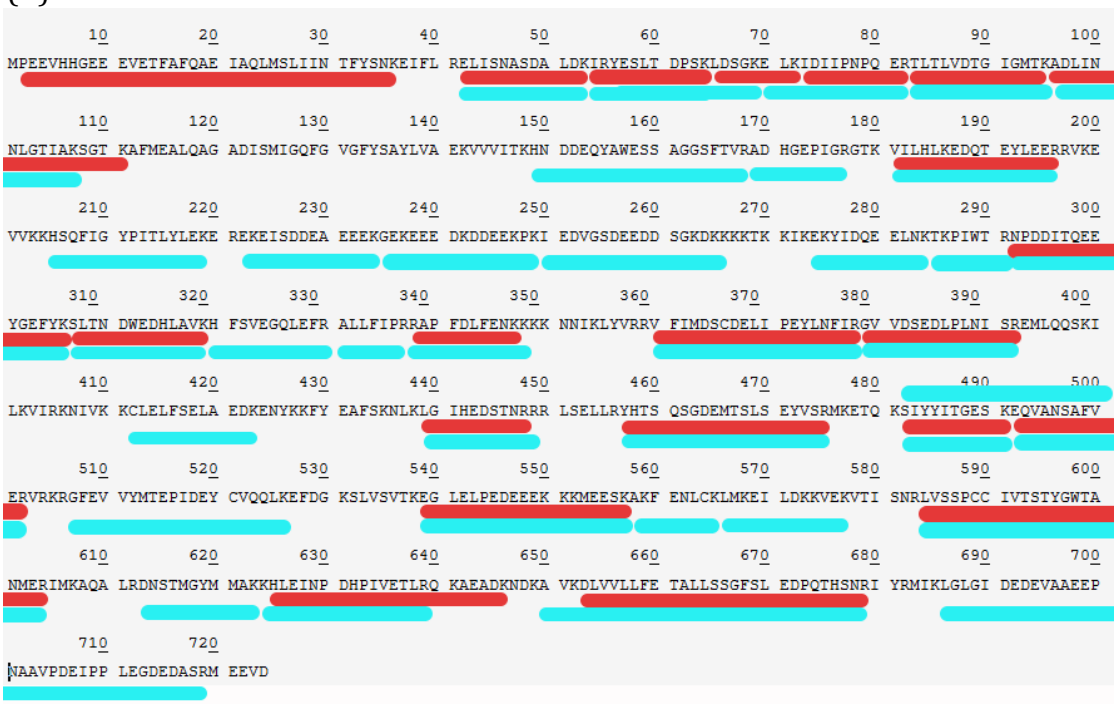

FIGURE 2-4: SEQUENCE COVERAGE OF HSP90 PROTEINS IN MS ANALYSES

Shown are the peptides detected at least in 2 MS analyses from the Maxis mass spectrometer (colored in red) or the Orbitrap mass spectrometer (colored in blue). The peptides are plotted for human Hsp90α in (A) and Hsp90β (B).

2.1.2.2 IDENTIFICATION OF PHOSPHORYLATION SITES

Despite limited sequence coverage, we were able to detect some phosphorylation sites on both human Hsp90 isoforms (Table 2-3). Interestingly, in GA-pulldown experiments followed by in-solution digestion and MS analysis by the MaXis mass spectrometer, more novel phosphorylation sites were identified as compared with analysis by Orbitrap even in

similar GA-pulldown experiments. On the contrary, in all the Orbitrap MS analyses, despite having higher sequence coverage, identification of phosphorylation sites was more limited. We detected overall fewer sites and only those that had been reported in proteomics studies except for Y667, which was also only identified once in our experiments. This could be due to the process of in-gel digestion in the absence of specific enrichment of phospho-peptides from our limited starting material. The in-gel digestion protocol further limited us in the volume that could be loaded onto the gel: in fact, a smaller amount of sample can be included in a standard in-gel digestion reaction than an in-solution digestion reaction. Even though Hsp90 proteins could be readily stained by colloidal Coomassie staining, the different phosphorylated species might be present in the gel band with insufficient amounts.

We also had no overlapping phosphorylation sites between two MS analyses, suggesting that different digestion protocols and LC-MS/MS systems had larger influence on the detection than we expected, especially since the starting amount of the material was limited. Interestingly, approximately half of the phosphorylation sites detected in MS analyses using the MaXis or the Orbitrap mass spectrometer, do not belong to overlapping regions (Figure 2-4). In those phosphorylation sites that belonged to overlapping regions, the abundance of a modified peptide resulted from in-gel vs in-solution digestion might deviate, giving the possibility that in analyses using one mass spectrometer, the abundance was below detection threshold. In a very special case of the peptide 584-604 of human Hsp90β, the peptide itself is rather long with 21 amino acid and contains several serines, threonines, tyrosines (in total 7 phosphorylatable residues) that are even next or close to one another (Figure 2-4). Precursor ion of this peptide suggested that there were more than one phosphorylation site and hence, the assignment for exact modified residues could be compromised.

	Hsp90α	**Hsp90β**
GA-pull down In-solution digestion MaXis MS	T19 S31 **T36** **Y38** S39 **T88** T109 S113 **T115** T594 **S595**	T14 S26 T31 **Y33** S34 **S45** **S48** T104 S108 T110 **S365** S586 S587 **T593**
GA-pulldown or IP In-gel digestion Orbitrap MS	**T99** **S231** **S263** **T317** **Y627** **T645** Y667	**T94** **S226** **S255** **T309** **S594** **T595** **Y596**

TABLE 2-3: PHOSPHORYLATION SITES DETECTED BY MS IN HEPG2, SNU182 AND HELA CELL EXTRACTS AFTER HSP90 ISOLATION.

In bold are sites that are reported on Phosphosite website (http://www.phosphosite.org/homeAction.do) (mostly detected in proteomics studies) and in red is the site we chose for detailed characterization in the next part. The sites from peptides that do not belong to overlapping regions are colored in blue.

There were a few phosphorylation sites detected in our analysis, such as T36, Y38 (Hsp90α) and corresponding T31, Y33 (Hsp90β) or S365 (Hsp90β only), etc that have just recently been added to the phosphosite database. The N-terminal phosphorylation sites T36 and Y38 (Hsp90α)/T31 and Y33 (Hsp90β) were detected in yeast and characterized in details by another group (Mollapour, S. Tsutsumi, et al. 2010; Mollapour, Tsutsumi, et al. 2011). The novel S365 phosphorylation site of Hsp90β was chosen to be the target for further characterization in my next part of the project.

Using two methods of isolation also allowed us to tackle the cellular Hsp90 population from different angles. Since in both methods I was able to isolate the majority of cellular Hsp90, I expected to compare also the interaction partners of Hsp90 from them. In contrast to MS results from GA-pulldown experiments, MS results from IP revealed a large number of interesting co-immunoprecipitated proteins such as Hsp70, Hsc70, STIP1, Cdc37, Aha1, CHIP, PP5, UNC-45, etc as cochaperones; cyclin-dependent kinase 1 (Cdk1), DNA repair protein Rad50, histone H1, importin β-1, exportin proteins (XPO1, XPO2, XPO5,…), etc as clients and DNA-dependent protein kinase (DNA-PK), 14-3-3 proteins, S100 calcium-binding protein (S100P) … as interactors that could be either or both. This was expected since GA either dissociates cochaperones and clients from Hsp90 complex or prevents transfer of client proteins to Hsp90; whereas in IP, Hsp90-client-cochaperon complexes could be preserved. Nevertheless, as our focus was phosphorylation as a post-translational modification type that contributes to tumor selectivity of Hsp90 drugs, we did not follow up any further on these co-IP hits.

Unfortunately, all the novel phosphorylation sites that we identified did not exhibit a clear correlation with the tumor specificity of Hsp90 inhibitors because either they were detected in both fraction of GA-bound and GA-unbound or were not detected reproducibly. Since our aim was to detect quantitative as well as qualitative differences in phosphorylation between cell lines, we did not include any specific phospho-peptide enrichment steps *in vivo* (before cell lysis) or *in vitro*. Our results could be limited due to the transient nature of the phosphorylation status of cellular Hsp90 proteins.

Furthermore, regarding to the tumor selectivity characteristics of Hsp90 inhibitors, on the contrary to what we hypothesized, the fraction of Hsp90 that contribute significantly to tumor specificity of Hsp90 inhibitors need not to be the majority. That would explain why without enrichment, our isolation methods were not robust enough for MS/MS identification later. Another possibility is another post-translational modification type, not phosphorylation, is responsible for tumor selectivity of Hsp90 inhibitors. This seems to be more likely under the light of recent study by Neckers and colleagues (Mollapour et al. 2014). In their work, Neckers and colleagues provided evidence that SUMOylation on the N-terminal of Hsp90 leads to more sensitivity to its inhibitors. Although SUMOylation of Hsp90 was reported previously (Panse et al. 2004), for the first time, the site of SUMOylation and its consequences for Hsp90 function were identified and characterized. It was unexpected, even to the authors that Hsp90 inhibitors had higher affinity for SUMOylated Hsp90 and as a consequence, increased SUMOylation could sensitize cells to Hsp90 inhibitors.

2.1.3 MRM-MS ANALYSIS OF SELECTIVELY KNOWN PHOSPHORYLATION SITES

In this special MS approach, we limited our analysis to 5 phosphorylation sites of human Hsp90 proteins: T36 and/or Y38, T90, Y309 (numbering is referred as in the α isoform) and S365 (only of the β isoform) (Table 2-4) and wanted to monitor the phosphorylation status of these sites in crude cell lysate without any isolation method. The sites were selected due to their importance for cancer progression or their being the target of cancer-related kinases. The MRM profile was constructed from four parameters that were

obtained from one or multiple standard LC MS/MS experiments: (i) chromatographic elution order of phosphorylated peptides (retention time window), (ii) phosphorylated peptide (precursor ion) mass to charge ratio (m/z) and charge state (z), (iii) characteristic b- and y-fragment ion m/z ratio, and (iv) collision energy required for fragmentation to obtain b- and y-fragment ions. This MRM-MS profile of each peptide would then be applied to monitor its status in cell lysate samples. This MRM-MS characterization step was done in collaboration with S.Link (MS facility, ZMBH, Heidelberg).

There were actually a few more phosphorylation sites that we also would like to select for this MS approach, for e.g. the two serine phosphorylation sites in the charge linker (S236 and S255). However, they weren't readily fitted to certain requirements of MRM-MS: the surrounding region contains series of lysine residues which make generating exact tryptic peptide with predicted mass not feasible or the peptide as digested by other proteases is either larger or smaller than the optimal range for the precursor mass. In addition to the phospho-peptides, we also selected other peptides from digestion of purified human Hsp90α and β (those that have good MS responses) to ensure the selection and characterization of Hsp90 proteins in complex samples. We also included peptides for the purpose of distinguishing between isoforms. In total, we include a list of approximately 90-100 transitions (precursor/fragment ion pairs) for MRM-MS analysis (Appendix Table S1).

For each phoshorylation site, we synthesized a tryptic peptide containing the specific site, except for T36 and Y38 which cannot be separated into two peptides because they are only 2 amino acids away from one another. Moreover, there were no lysine or arginine residues nearby in this N-terminal region for tryptic cleavage so that we had to use Glu-C digestion, which generated a relatively large peptide. These differences later turned out to be quite problematic since the large peptide containing these single or double phosphorylation sites were not readily detected even in the synthesized form (which we could utilize in much more abundant quantity than in cell lysate samples). Therefore, we gained no MS results for these phosphorylation sites in cell lysate samples.

Site (numbering as in Hsp90α)	Phosphorylated synthetic petide	Reference
T36	IAQLMSLIIN**T**FYSNKE	(Mollapour, S. Tsutsumi, Kim, et al. 2011), (Mollapour, Tsutsumi, et al. 2011)
Y38	IAQLMSLIINTF**Y**SNKE	*ditto*
T36/ Y38	IAQLMSLIIN**T**F**Y**SNKE	*Ditto*
T90	TL**T**IVDTGIGMTK	(Wang et al. 2009; Wang et al. 2012)
Y309	NPDDITN/QEE**Y**GEFYK	(Duval et al. 2007)
S365 (Hsp90β)	VFIMD**S**CDELIPEYLNFIR	This work

TABLE 2-4: SELECTED PHOSPHORYLATION SITES TO BE MONITORED IN MRM-MS APPROACH

For the rest including T90, Y309 and S365 phosphorylation peptides, we could detect and monitor their transitions well when using synthetic peptides. However, only the non-phosphorylated forms of the peptides were found in cell lysates, except for the S365-containing peptide.

The identification of S365-phosphorylated peptide was also not straightforward: Only MRM-MS was not enough because the transitions eluted in the expected retention time window but with low intensities and were interfered by other signals. Therefore, a further fragmentation step was included in Q3 (MS^3) and MS^3 scans were recorded. In parallel, the MS^3 fragmentation patterns of transitions from S365-phosphorylated synthetic and other peptides (both non-phosphorylated and phosphorylated) were also generated to build up a MS^3 "library". We then could perform "library identification", i.e. comparing the MS^3 fragmentation spectrum of interesting transitions with that of each component in our library to identify the transition that have the most similar MS^3 fragmentation pattern (Appendix Figure S1, in cooperation with S. Link, MS facility, ZMBH). In our case, the MS^3 fragmentation spectra of the transitions of interest were indeed matched well with that of corresponding transitions from S365-phosphorylated synthetic peptide under identified MS conditions, allowing us to confirm the presence of S365-phosphorylated peptide in HELA crude lysate samples. The low signal intensity of S365-phosphorylated parental peptide and transitions suggested their substoichiometric abundance as compared with the non-phosphorylated counterpart. However, we were unable to conclude more in details because due to interference of MS^3, relative quantification between phosphorylated versus non-phosphorylated forms of this peptide was not possible any more. The low abundance of cellular S365-phosphorylated Hsp90 proteins could be the result of dynamic phosphorylation/dephosphorylation cycle and/or client-specific activity of Hsp90. Besides, we could not completely rule out the possibility that in the only processing procedure of in-solution or in-gel digestion, the total amount of S365-phosphorylated peptide was reduced or became harder to detect in MS due to for e.g. instability or being less well-ionized than the unmodified counterpart. This will be further discussed in the next section.

All Hsp90 petides containing T90 or Y309 were detected in non-phosphorylated forms in HELA cell extract samples. Our data provided evidence that under normal conditions, those sites were not phosphorylated at all or their basal phosphorylation levels are lower than MS detection threshold. Due to the lack of detected phosphorylated forms of these peptides, we did not continue with relative quantification to compare between phosphorylation status. In general, the MRM-MS succeeded in detection of most phosphorylation sites that we selected. In normal HELA samples, the selected phosphorylation sites of Hsp90 proteins were dominantly in unmodified form, indicating that their phosphorylations are highly specific in response to their particular stimulus or environmental signals such as overexpression of PKA for T90 or VEGF for Y309.

During optimization procedure for MRM-MS, we recognized other requirements of this approach such as the parent peptides must be accurately produced by protease digestion and should not be either too small or large (m/z value between 400 to 1000); the characterization of peptides and transitions might require purified or synthetic materials; the b-/y-fragment ions also should contain at least 4 amino acids and should not be complementary; the relative stoichiometric ratio between phosphorylated peptide and its non-phosphorylated counterpart should be in a certain range to ensure confidently detection for both forms; etc. For those reasons, our quantification for the selected phosphorylation sites of Hsp90 proteins was not complete.

Nevertheless, with modified and coupled approaches such as the utilization of phosphatase treatment or spiked-in of stable isotope-labeled standards, the application of MRM-MS as a quantitative method for a number of selected proteins or other modification sites is highly feasible.

2.2 CHARACTERIZATION OF PHOSPHORYLATION AT SERINE 365 IN HUMAN HSP90β

2.2.1 IDENTIFICATION AND VERIFICATION OF S365 PHOSPHORYLATION IN HUMAN HSP90β

The phosphorylated peptide of serine 365 on Hsp90β has first been detected in HepG2 and Snu182 cell lysates using the MaXis mass spectrometer (see section 2.1.2, Table 2-3). The tryptic peptide 360-378 from Hsp90β was fragmented well, yielding a number of b and y-ions series, which enabled exact assignments of 16 out of 19 amino acids of the peptide. Parent mass of the peptide and the a-6th ion allowed specifically identification of the phosphorylation site to serine 365. Moreover, there wasn't any other potential site in the peptide sequence (Figure 2-5B). It should be mentioned that there was also MS detection of the same peptide but in non-phosphorylated form. It was also well-fragmented and the b, y-ion series covered most of the sequence, too (data not shown). This observation implies that the population of Hsp90 proteins in the cells is heterogenous: some of which are phosphorylated at serine 365, others are not. The ratio between phosphorylated and non-phosphorylated Hsp90 could well be an important factor to determine the affinity of the whole population to inhibitors.

Interestingly, the cysteine residue next to serine 365 phosphorylation site was detected unmodified (Figure 2-5A) despite treatment with DTT and iodoactemide in both in-solution and in-gel digestion methods, whereas the same cysteine residue on the corresponding non-phosphorylated peptide was detected as alkylated form, suggesting that the phosphorylation at serine might influence the alkylation reaction of this cysteine or result in different accessibility and conformation for alkylation.

However, phosphorylation on serine 365 of human Hsp90β was not readily detected in all MS analyses by the Orbitrap mass spectrometer despite our attempt of using Preferred Mass list, indicating that this S365 phosphorylation was not abundant and may not be as well-selected by the ion trap in Orbitrap MS as by the quadrupole in MaXis MS. Several attempts later using synthetic phosphorylated vs non-phosphorylated peptides and MS detection on the Orbitrap MS revealed that the lack of modification on cysteine of the peptide made it unstable and thus, hindered further detection. Even with synthetic peptides, after treatment with DTT and iodoacetamide as we did for Hsp90 protein before digestion or not as control, the intensity of the phosphorylated and non-alkylated peptide detected in MS was at least 100-fold less than that of peptides which have all other combination between phosphorylation and alkylation status (Figure 2-6). Of note, with synthetic peptides, we could use in high amount and defined starting material, unlike with complex lysate samples in which we had little control over these factors. This finding suggested that the combination of phosphorylation and not-being alkylated status caused the bad MS response of the modified peptide. The MS characterization of S365-phosphorylated synthetic peptide was done in cooperation with L. Behrens, MS facility, ZMBH.

Indeed, this could explain why by the time we identified the S365 phosphorylation site of human Hsp90β, there was no phosphoproteomics data for it. Only later in human ES and iPS as well as Jurkat cells (T-cell leukemia cell line), this S365 phosphorylation was also reported (Phanstiel et al. 2012) (Phosphosite database).

We had to use the MRM-MS technique followed by MS^3 and library identification to verify this phosphorylation site (see section 2.1.3, page 47). Indeed, S365 phosphorylation was confirmed in HELA cells (Appendix Figure S1): the corresponding peptide was identified in the phosphorylated and non-alkyated form.

(A)

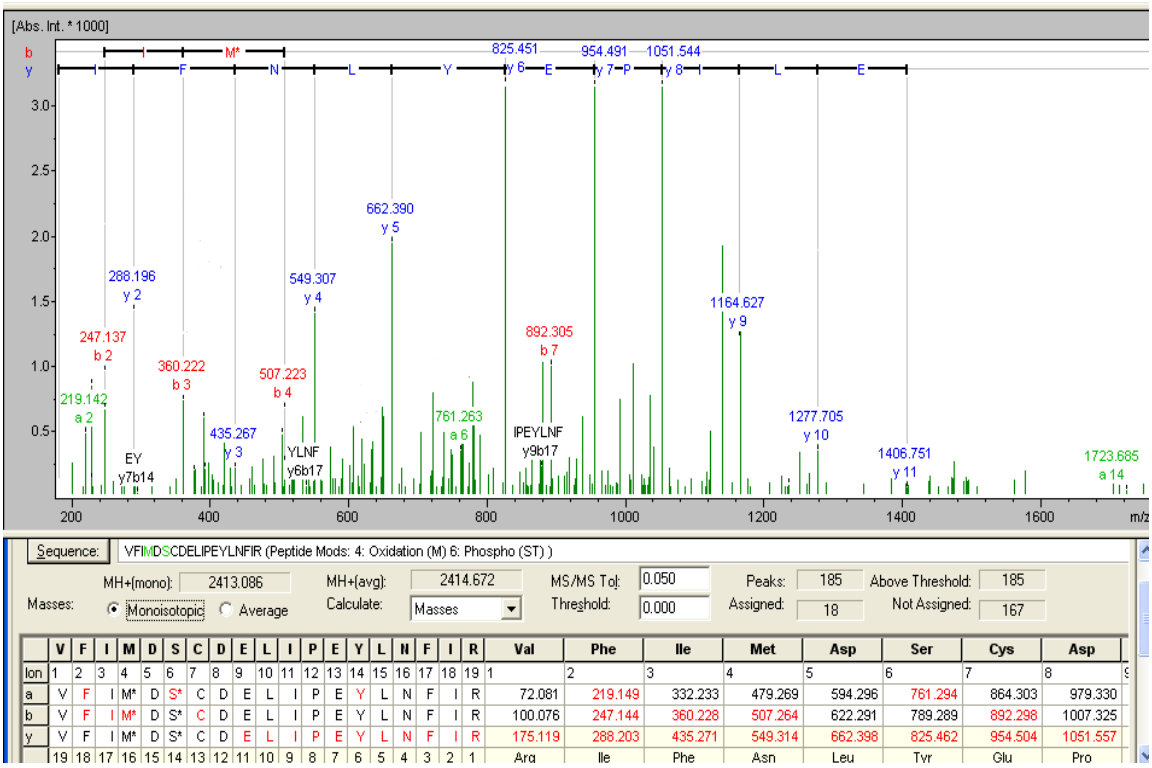

(B)

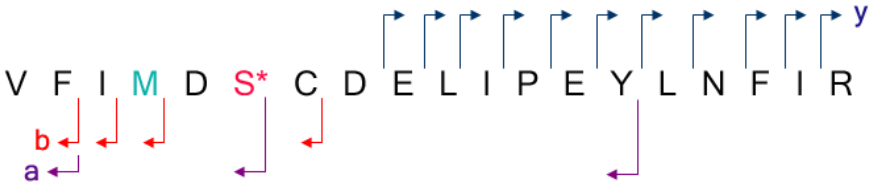

FIGURE 2-5: IDENTIFICATION OF S365 PHOSPHORYLATION IN HUMAN HSP90β.

(A) Screenshot of MS/MS spectrum of peptide 360-378 containing S365 phosphorylation in human Hsp90β (Biotools, Bruker).

(B) Peptide 360-378 of human Hsp90β with detected a, b, y ions marked with violet, red and blue arrows, respectively.

FIGURE 2-6: MRM-MS DETECTION OF SYNTHETIC PEPTIDES CONTAINING THE S365 PHOSPHORYLATION SITE IN PHOSPHORYLATED OR NON-PHOSPHORYLATED FORM TREATED OR NOT TREATED WITH IODOACETAMIDE

The phosphorylated peptide is treated without (A) or with (B) iodoacetamide which modifies its cysteine to the carbamidomethyl form.

Similar treatment was performed for non-phosphorylated peptide in (C) and (D). All 4 samples were injected to the LC-MS system at 100 fmol.

The normalized detection levels (NL) of all transitions in (A) are in 10^4 range, at least 100-1000x less than those of transitions in (B), (C), (D), indicating that the phosphorylated and cysteine-modifed form of the peptide is not as readily detected as other forms.

(A)

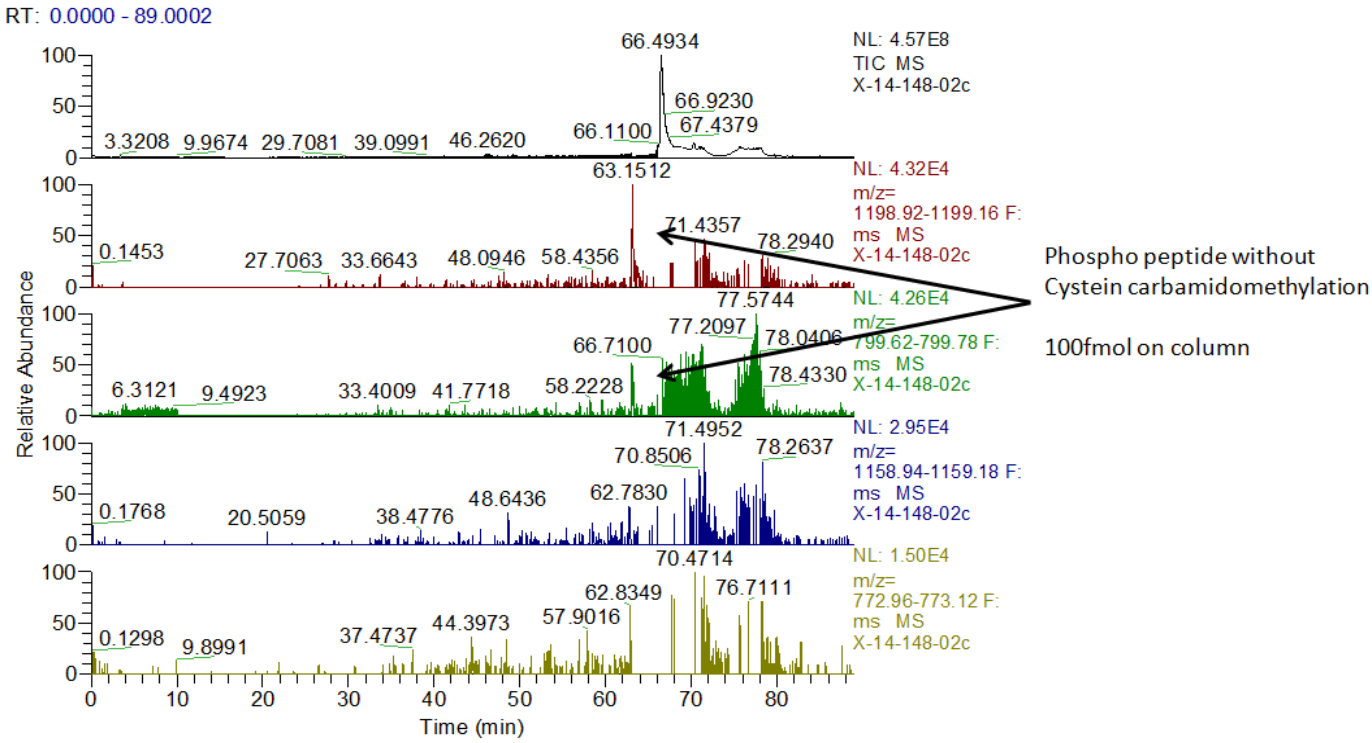

(B)

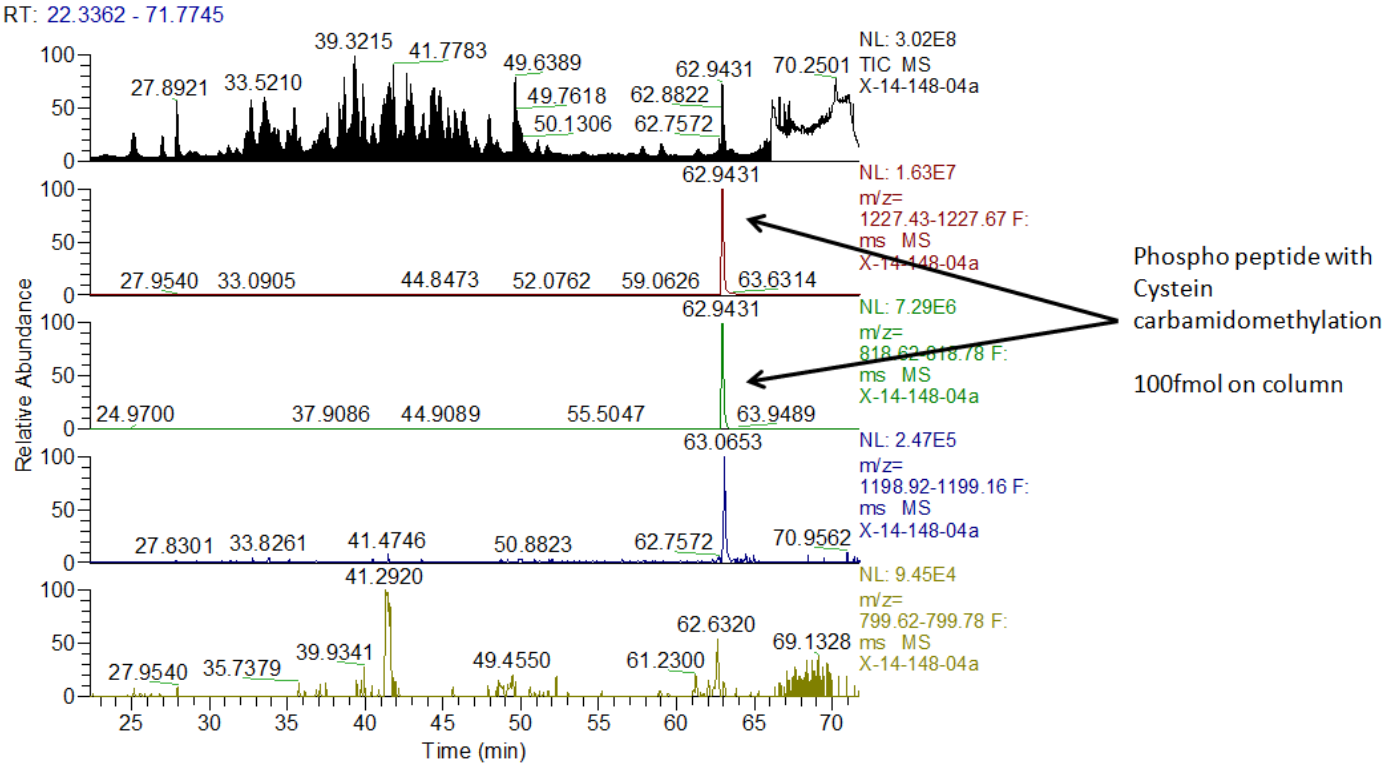
RT: 22.3362 - 71.7745
NL: 3.02E8
TIC MS
X-14-148-04a
NL: 1.63E7
m/z=
1227.43-1227.67 F:
ms MS
X-14-148-04a
NL: 7.29E6
m/z=
818.62-818.78 F:
ms MS
X-14-148-04a
NL: 2.47E5
m/z=
1198.92-1199.16 F:
ms MS
X-14-148-04a
NL: 9.45E4
m/z=
799.62-799.78 F:
ms MS
X-14-148-04a
Relative Abundance
Time (min)
Phospho peptide with
Cystein
carbamidomethylation
100fmol on column

(C)

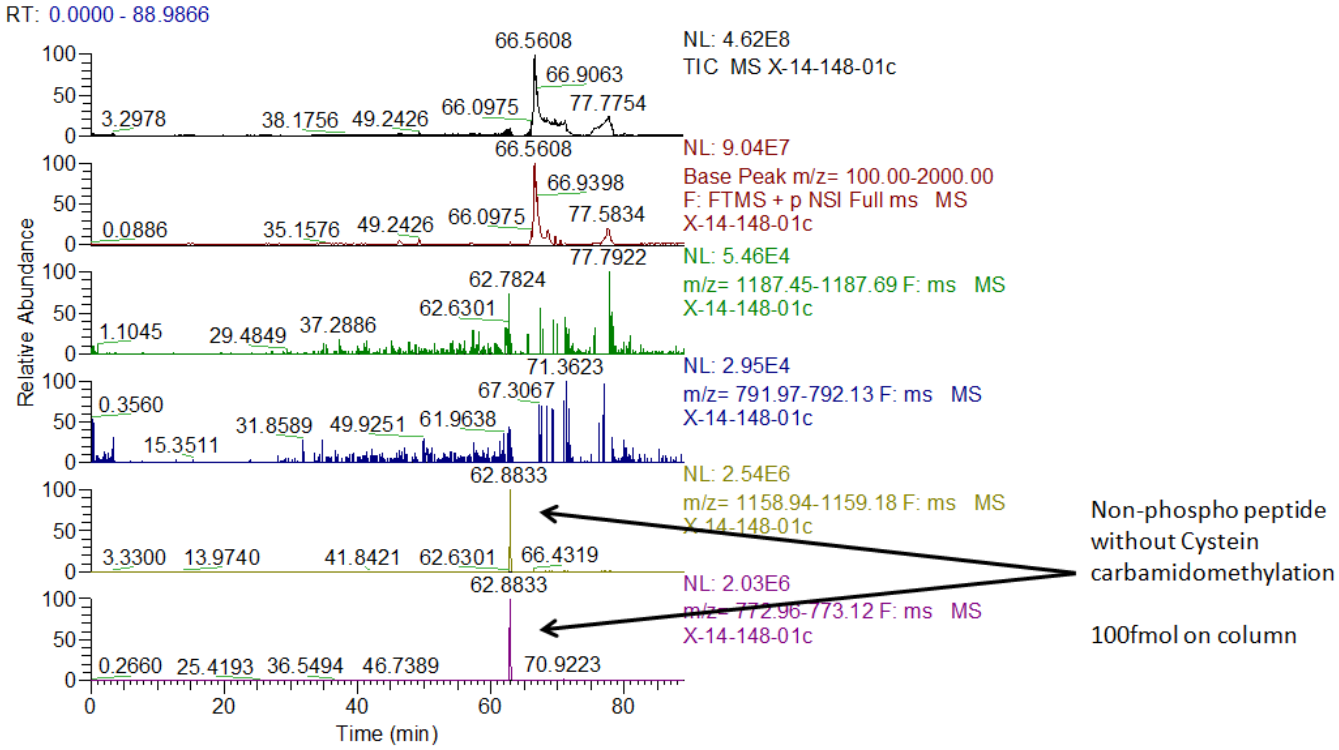
RT: 0.0000 - 88.9866
NL: 4.62E8
TIC MS X-14-148-01c
NL: 9.04E7
Base Peak m/z= 100.00-2000.00
F: FTMS + p NSI Full ms MS
X-14-148-01c
NL: 5.46E4
m/z= 1187.45-1187.69 F: ms MS
X-14-148-01c
NL: 2.95E4
m/z= 791.97-792.13 F: ms MS
X-14-148-01c
NL: 2.54E6
m/z= 1158.94-1159.18 F: ms MS
X-14-148-01c
NL: 2.03E6
m/z= 772.96-773.12 F: ms MS
X-14-148-01c
Relative Abundance
Time (min)
Non-phospho peptide
without Cystein
carbamidomethylation
100fmol on column

(D)

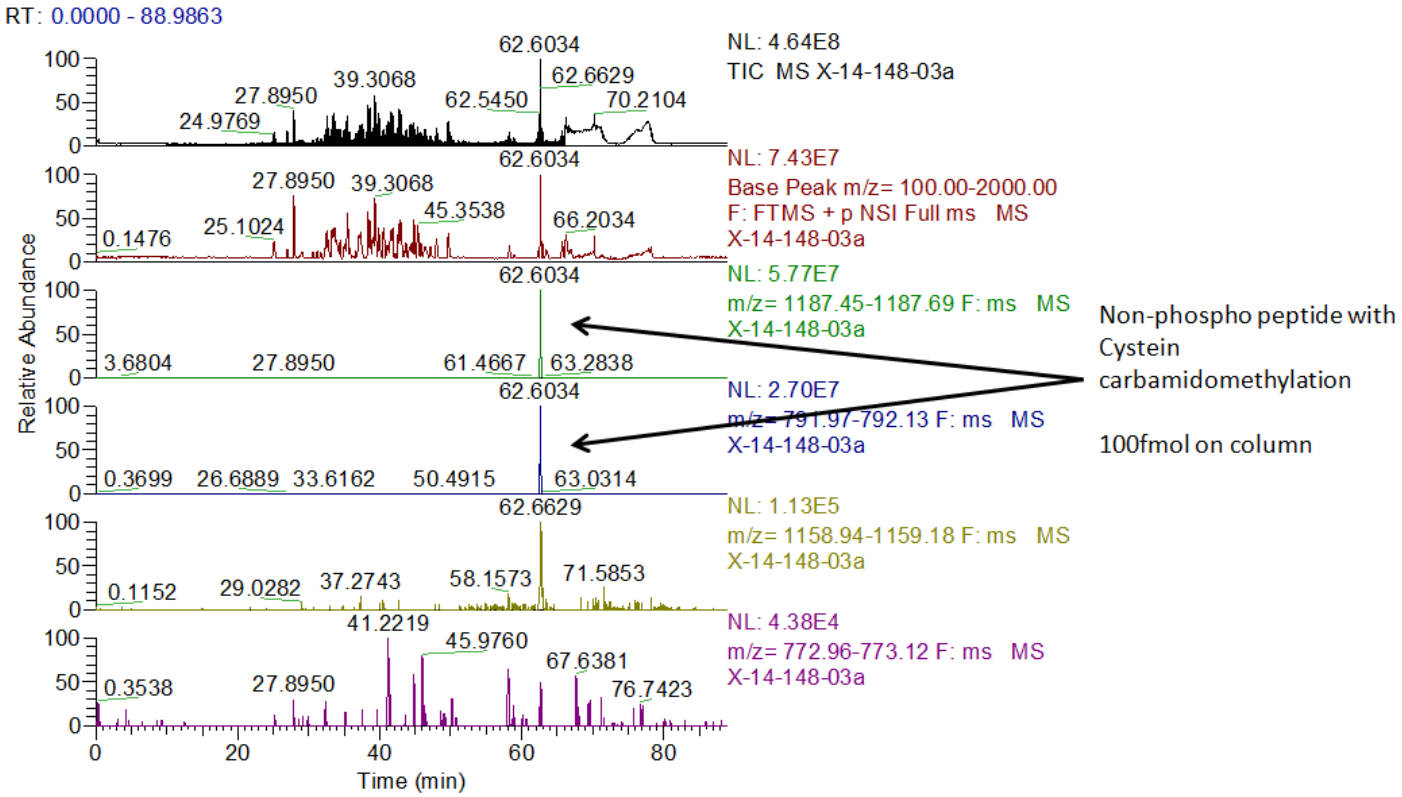
RT: 0.0000 - 88.9863
NL: 4.64E8
TIC MS X-14-148-03a
NL: 7.43E7
Base Peak m/z= 100.00-2000.00
F: FTMS + p NSI Full ms MS
X-14-148-03a
NL: 5.77E7
m/z= 1187.45-1187.69 F: ms MS
X-14-148-03a
NL: 2.70E7
m/z= 791.97-792.13 F: ms MS
X-14-148-03a
NL: 1.13E5
m/z= 1158.94-1159.18 F: ms MS
X-14-148-03a
NL: 4.38E4
m/z= 772.96-773.12 F: ms MS
X-14-148-03a
Relative Abundance
Time (min)
Non-phospho peptide with Cystein carbamidomethylation
100fmol on column

Position of serine 365 on human Hsp90β

Serine 365 on human Hsp90β locates in a helix belonging to the middle domain (mH2, (Karagöz et al. 2014)) of the chaperone, facing into the "inner space" that formed between the two protomers in the closed conformation of the dimer. Therefore, in principal, the site is not accessible to kinases and phosphatases when the Hsp90 is in its closed conformation, implicating that phosphorylation and dephosphorylation of this site must happen when Hsp90 protein is in open conformation and the phosphorylated or unphosphorylated form of Hsp90 can then be trapped by converting into the closed conformation. These events can also be coupled with Hsp90's client protein binding and release. Such dynamic events of phosphorylation and dephosphorylation on the one hand, would be challenging for us to identify the involved kinase or phosphatase but on the other hand, would be highly competent for fine-tuning the chaperone. The middle domain of Hsp90 is known as binding site for client proteins such as Cdk4, v-src, glucorcorticoid receptor, Tau, etc and some cochaperones like Aha1, Unc-45, etc (Meyer et al. 2003; Hawle et al. 2006b; Vaughan et al. 2006; Scroggins et al. 2007; Street et al. 2011; Karagöz et al. 2014; Lorenz et al. 2014). Therefore, it is very likely that phosphorylation of serine 365 of the middle domain can directly influence both client and cochaperone interactions of Hsp90 proteins. In addition, it can also participate in modulating dynamic conformational changes of Hsp90 in the N- and C-terminal parts.

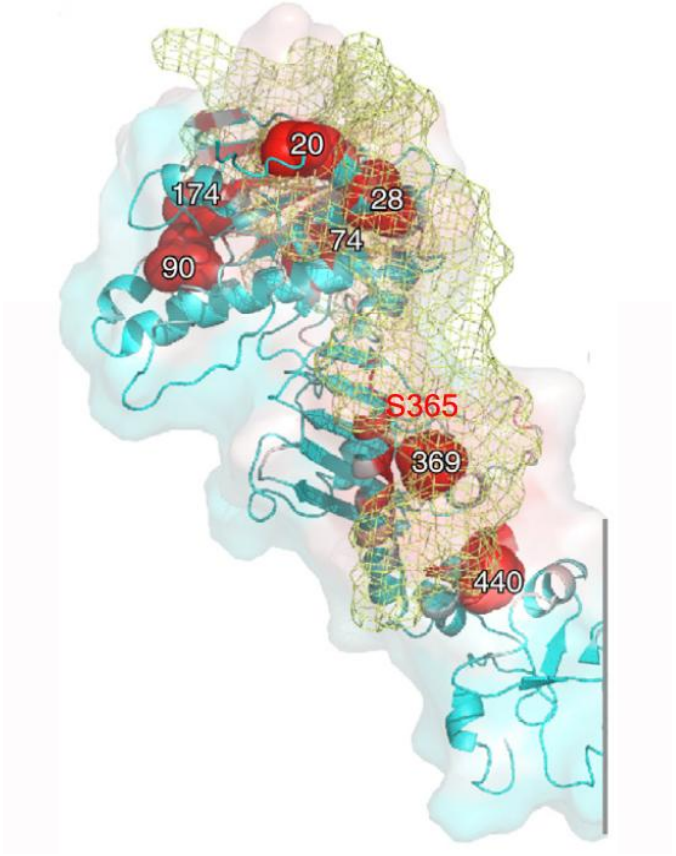

FIGURE 2-7: POSITION OF S365 IN AN HSP90-CLIENT COMPLEX.

Tau (yellow mesh) in complex with human Hsp90β (cyan cartoon). Leucine residues of Hsp90 that belong to binding surface are depicted in red spheres. Serine 365 is marked in red. Adapted from (Karagöz et al. 2014).

Isoform-specific conservation of S365

This serine phosphorylation site of human Hsp90β is specific for this iosform since the corresponding residue in Hsp90α is an asparagine (N) – which cannot be

phosphorylated. Interestingly, in *Saccharomyces cerevisiae*, the homologous position is occupied by the phosphomimetic residue glutamate (E). Alignment of several other homologous sequences of cytosolic Hsp90 proteins (normally two isoforms) reveals intriguing pattern of evolution: the serine residue is conserved in all β isoform proteins whereas in all α isoform proteins, the corresponding residue is asparagine and also highly conserved (Figure 2-8). These isoforms are differed in their expression and induction mechanism as well as cell-type specificity and functions, nonetheless, these differences are still not fully characterized (Subbarao Sreedhar et al. 2004; Kuo et al. 2007; Millson et al. 2007; Milicevic et al. 2008; Gao et al. 2013; Silva et al. 2013). In the cellular context, Hsp90α emerges as a fast-response, cytoprotective isoform; while Hsp90β seems to be associated with long-term cellular adaptation and facilitates cellular evolution. The isoform-specific conservation at this residue in Hsp90 proteins suggests that this serine phosphorylation could involve in isoform-specific tasks of Hsp90 such as regulating certain clients or upon response to particular conditions. The isoform-division cellular tasks of Hsp90 proteins could be performed simply by the switch of phosphorylatable and non-phosphorylatable residues. It can be highly informative to elucidate these isoform-specific tasks in relation to the phosphorylation status of serine 365 in human Hsp90β. However, in the scope of this project, I do not focus on the isoform-specific issues of Hsp90 proteins, but rather on its effects on the human Hsp90β isoform only.

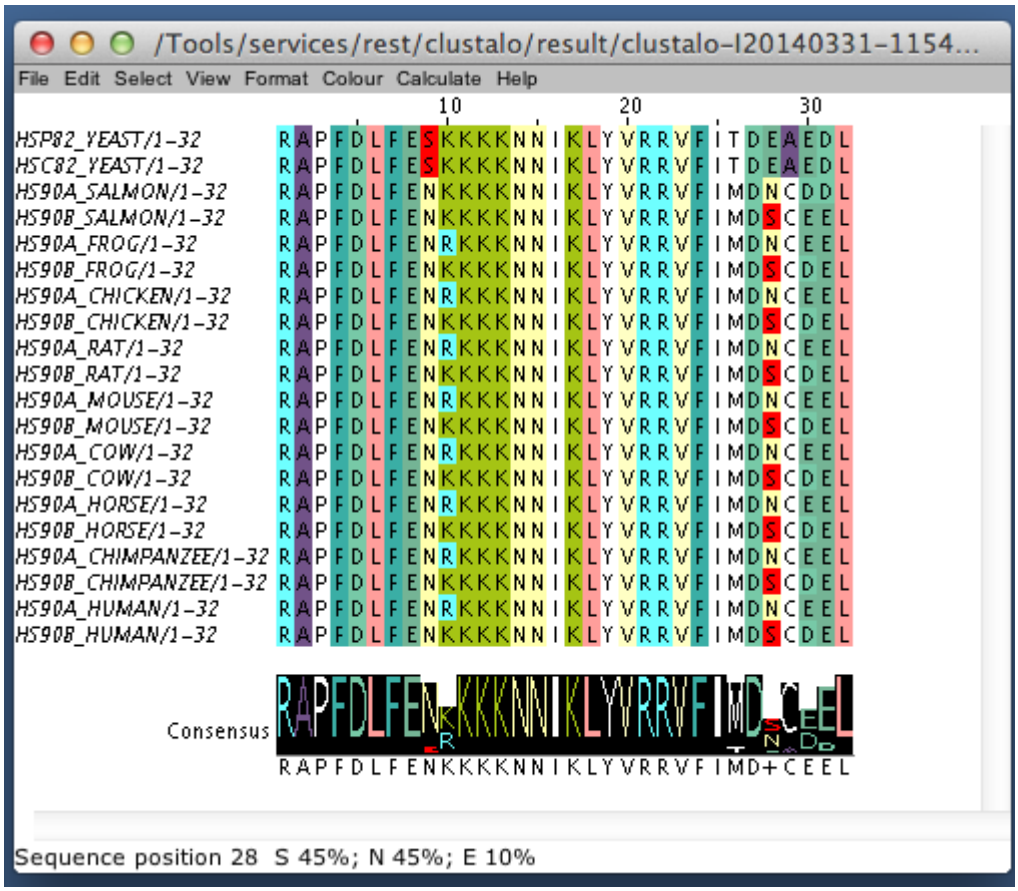

FIGURE 2-8: SEQUENCE ALIGNMENT OF HSP90 PROTEINS IN EUKARYOTES DEMONSTRATES A POSSIBLE EVOLUTION ROLE OF RESIDUES AT THIS POSITION (365 ON HUMAN HSP90β).

For each organism, two cytosolic isoforms were taken for alignment. As shown in consensus sequence, apart from yeast which has in both isoforms glutamate (E) at this corresponding position, all other organism exhibit a high conservation of serine (S) for the beta isoform and asparagine (N) for the alpha isoform. Sequence alignment was performed by online Clustal Omega tool of EMBL-EBI (Link: http://www.ebi.ac.uk/Tools/msa/clustalo/).

The presence of a glutamic acid at the corresponding position which resembles the phospho-mimetic state of the serine residue in both cytosolic Hsp90 isoforms of *Saccharomyces cerevisiae*, the simplest eukaryotic organism, is also intriguing. It has been suggested that the phosphorylation patterns in yeast and man are quite different despite that the majority of yeast phosphorylation sites are conserved residues also in the human proteins (Gnad et al. 2010; Soroka et al. 2013). In our case, on the contrary, the need for a negative charge at this position seems to be conserved and is fulfilled either by glutamic acid in yeast homolog or phosphorylation of serine in human Hsp90β. Given the flexibility gained from phosphorylation of serine residue in human Hsp90β instead of glutamic acid residue in yeast and the complete replacement into asparagine in the α isoform, it can be envision that the role of this phosphorylation site is modulated in a finer manner or tuned down in human Hsp90 homolog as compared with its yeast counterpart. Due to the enlargement of human Hsp90 clientele, the increase in cellular processes in adaptation to environmental stimuli and the evolution of protein kinase family after the divergence of higher eukaryotes from yeast, many other phosphorylation sites of Hsp90 protein could have been utilized and took over part of the role. It is also conceivable that the combination between S365 phosphorylation and other modifications (either on the same Hsp90 molecule or on the interaction partners) in higher eukaryotes becomes more critical.

Potential kinase

Serine 365 of human Hsp90β is followed by acidic residues and hence, is well-matched to phosphorylation recognition motif of CK2 kinase. However, in *in-vitro* phosphorylation assay using CK2 and subsequent MS analysis, S365 phosphorylation was not detected together with all other CK2-targeted phosphorylation sites on human Hsp90β except two serines at the linker region (S226 and S255). This result suggested that additional specific *in vivo* conformation and/or associated factors might be required for serine 365 phosphorylation of human Hsp90β. Moreover, besides being a kinase that phosphorylates many other sites in human Hsp90 proteins, CK2 is also a client protein of Hsp90, making it technically impossible to test for *in vivo* phosphorylation of this particular serine residue of human Hsp90β by CK2 without a specific antibody that recognizes uniquely the phosphorylated S365. We attempted to produce such an antibody using purified phosphomimetic variants as well as the phosphorylated peptide, however, both approaches did not yield successful results. Therefore, so far, our method to demonstrate *in vivo* phosphorylation of S365 in human Hsp90β is limited to MRM-MS.

2.2.2 *IN VIVO* S365 PHOSPHORYLATION IS BENEFICIAL FOR HSP90 CHAPERONE ACTIVITY

General chaperone activity

In order to gain more insights into the impact of serine 365 phosphorylation on the function of human Hsp90β, we constructed non-phosphorylatable and phospho-mimetic variants of human Hsp90β and introduced them as sole source for Hsp90 in yeast. We used alanine replacement as non-phosphorylatable (S365A) and glutamic acid as phospho-mimetic variants (S365E) as generally utilized in the field of phosphorylation studies. We also included another non-phosphorylatable variant by asparagine replacement for serine 365, which also mimicking the corresponding residue on human Hsp90α. While the human wild-type Hsp90β protein and the phosphomimetic variant (S365E) were able to complement the lethal phenotype of the double deletion of the endogeneous yeast Hsp90 genes similarly, two non-phosphorylatable variants of Hsp90β complemented more poorly (Figure 2-9A), indicating that phosphorylation of Hsp90β is important for its full functionality at least in *Saccharomyces cerevisiae*.

The yeast cells containing only human Hsp90β protein (wild-type or mutants) also exhibited another striking phenotype: their overall size was three to five-fold bigger than that of the isogenic yeast strain that habors at least one copy of yeast *hsp90* genes (Figure 2-9B). This morphological effect demonstrated that there were abnormalities in yeast cell cycle control and it is very likely that involved proteins in this process are regulated by Hsp90. Indeed, in *Saccharomyces cerevisiae*, the kinase Cdc28 (corresponding human homolog Cdk1), the master player of yeast cell cycle, together with the Cla4 protein kinase, which is involved in septin formation and subsequently bud elongation, have been shown to interact with Hsp90 (Mollapour, S. Tsutsumi, et al. 2010; Hsieh et al. 2013) and thus, very likely are client proteins of Hsp90. Another well-known client protein of Hsp90, heat shock factor-1 (Hsf1), was also reported to be related to spindle pole body duplication (Zarzov et al. 1997), a process that eventually could lead to abnormal cell size, too. Apparently, human Hsp90 proteins are less potent in chaperoning yeast client proteins as compared to yeast Hsp90, partially due to their much weaker ATPase activity as well as their altered interactions with yeast cochaperones. Therefore, it is likely that these yeast protein kinases were less chaperoned by the human wild-type Hsp90β or variant proteins and thus, result in such morphological change.

To test whether yeast strains harbouring only human Hsp90β proteins suffered severe defects in cell cycle progression, we performed cell cycle analysis of these strains using Flow cytometry. The results confirmed that all four yeast strains containing human Hsp90β wild-type and phosphomutants were haploid with more cells were in G2/M phase than wild-type yeast carrying endogeneous Hsp90 proteins, nevertheless, no higher DNA content were observed (Figure 2-10), ruling out the possibility that cell cycle in these yeast strains were fully arrested but rather only delayed or prolonged. The budding and growth of daughter cells happened eventually.

Moreover, on top of the overall large size of yeast cells containing human Hsp90β proteins, the largest size effect belonged to the non-phosphorylatable variant S365A while phospho-mimetic variant S365E had almost an identical cell size to that of wild-type Hsp90β (Figure 2-9B). This phenotype provided us with hints that wild-type Hsp90β could be phosphorylated in *Saccharomyces cerevisiae* and phosphorylation at S365 participates in chaperone activity of the protein for cell-cycle-control client proteins.

(A)

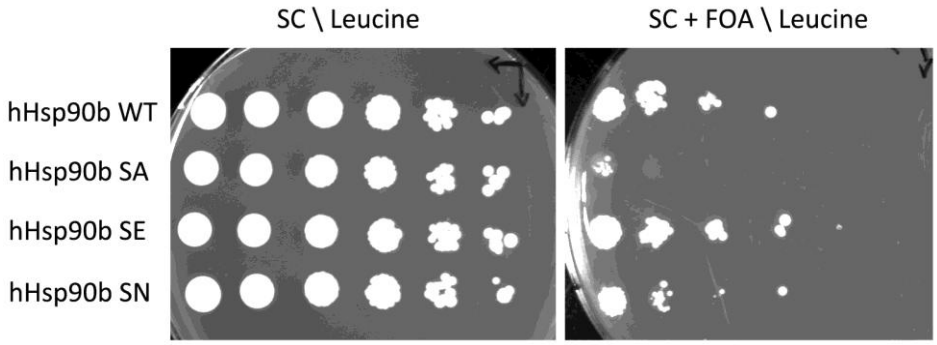

(B)

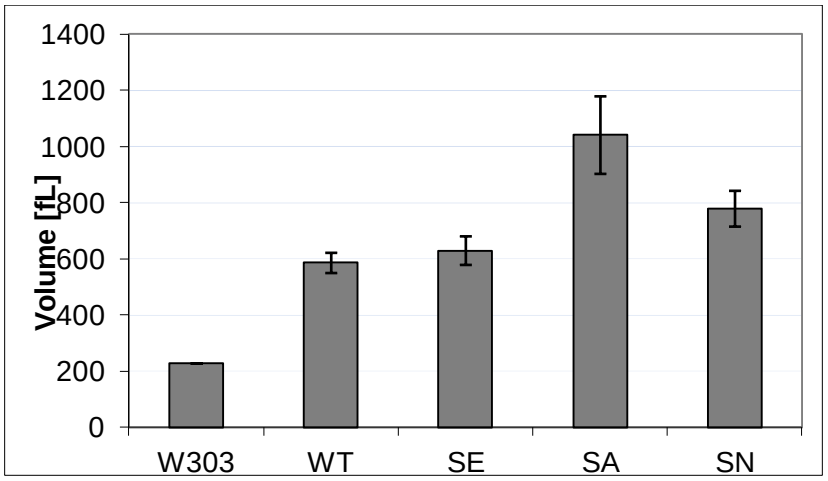

FIGURE 2-9: GENERAL IN VIVO FUNCTION AND PHENOTYPE OF YEAST CONTAINING EITHER HUMAN HSP90β WILD-TYPE OR S365 PHOSPHO-MUTANT PROTEIN AS THE SOLE SOURCE OF HSP90 PROTEIN.

(A) Complementation assay: Yeast cells containing either human Hsp90β wild-type (WT) or phosphomutant protein (SA: S365A; SE: S365E, SN: S365N), were tested whether they could complement the double deletion of both yeast Hsp90 cytosolic isoforms.

(B) The average cell volumes of yeast cells in (A): W303 is the yeast strain containing yeast Hsp90; the others are isogenic yeast strains with *hsp82* and *hsc82* genes deleted and instead the human hsp90β encoding gene on a plasmid was introduced (labeled as in A). The data are expressed as mean ± standard error of the mean (SEM) from n>=70 single cells. Experiments were performed in collaboration with R. Knieß.

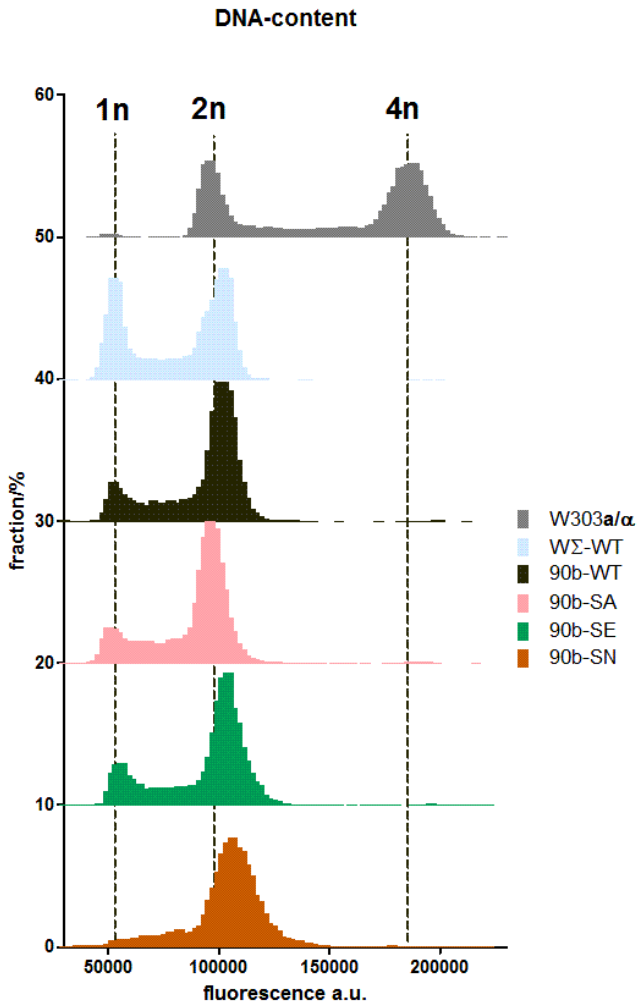

FIGURE 2-10: CELL CYCLE ANALYSIS OF YEAST STRAINS CONTAINING EITHER YEAST HSP90 OR THE ISOGENIC YEAST STRAINS CONTAINING ONLY HUMAN HSP90β AS THE SOLE SOURCE OF HSP90 PROTEIN.

W303a/α: yeast strains containing yeast Hsp90 and the isogenic strains with human Hsp90β proteins (WT: wild-type; SA: S365A; SE: S365E, SN: S365N). Experiments were performed in collaboration with R.Knieß.

Client-specific effects

Even though plating efficacy of the non-phosphorylatable Hsp90 variants on FOA medium was much lower as compared to wild-type and S365E variant, once adapted to grow with Hsp90β-S365A or S365N as sole source of Hsp90, these variants grew with slightly slower rates as compared to that of strains harbouring the wild-type (Figure 2-11). Nevertheless, they could still be utilized to query the possible role of serine 365 phosphorylation for distinct aspects of chaperone function.

R. Knieß in the lab developed GFP-based reporter assays in yeast to analyze the activity of selected Hsp90 clients, including the mammalian glucocorticoid receptor (glucocorticoid response) and three endogeneous yeast Hsp90 clients: the heat shock factor-1 HSF-1 (heat shock response), the mitogen-activated protein kinase (MAPK) Ste11 (pheromone response) and the Heme activator protein (Hap1).

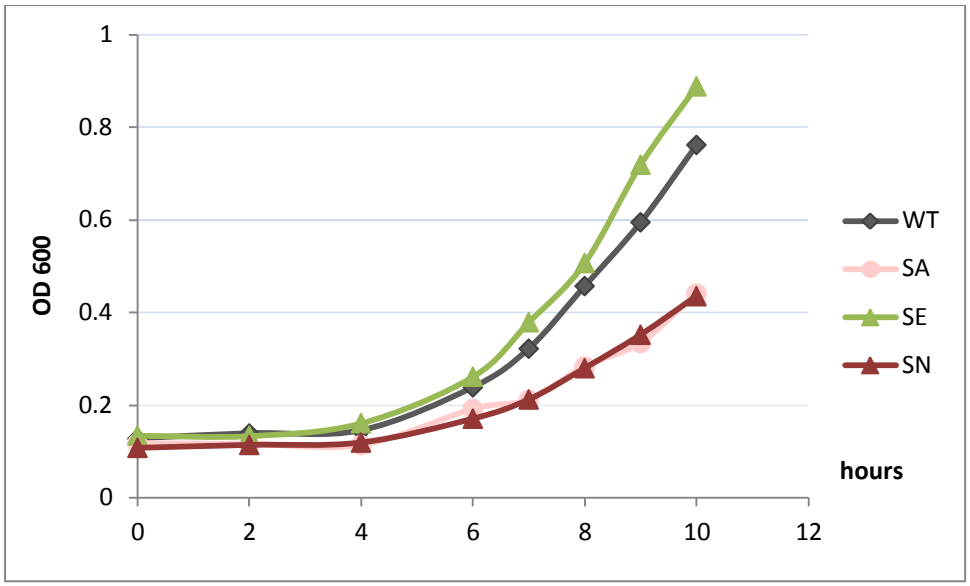

FIGURE 2-11: GROWTH CURVE OF YEAST STRAINS CONTAINING EITHER HUMAN HSP90β WILD-TYPE OR S365 PHOSPHO-VARIANT PROTEIN AS THE SOLE SOURCE OF HSP90 AT30°C.

The growth curve for WT: wild-type is in black; SA: S365A in pink; SE: S365E in green and SN: S365N in brown.

The mammalian steroid receptor GR is a well-characterized Hsp90-dependent transcription factor that has been applied as a sensitive readout for Hsp90 function in yeast in several studies (Bohen 1995; Nathan & Lindquist 1995; Chang et al. 1997; Mollapour, Shinji Tsutsumi, et al. 2010; Mollapour, Tsutsumi, et al. 2011; Mollapour et al. 2014). To examine the potential influence of S365 phosphorylation on the chaperoning of GR by human hsp90β, yeast strains with wild-type, S365A, S365E and S365N mutants were transformed with a plasmid that constituitively expressed GR. The strain was further integrated into the genome a fragment carrying glucocorticoid-response elements followed by GFP reporter gene. The cells were treated with doxycyclin to initiate the response and GFP expression was monitored in the time course of 6 hours. GFP signals in different strains were normalized by another fluorescence signals under regulation of translation elongation factor-1 (TEF) promoter which represents overall translation in the cell at the same time point. Our data showed that GR response was weakened in yeast containing S365A and S365N – the two non-phosphorylatable variants – as compared with that in yeast having human Hsp90β wild-type or S365E-phosphomimetic mutant (Figure 2-12A). Further analysis revealed that the activation rate constants for GR response of wild-type or S365E were approximately double that of the other two variants (Appendix Figure S2), which strongly demonstrated that phosphorylation of human Hsp90β-S365 was important for chaperoning of the steroid receptor GR.

Next, we employed the similar reporter system for two endogeneous yeast Hsp90 client proteins: the kinase Ste11 in pheromone response and HSF-1 in heat shock response. Ste11 is one of the kinase participated in a MAPK signaling cascade that transmit and relay mating signal in *Saccharomyces cerevisiae* (Zhou et al. 1993; Kjærulff et al. 2005). Its stability and activity require Hsp90 and Cdc37 (Louvion et al. 1998; Abbas-Terki et al. 2000). To look at the chaperoning of Ste11 by human wild-type hsp90β and phospho-mutant proteins, we constructed a pheromone response element in front of GFP gene and integrated the whole cassette into yeast genome as for GR's response element. The response was initiated by addition of alpha factor and GFP signals were measured during 7 hours. The signals were normalized as described before to overall protein translation. We obtained similar results: S365A and S365N both exhibited much reduced pheromone response than wild-type and

S365E (Figure 2-12B). The data qualified well as evidence for strong impact of S365-phosphorylation on chaperoning Ste11 kinase.

(A) Glucocorticoid response

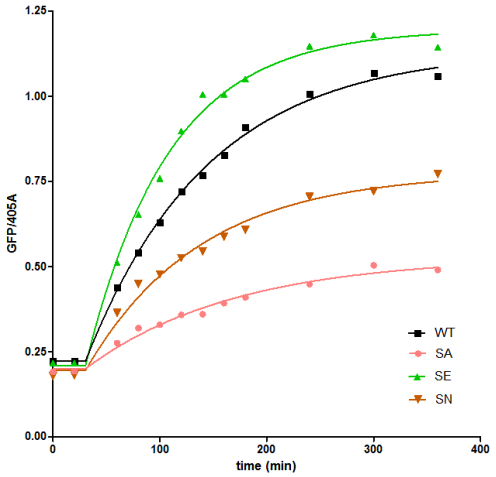

(B) Pheromone response

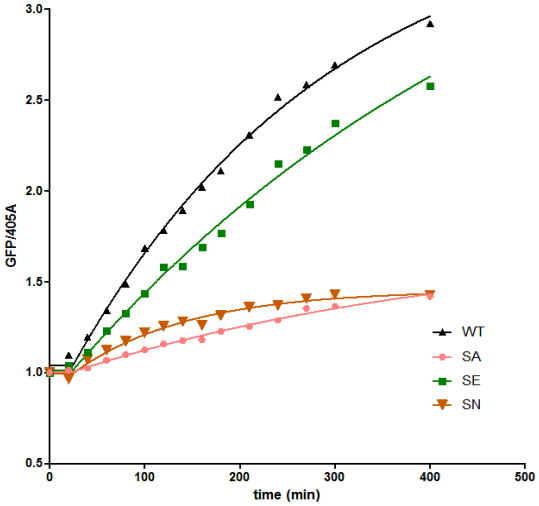

(C) Heat shock response

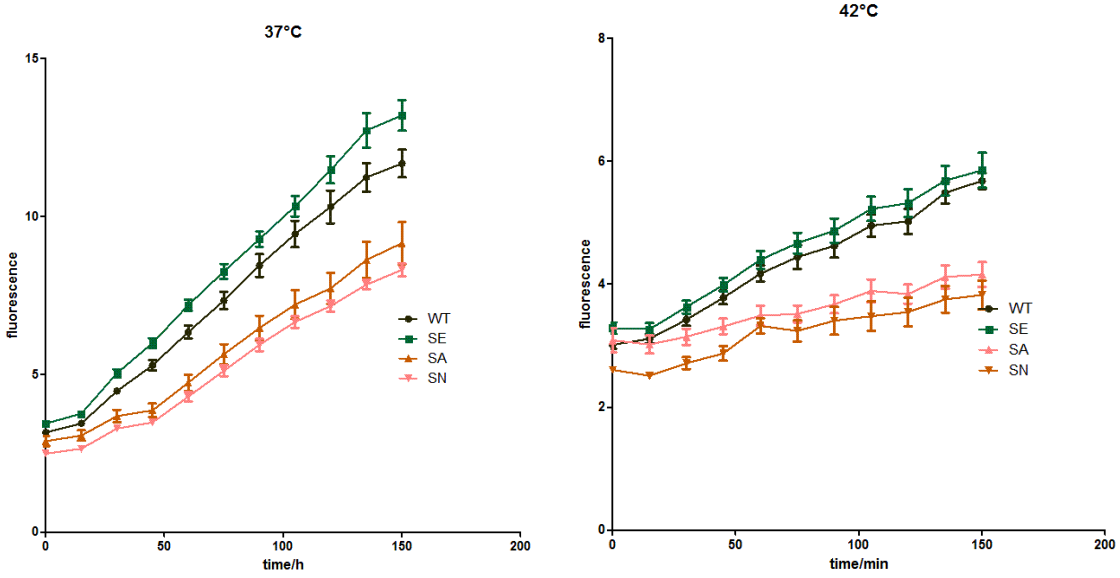

FIGURE 2-12: IN VIVO S365 PHOSPHORYLATION IS BENEFICIAL FOR HSP90 CHAPERONE ACTIVITY.

Constructs of corresponding response elements followed by GFP were introduced into yeast containing either human Hsp90β wild-type (WT); S365A (SA); S365E (SE) or S365N (SN) as the sole source of Hsp90 protein. Time-course GFP signals were recorded and normalized with the signal from TEF promoter which represent overall translation activity of each cell. In A, B and C, response signals were labeled in black for WT, pink for SA, green for SE and brown for SN.

(A) Glucocorticoid response (B) Pheromone response. (C) Heat shock response at 37°C (left) or 42°C (right).

In C, the response is expressed as mean ± SEM from 4 independent clones. Experiments were done in collaboration with R. Knieß.

In the case of HSF-1, heat shock response element was placed in front of GFP gene and integrated into the yeast genome similar as in the other cases. Yeast cells were grown at 25°C and heat shocked at either 37°C or 42°C. GFP signals and overall translation signals were monitored during 2.5 hours. The results of the heat shock response were similar to the results of both glucocorticoid and pheromone response (Figure 2-12C). Therefore, same as for glucocorticoid receptor and the MAPK Ste11, S365-phosphorylation status appears to be an important determinant for effective chaperoning HSF-1 in yeast.

Finally, we assessed the effect of S365-phosphorylation on chaperoning another Hsp90 client in yeast, HAP1. HAP1 is a heme-activated transcription factor that mediates the effects of oxygen on gene transcription in the yeast *Saccharomyces cerevisiae*. Previous studies showed that in the absence of heme, HAP1 is bound to Hsp70, Hsp40 and Hsp90 as well as other proteins in a high molecular weight complex and is repressed. Heme promotes the dissociation of the complex and activates HAP1, which in turn binds to DNA and stimulates transcription of target genes (Zhang et al. 1998; H. C. Lee et al. 2002; Lan et al. 2004). In this case, HAP1 is similar to glucocorticoid receptor, as both were kept by the Hsp90 complex in a ligand-activation-competent conformation.

We employed a heme-response element followed by GFP gene integrated into the yeast genome to examine the influence of S365-phosphorylation of Hsp90 on HAP1 chaperoning. Surprisingly, in this case, neither non-phosphorylatable mutant S365A and S365N nor phosphomimetic mutant S365E displayed significant difference as compared to wild-type (Figure 2-13).

Taken together, these data showed that the S365-phosphorylation status of human Hsp90β is not involved uniformly in all interactions of Hsp90 with client proteins. While this modification significantly influences the interaction or activity of some transcription factors and kinase include HSF-1, glucocorticoid receptor and MAPK Ste11, it seems not to participate in interaction with and chaperoning of the HAP1 transcription factor.

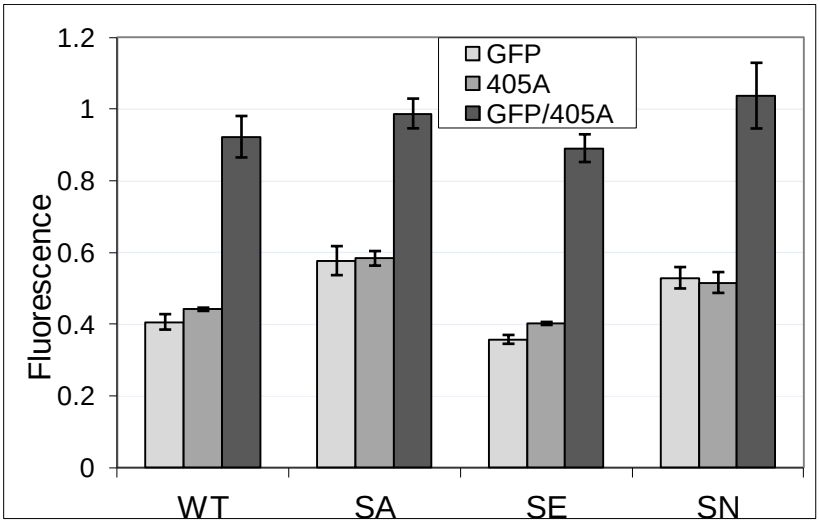

FIGURE 2-13: PHOSPHORYLATION STATUS AT S365 OF HUMAN HSP90β HAS MINIMAL IMPACT ON HEME ACTIVATOR PROTEIN (HAP) ACTIVATION

The HAP response is expressed as mean ± SEM from 4 independent clones. Experiments were performed in collaboration with R.Knieß.

2.2.3 PHOSPHO MUTANTS AT SERINE PHOSPHORYLATION SITE ALTERS INTERACTION OF HSP90 PROTEIN WITH COCHAPERONES *IN VITRO*

To elucidate the mechanism how S365 phosphorylation contributes to mediation of Hsp90 function, I purified recombinant human wild-type and phospho-mutant Hsp90β proteins from *E.coli* for *in vitro* assays. All S365 mutants behaved almost identical as wild-type human Hsp90β protein in expression and purification from *E.coli*, indicating that the overall structures of the mutant proteins were minimally affected by the amino acid exchange itself.

Limited proteolytic assay by Trypsin

A partial digestion of purified Hsp90 proteins by Trypsin was also performed. The result showed that all mutants and wild-type have indistinguishable digestion pattern (Figure 2-14), confirming that these proteins have almost equal stability under the storage conditions. Interestingly, in the presence of AMPPNP which induces the close conformation of Hsp90, subtle variations could be observed for all the phospho-mutant proteins (S365A, S365E, S365N) as compared to the wild-type protein. In general, the S365 phospho-variant proteins seemed to be more protected from tryptic digestion in the presence of AMPPNP than all other proteins as the overall digestion was delayed (see Figure 2-14 in (C) and (D)). Especially in the case of S365A, the tryptic digestion pattern was even slightly alterred with the appearance of higher molecular-weight bands, indicating that in the structure of this phopho-variant, at least one tryptic site was protected in the presence of AMPPNP. However, the differences were relatively small and thus, should not disturb significantly our subsequent *in-vitro* experiments using these purified proteins.

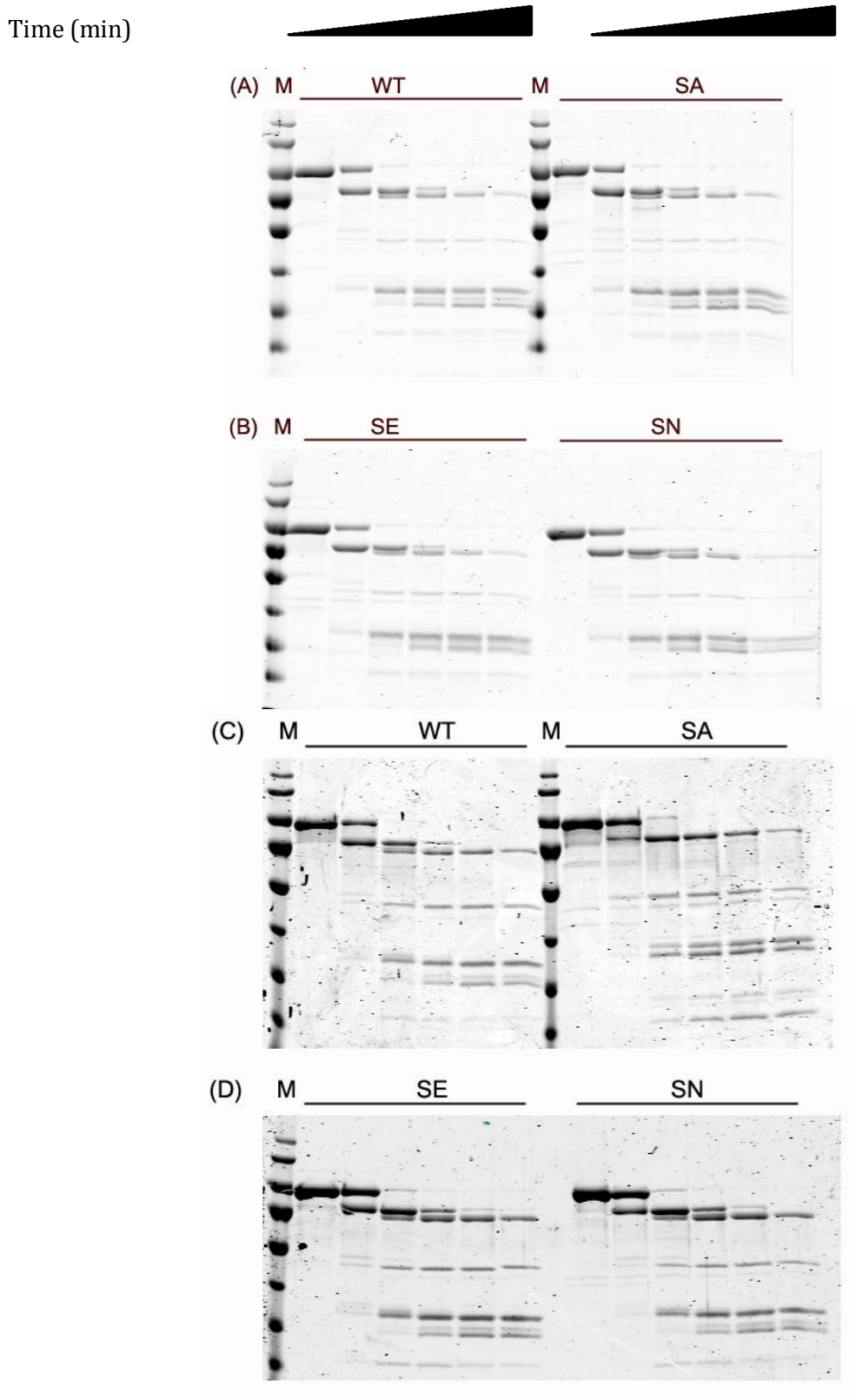

FIGURE 2-14: LIMITED PROTEOLYSIS ASSAY OF PURIFIED HSP90 PROTEINS

Purifed Hsp90 proteins (wild-type: WT, S365A: SA, S365E: SE and S365N: SN) were digested individually by Trypsin (E:S=1:100) at 37°C. At different time points (0, 1, 5, 10, 15, 20min), identical amount of each digestion reaction was taken for SDS-PAGE. In (A) and (B): without nucleotide, in (C) and (D): in the presence of AMPPNP.

***In vitro* binding to GA**

A similar pulldown experiment using biotinylated-GA was performed for purified proteins instead of cell lysates to examine whether the single S365 phosphorlyation status of Hsp90β mimicked by exchanging into glutamic acid would alter binding to GA. Besides, S365E – the phospho-mimetic variant, I also included the purified human Hsp90β and Hsp90α wild-type proteins as controls for non-phosphorylation status of Hsp90. In this experiment, the wild-type tagged Hsp90β protein (His6x-SUMO-Hsp90β) was used, enabling me to distinguish and evaluate quantitatively (if necessary) the β versus α isoform on SDS polyacrylamide gels after Coomasie staining without the need of Western blotting since any antibody for Hsp90 might recognize the isoforms with different efficiency.

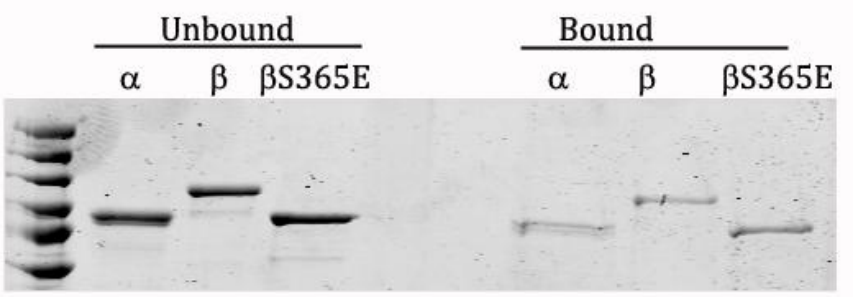

FIGURE 2-15: GA-PULLDOWN OF EITHER HUMAN HSP90 ISOFORMS AND THE PHOSPHO-MIMETIC MUTANT OF HSP90β (βS365E)

SDS-PAGE of unbound and bound fractions from GA pulldown is shown. The Hsp90β isoform was purified without cleavage of N-terminal His6-SUMO tag to allow distinguishing between two isoforms by Coomasie staining.

All three tested proteins exhibited a very similar binding behavior to GA: only a minority fraction was bound whereas the majority stayed unbound in flowthrough. Binding to GA was hardly influenced by the single S365 phosphorylation status of Hsp90β imitated by exchange of serine into an acidic amino acid. Notably, in the very similar experimental conditions (binding buffer, incubation time and temperature, amount of biotinylated-GA and streptavidin beads, etc), a bigger fraction of cellular Hsp90 (from comparable total amount in lysate input) was bound to GA as compared with purified Hsp90 (see section 2.1.1, page 40). This observation confirmed the findings reported by Kamal *et al.* that cellular Hsp90 consisted of a high-affinity conformation which differs significantly from purified Hsp90 in binding to GA and other Hsp90 inhibitors (Kamal et al. 2003).

***In vitro* glucocorticoid receptor (GR)-activation assay**

To dissect the underlying mechanism for the phenotype observed in yeast for glucocorticoid response, I reconstituted the minimal *in vitro* activation chaperone system for this client and assessed the impact of different S365 phospho mutants. A minimal activation chaperone system for glucocorticoid receptor comprises of Hsp40, Hsp70, HOP, p23 and Hsp90 (Dittmar et al. 1996; Dittmar & Pratt 1997; Dittmar et al. 1997). Earlier studies by Pratt and coworkers characterized not only these central proteins involved but also their general order in which they enter and exit the activation pathway (Y Morishima et al. 2000; Kanelakis et al. 2002) as depicted in Figure 1-2 , page 14. Most recent work by Kirschke *et al.* revealed even more interesting details referring to activity of each chaperone on GR during the process: Upon binding to the Hsp40-Hsp70 system, GR is partial unfolded, while interaction with Hsp90 then reverses this inactivation and promotes ligand binding. Together, the two chaperone system coordinate to ensure GR stability, function and regulation.

Along with other members of the steroid hormone receptor (SHR) family, GR represents one of the most stringent Hsp90 clients (Taipale et al. 2012). Similar to other proteins of the family, GR consists of three major functional domains: an N-terminal

activation domain, a DNA-binding domain (DBD) and a ligand binding domain (LBD), linked by a short, flexible hinge-region (Kumar & Thompson 1999). The receptor activity is regulated through its C-terminal ligand binding domain (LBD). All LBDs have a similar mostly helical structure with the ligand binding pocket located in the core of the protein. In the absence of ligand, LBDs are assumed to be dynamic, while the ligand provides both structural stability for LBD and allosteric control of the LBD's ability to interact with co-regulator proteins to modulate transcription (Bain et al. 2007). This important domain is also the interaction part of GR with Hsp90 (Howard et al. 1990). The *in vivo* function of GR strictly depends both on the interaction of the GR-LBD with the Hsp90 chaperone machinery and chaperone activity from the chaperone complex (Bresnick et al. 1989; Picard et al. 1990; Bohen 1995). Like most stringent Hsp90 clients, biochemical studies of GR have been hampered by the difficulty to obtain stable and functional apo protein for *in vitro* investigations. Since the wild-type GRLBD is a rather unstable and poor-soluble protein, I utilized a single solubility enhancing mutation (F602S) to obtain workable quantities of GRLBD while making least change to the wild-type protein (Bledsoe et al. 2002; Ricketson et al. 2007; Seitz et al. 2010; Lorenz et al. 2014). The GRLBD(F602S) were also purified in the apo state with an N-terminal MBP tag since it enhanced stability over long experimental time courses. This N-terminal MBP tag had already been verified to not interfere with *in vitro* experiments using the same chaperone system (Kirschke et al. 2014). MBP-GRLBD(F602S), referred to as GRLBD unless otherwise specified, was purified in the presence of ligand (dexamethasone) followed by extensive dialysis to remove the ligand.

Ligand binding was monitored by microscale thermophoresis measuring the alterations in thermophoretic mobility behavior of fluorescein labeled dexamethasone (F-dex) as it is bound to GRLBD. Taken into account that the ligand affinity of GRLBD was unaffected but rather the fractions of ligand-binding competent proteins were differentially affected by the minimal chaperone system, we fitted the data using the quadratic equation for tight-binding substrates (see section 3.2.3) to calculate this ligand-binding competent fraction with the constraint of a constant dissociation constant (Kd). We applied the Kd of 150nM as reported by Kirschke *et al*, 2014 in which very similar experimental conditions were used. The ligand-binding competent fraction from here on will be referred to as "active fraction".

In our experiments, GRLBD was partially unfolded by the Hsp70-Hsp40 system, which was in agreement with the study by Kirschke *et al*, 2014. Also, addition of Hsp90 together with the cochaperones HOP, p23 led not only to restoration of active GR fraction as in the absence of chaperones and adaptor proteins but also to further enrichment this active fraction. The highest ligand-binding competent fraction of GRLBD was obtained in the presence of the minimal chaperone system with Hsp90β S365E phosphomimetic variant (

Figure **2-16**), indicating that this variant exhibited an enhanced chaperone activity for GRLBD as compared with all other Hsp90 tested in this experiment. Of note, the wild-type Hsp90β protein as expressed and purified from *E.coli* was absolutely in non-phosphorylated form and therefore, behaved similar to S365A and S365N in this *in-vitro* experiment as expected.

This result confirmed the positive effect of phosphorylation at S365 of human Hsp90β for GR response although with a lesser extent than observed in the *in-vivo*-system. The variations in modulation capacity of S365 phosphorylation in *in-vivo*- versus *in-vitro*-experiments could be explained by several possible reasons. First, in the yeast reporter system, we observed not only higher maximal response but also increased in activation rate of wild-type and S365E phospho-mimetic mutant than S365A and S365N nonphosphorylatable mutants (Figure 2-12). Therefore, additional time-course *in-vitro*-experiments may provide more comparable effects between the S365 phospho-mutants with

results in *in-vivo* model. Secondly, in contrast with *in-vivo* settings, *in-vitro* reactions included only the minimal chaperone system of most important proteins involved in the chaperoning process of GR. Additional factors such as the Cyp40/Cpr6 which was shown to also be present in the Hsp90-GRLBD-HOP complex (Lorenz et al. 2014) might be responsible for another enhancement onto the final response that was observed in yeast. Since for most tested clients including not only glucocorticoid receptor but also heat shock factor and Ste11 kinase, the S365E phosphomimetic variant provided better chaperone effect than S365A and S365N non-phosphorylatable variants, it is equally possible that the impact of phosphorylation is direct on client interaction(s) or indirect via cochaperone(s) that participate in the Hsp90-client complex, or the combination of both. The latter possibility also has been studied and is described in the next part.

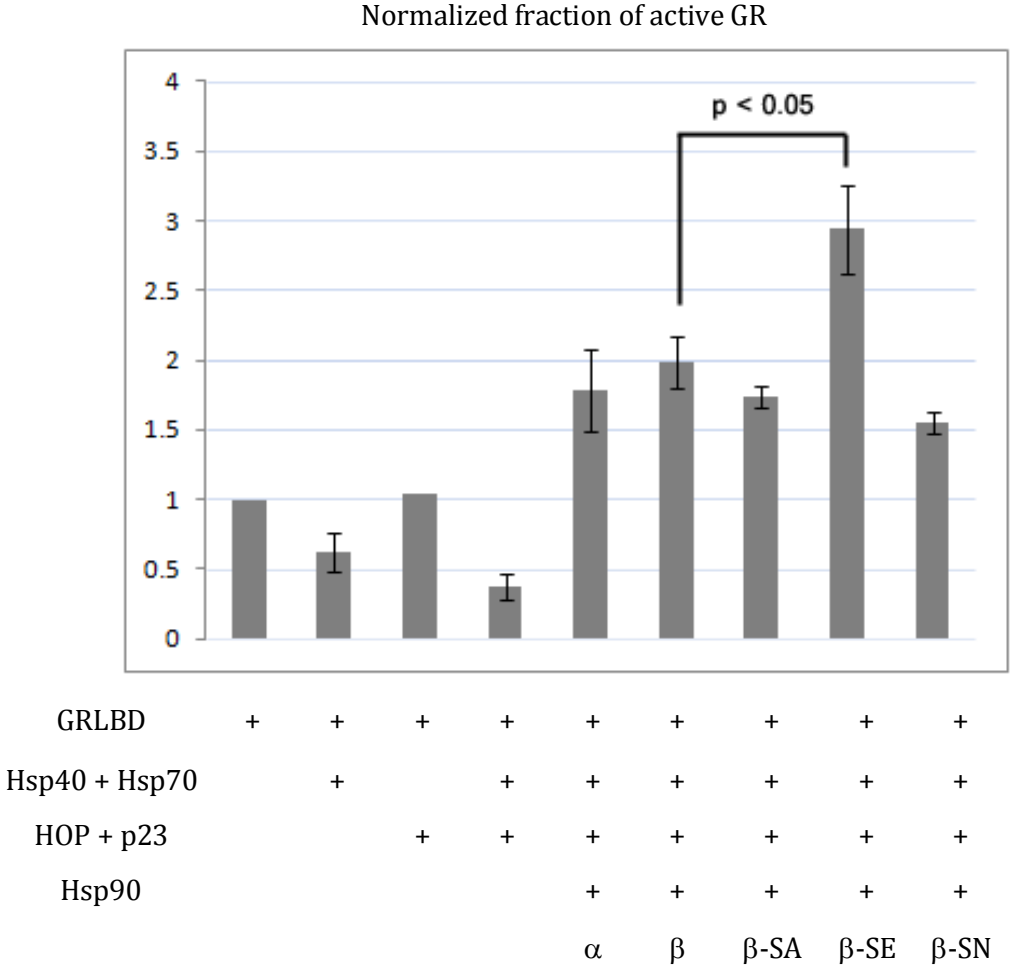

FIGURE 2-16: PHOSPHOMIMETIC VARIANT (S365E: β-SE) OF HSP90β EXHIBITED ENHANCED CHAPERONE ACTIVITY IN *IN VITRO* MINIMAL GR-ACTIVATING SYSTEM

as compared with human Hsp90α (α), human Hsp90β wild-type (β) and non-phosphorylatable variant proteins (S365A: β-SA and S365N: β-SN). The minimal GR-activting system includes Hsp70, Hsp40, HOP, p23 and different Hsp90 proteins. The activity of activated GR was measured as binding affinity to fluorescein dexamethasone using microscale thermophoresis. SEM were calculated for 2-3 repeats. A Student's t-test was performed for the system with the wild-type Hsp90β and S365E protein.

Another difference in the experimental setup for *in-vivo* vs *in-vitro* experiments was the output that I monitored. In the system consisted of purified chaperones and cochaperones that activate GR, binding to F-dex was measured as indicator for GR's activity; whereas in the yeast model system, transcriptional activation activity of GR was recorded. It

is proven that Hsp90 does not involve only in restoring the binding capacity of GR for ligand but also in later events as the GR-Hsp90 complex is translocated into the nucleus. S365 phosphorylation might also have an impact on these subsequent steps such as altering the transport of GR-Hsp90 complex into the nucleus or the release of ligand-bound GR from Hsp90 complex. These later steps from ligand binding to activation of target genes of GR response were not investigated in the *in-vitro* experiments. Further dissecting of these possibilities using *in-vitro* system would be quite challenging as well.

Last but not least, different constructs of glucocorticoid receptor were utilized in the two systems: full-length wild-type rat glucocorticoid receptor in the yeast model and GRLBD(F602S) in biochemical experiments. The F602S mutant I employed in the purified-protein system was shown to be less dependent on Hsp90 *in vivo* in a way that it responds to lower concentrations of dexamthasone than does wild-type GR as well as still retains partial response upon reduction of Hsp90 levels or in presence of geldanamycin (Bohen 1995; Ricketson et al. 2007). IP experiments also indicated that the F602S mutant binds with less affinity or more transient with Hsp90 (Ricketson et al. 2007). However, it should be emphasized that signal transduction by wild-type and F602S GR was similarly affected by a number of Hsp90 mutants, and, more importantly, the individual Hsp90 mutants followed the same order of severity within the spectrum of mutant (Bohen 1995). So in principle, Hsp90 functions in a similar manner to chaperone both wild-type and F602S mutant and the F602S mutant is still valid as an effective tool for testing effects of Hsp90 mutants. Nevertheless, I could not completely rule out the possibility that dependency of the F602S mutant on Hsp90 chaperone activity for ligand binding is lower than that of wild-type glucocorticoid receptor.

Interaction with cochaperones

I also looked at the effect of S365 phosphorylation on association with different cochaperones using the purified phospho-mutant and wild-type proteins. In these *in vitro* experiments, in contrast with *in vivo* models, I expected to observe distinguished impacts between S365E phosphomimetic variant and all three other Hsp90 proteins including wild-type protein and non-phosphorylatable variants S365A and S365N, since wild-type Hsp90β protein expressed and purified from *E.coli* was also not phosphorylated.

HOP (Hsp70/Hsp90 organizing protein)

The Hsp70/Hsp90 organizing protein HOP has the unique ability to interact with both Hsp70 and Hsp90. This simultaneous binding of HOP to the two chaperones is critical for coordination between these systems as it facilitates client transfer which is the first step and prerequisite for later folding process on the Hsp90 system. Since detected in many Hsp90-client complexes, HOP is referred to as a general cochaperone required for chaperoning most Hsp90 clients even though on its own this protein has no chaperoning activity. For that reason, it is comprehensible to hypothesize that the effects I observed in the yeast model system for different client proteins were mediated via such a general cochaperone like HOP.

To study the interaction of HOP and human hsp90β wild-type or S365 phospho-mutants, I employed size-exclusion chromatography (SEC) and purified proteins. HOP and Hsp90 protein(s) were incubated for 30min at 30°C with a 1:1 molar ratio to form the complex. Each protein alone was also prepared in the same buffer and incubated under identical conditions as controls. The protein alone or mixture(s) was then loaded onto a Superdex 200 analytical column and elution fractions were analyzed on SDS-PAGE. The difference in size of HOP (60kDa) and Hsp90 proteins (90kDa) allowed me to identify those proteins in the elution fractions without the need of further confirmation method such as Western blotting.

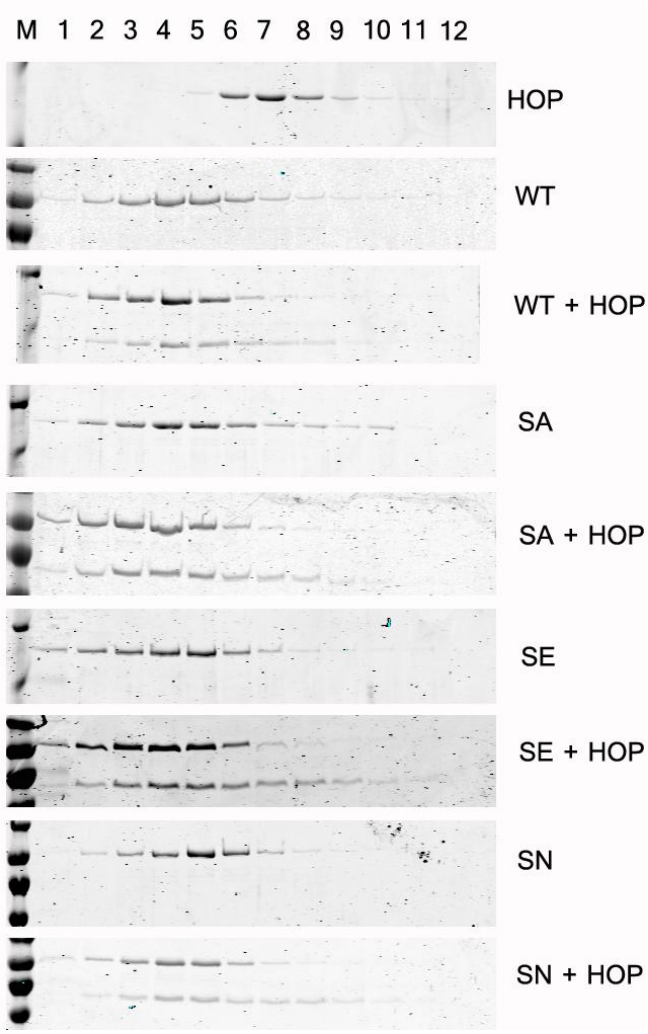

FIGURE 2-17: INTERACTIONS OF PURIFED HUMAN WILD-TYPE HSP90β AND S365 PHOSPHO MUTANT PROTEINS WITH HOP ARE HIGHLY SIMILAR.

SDS-PAGE of size-exclusion chromatography fractions (1-12) from a Superdex 200 PC 3.2/30 analytical column of HOP or human Hsp90β wild-type (WT) and S365 phospho-mutants (S365A: SA; S365E: SE: S35N: SN) as single protein alone and each Hsp90 protein forming complex with HOP as indicated.

As expected, HOP eluted in later fractions than Hsp90 proteins when each of them was injected alone. However, when HOP was incubated with either wild-type Hsp90β or S365 mutant proteins, a complex was successfully formed as HOP protein was shifted to co-elute with Hsp90 in higher molecular weight fractions (Figure 2-17). I observed no significant variation between complex formation of HOP and all Hsp90 proteins, indicating that S365 phosphorylation has no effect on association of HOP and human Hsp90β under these conditions. Of note, in this interaction experiment with HOP and the *in-vitro* assay using the minimal GR-activating system, the similar experimental conditions which Hsp90 : HOP molar ratio is 1:1 was applied. No significant difference was observed in interaction of Hsp90 proteins with HOP, indicating that the improved impact of S365E and cochaperones for GR activation was not likely to originate from indirect alterations in interaction of S365E and this cochaperone. It is intriguing, though, to see how HOP and those cochaperones that are already included in the minimal GR-activating system such as Hsp70 and p23 would interact with Hsp90 when they are used with lower physiological concentrations (in substoichiometric ratio as compared to Hsp90 proteins). It is possible that under those conditions, a binding preference to one variant could be revealed.

Aha1 (Activator of Hsp90 ATPase activity-1)

Aha1 is the only Hsp90 cochaperone that can accelerate the weak ATPase activity of Hsp90. Nevertheless, the contribution of Aha1 to Hsp90 chaperone activity is still enigmatic. While for some clients such as ErbB2, v-src, Cdk4, c-Raf, etc, Aha1/Hsp90 interaction is proven to be important (Panaretou et al. 2002; Lotz et al. 2003; Holmes et al. 2008; Mollapour, Tsutsumi, et al. 2011), for some others such as HSF, GR and CFTR, the decreased Aha1 interaction with certain Hsp90 post-translational modified variants seems to have minimal or even beneficial effects (Mollapour, Tsutsumi, et al. 2011; Mollapour et al. 2014). The various influences are obviously client-specific or cellular Aha1 concentration-dependent, representing a complicated relationship of modulation between this cochaperone and Hsp90 protein.

The involvement of Aha1 in chaperoning HSF1 and GR makes it a candidate for our *in vitro* investigation of the impact from S365 phosphorylation on Hsp90 chaperone based on the results from the yeast reporter system. Moreover, the majority of its interaction surface with Hsp90 is along the chaperone's middle domain, where S365 phosphorylation site is located even though on the opposite side.

I also performed similar SEC experiments to look at complex formation between purified human Hsp90β protein(s) and (yeast) Aha1, however, very little complex was observed under similar conditions as for HOP despite my several attempts by modifying the incubation duration and presence of nucleotide (data not shown). Hence, I labeled (yeast) Aha1 with Hilyte 488 C2 maleimide and used it in only substoichiometric amount with Hsp90 to shift Aha1 as much as possible into the complex. The fluorescence labeling provided me with the necessary sensitivity to detect such small quantities of Aha1 in complex with Hsp90. Despite the low efficiency of complex formation between human Hsp90β(s) and (yeast) Aha1, fluorescence detection coupled with SEC enabled me to assess differences between human Hsp90β wild-type and S365 phospho-mutants in binding with Aha1.

Indeed, S365E phosphomimetic mutant displayed a diminished complex amount as compared with all other Hsp90 proteins including wild-type and nonphosphorylatable variant proteins (Figure 2-18). This observation is similar to another recently reported phosphorylation on human hsp90α (T36) which also attenuates Hsp90 interaction with Aha1 and displayed enhanced chaperone activity for GR (Mollapour, Tsutsumi, et al. 2011) although these two phosphorylation sites seem to be unrelated. However, investigation of T36-phosphorylation only showed in GR activation assay elevated effect of the phospho-mimetic variant (T36E) over wild-type and non-phosphorylatable variant (T36A) in yeast and human cells, suggesting that the protein is not phosphorylated at this position *in vivo*. Our data demonstrated a different scenario, as both wild-type and phospho-mimetic variant (S365E) exhibited similar *in vivo* activation levels and higher than that in case of two other non-phosphorylatable variant (S365A and S365N). The wild-type protein seems to be phosphorylated at S365 in yeast. Moreover, the modulation amplitude of S365 phosphorylation was less than that of T36, suggesting an intermediate level of regulation provided by this S365 phosphorylation for Hsp90β.

(A)

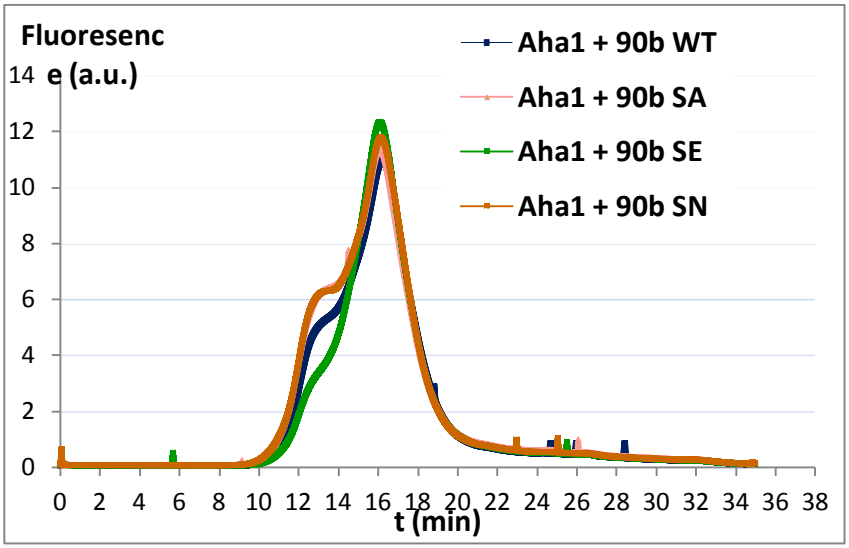

(B)

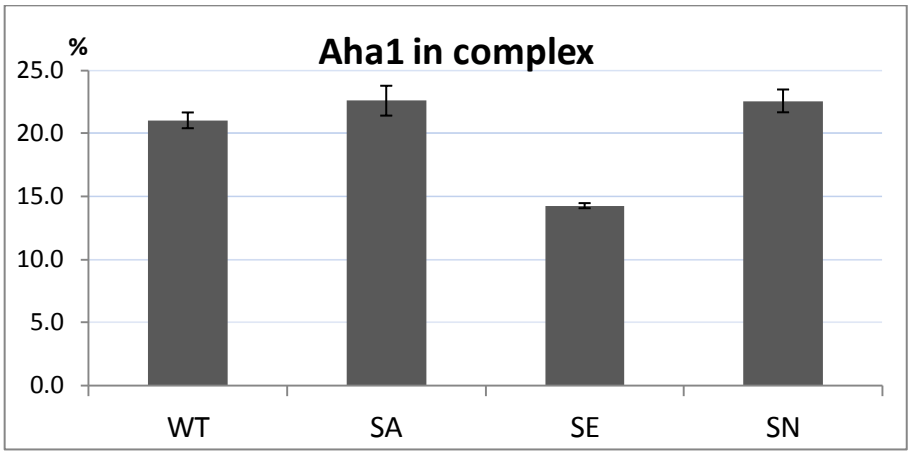

FIGURE 2-18: REDUCED INTERACTION OF PURIFED HUMAN HSP90β S365E (SE) PHOSPHOMIMETIC MUTANT WITH AHA1

as compared with wild-type (WT) and nonphosphorylatable mutants S365A (SA) and S365N (SN).

Aha1 protein was labeled with Hilyte 488 C2 maleimide and incubated with purified human Hsp90β protein(s) for 15minutes at 30°C before loaded onto a Superdex 200 PC 3.2/30 analytical column. Both UV280 and fluorescence signals were recorded.

(A) Overlay of fluorescence detection coupled with SEC for samples containing labeled Aha1 and different human Hsp90β protein(s): WT (blue), SA (pink), SE (green) and SN (brown).

(B) Quantification of Aha1 in complex as percentage with total Aha1 by summation of fluorescence signal detected in time duration from 10-13.75min in SEC elution profile. The values are expressed as average ± SEM from 2 independent repeats.

Cdc37 (Cell division cycle 37 protein)

Cdc37, one of the essential cochaperones of Hsp90, plays a specialized and crucial role in the maturation of many members from the protein kinase family, an important class of Hsp90 clients, such as EGFR, v-src, Lck, Raf-1, Cdk4, etc. Cdc37 acts as an adaptor to load these kinase clients onto the Hsp90 complex for further conformational activation. Even though the impact of S365 phosphorylation we observed in yeast model was not limited to the only kinase client Ste11 that we used, it is possible that these impacts can be mediated via

interactions of modified Hsp90 with Cdc37 as a few studies have shown that this cochaperone is not completely restricted to kinases as substrates (Rao et al. 2001; X. Wang et al. 2002). Therefore, I decided to investigate the interaction of human wild-type Hsp90β or phospho-variant proteins with human Cdc37 using purified proteins. Similar SEC was performed to assess complex formation between purified human Hsp90β protein(s) and human Cdc37 under similar conditions as for HOP. The results were also comparable to the case of HOP (data not shown). However, taken from the experience with HOP, I further investigated binding of Cdc37 and Hsp90(s) using isothermal titration calorimetry (ITC) since Cdc37 could be conveniently purified and concentrated to high concentration to be used in ITC. While this is not the case for Aha1, similar labeling as for Aha1 was not applicable for human Cdc37 due to the presence of 9 cysteines in total on this protein, which would definitely complicate the labeling outcome. The ITC result provided us with evidence that the phospho-mimetic variant S365E binds Cdc37 with an impaired affinity while both two non-phosphorylatable variants (S365N and S365A) binds with similar affinity as compared with wild-type human Hsp90β in the simple context of purified proteins (Figure 2-19 and Table 2-5).

The decreased binding of Cdc37 is quite complicated to correlate with client activation effect. Partially it is due to the complexity and dynamic nature of Cdc37-and-Hsp90-mediated protein kinase activation cycle as depicted in Figure 1-8 from work of Neckers and colleagues: several phosphorylation and dephosphorylation events needs to happen in a sequential order to drive the cycle unidirectionally (Xu et al. 2012). The impact of S365 phosphorylation on Hsp90β seems to relate with Y313 phosphorylation on Hsp90α: they both weaken Hsp90-Cdc37 interactions. Nevertheless, it depends on the timing of phosphorylation/dephosphorylation in the cycle to decide whether their biological relevance is really similar. The couple of S365 phosphorylation with one or another phosphorylation site involved might help to integrate the role of S365 phosphorylation (if any) into the cycle. The presence of a kinase client might also be necessary. As S365 phosphorylation significantly affects Cdc37 binding to Hsp90 in a negatively way, it is potential that this phosphorylation event occurs to displace Cdc37 out of Cdc37-kinase client-Hsp90 complex and even prepares for association of another cochaperone that acts downstream in the complex, however, not Aha1. Looking from another angle, dephosphorylation of S365 phosphorylation (probably by PP5) may free a sub-population of Hsp90 (that for e.g. engaged by other cochaperone and clients) so that Cdc37 can bind effectively for the kinase activation cycle to start.

	WT	**SA**	**SE**	**SN**
Kd (μM)	0.83 ± 0.14	1.21 ± 0.25	6.08 ± 2.02	0.59 ± 0.1

TABLE 2-5: DISSOCIATION CONSTANTS OF HUMAN HSP90β WILD-TYPE OR PHOSPHO-VARIANT PROTEINS TO CDC37 IN VITRO.

The dissociation constants (Kd) were calculated from ITC data using Origin software and are expressed as average ± SEM from 2 independent measurements.

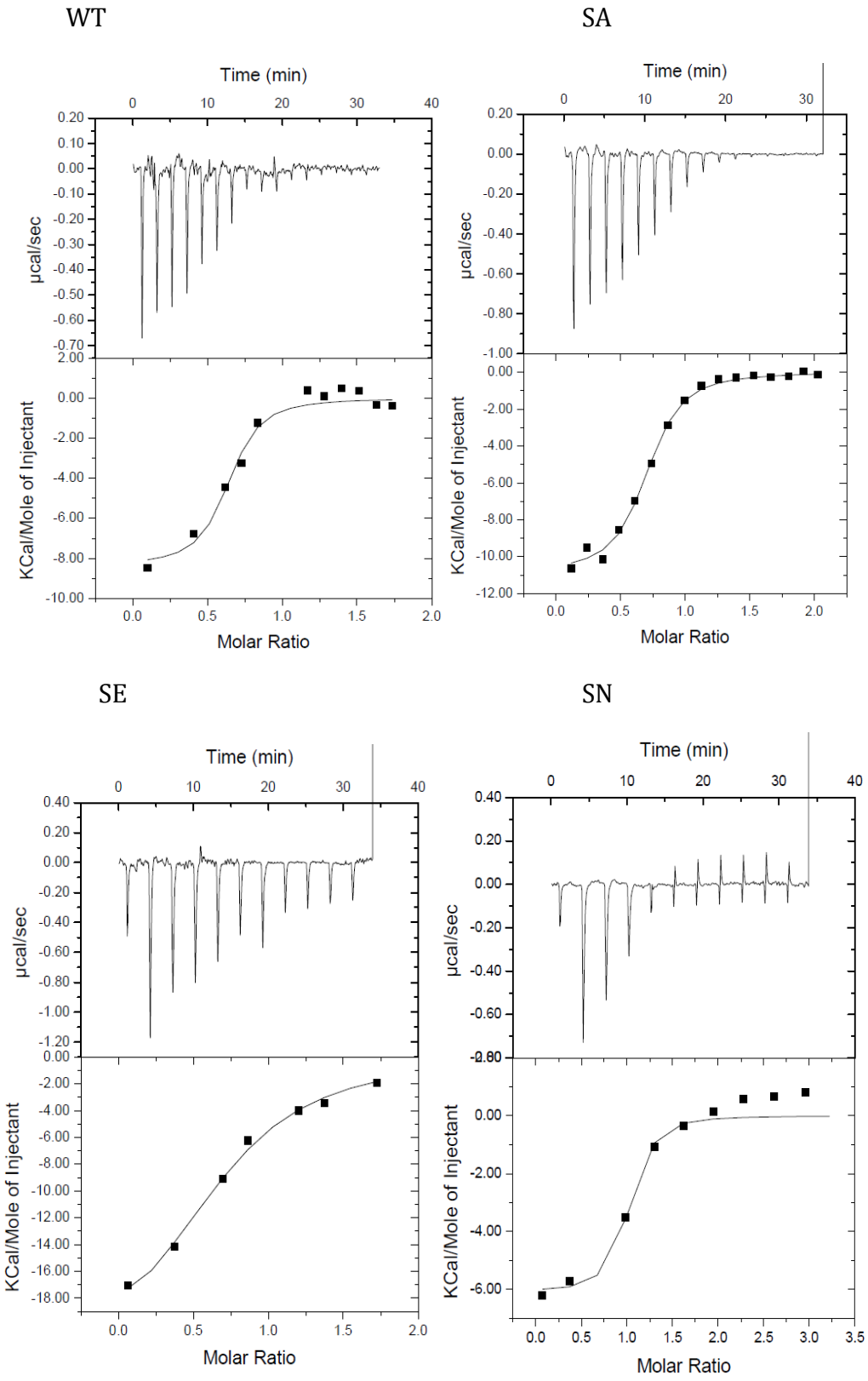

FIGURE 2-19: HUMAN HSP90β S365E PHOSPHOMIMETIC MUTANT EXHIBITED AN IMPARED AFFINITY FOR CDC37

as compared with wild-type (WT) and non-phosphorylatable mutants S365A (SA) and S365N (SN).

Isothermal titration calorimetry (ITC) profile of human Cdc37 binding to human Hsp90β wild-type or variant proteins. Titrations of 300-400µM Cdc37 into 30-35µM Hsp90 protein(s) were measured on a Microcal ITC200 microcalorimeter at room temperature. Both proteins were dialyzed into buffer containing 25mM Hepes, 50mM KCl, 5mM $MgCl_2$ and 10% glycerol. The raw data (top panels) and their integrated data (bottom panels) of heat

changes are shown. Integrated data were fitted using a non-linear least square fit to one site model by Origin software (OriginLab).

2.2.4 CONCLUSIONS

Inspired from the results of previous part, we set out to characterize the phosphorylation at serine 365 in human Hsp90β. This phosphorylation site is quite interesting as it is located in the middle domain of Hsp90, where a number of both cochaperone and clients already share binding surface. Although the position of S365 in 3D structure limits its phosphorylation when Hsp90 is in the closed form, it is still probable that the site can be phosphorylated at other steps in the conformational cycle of Hsp90 or at times when the kinase is directly recruited to Hsp90 as client or cofactors. This is in line with our predicament in MS detection for this specific phosphorylation site since it is highly likely that S365-phosphorylated Hsp90 form is not the dominant form of Hsp90 or easy to be "caught in the act". This was also further supported by the fact that at the time we first detected this serine phosphorylation in human Hsp90β, despite the fact that several of Hsp90 phosphorylation sites are detected in proteomics studies, the site was not reported. Only much later, it was confirmed to be phosphorylated in human ES and iPS as well as Jurkat cells (T-cell leukemia cell line) by two independent studies (Phanstiel et al. 2012)(Phosphosite database). Surprisingly, the sequence surrounding matches well with CK2-recognition motif which suggests constitutive phosphorylation due to the constitutive activity as well as ubiquitous distribution of the kinase. However, since one of Hsp90 cochaperone is the phosphatase PP5 and together with the specific position of S365, it would still be regulatable and can cycle between phosphorylated and dephosphorylated states.

The most recent publication highlighting the client binding surface of Hsp90 and Tau has provided also additional evidence for us that the serine 365 is indeed very close to and might as well directly participate in interaction with Tau and other client proteins. It is conceivable that phosphorylation at this position could have significant impact on client binding of Hsp90. Using a reporter system in which the activity of downstream GFP placed under response elements that is regulated by Hsp90 clients such as glucocorticoid receptor, heat shock factor, Ste11 and heme-activated protein, we were able to monitor the impact of human Hsp90β either wild-type or phospho-mutant proteins when they are expressed as the single source of Hsp90 chaperone in yeast cells. As an improvement, we added to the classical experimental design of Hsp90 reporter-systems the use of fluorescence-activated cell sorting (FACS) device for readout. In this way we could further select out the non-responding population of yeast cells (which are dead or cell cycle-arrested) that would otherwise affect our averaging across total population. The utilization of GFP as output signal and FACS also enabled us to circumvent the cell lysis step, which is quite tedious for yeast cells and might result in partial lysis, as well as the enzymatic reaction step that was required for β-galactose or luciferase activity assay. Therefore, we could process more samples for one assay while monitoring in addition the overall growth and viability of yeast cells during the response to the treatment. Our data supported the hypothesis that S365 phosphorylation could influence Hsp90 in client interaction in a beneficial manner. All reporter systems, except heme activator protein (HAP), displayed a uniform general pattern of impact in which both the wild-type protein and phospho-mimetic variant (S365E) chaperoned Hsp90 client better and resulted in faster and/or higher expression level of the downstream GFP reporters than both non-phosphorylatable variant (S365A and S365N). On the one hand, the wildtpye Hsp90β protein seems to be phosphorylated at S365 in yeast cells and S365 phosphorylation seems to promote the chaperone activity of Hsp90 for important clients such as GR, Hsf-1 and Ste11. On the other hand, our findings indicate that other specific client proteins like HAP may utilize other binding surfaces or is chaperoned by Hsp90 in another manner that does not

require S365 phosphorylation. Moreover, our *in vivo* experiments cannot exclude the involvement of altered cochaperone interaction caused by the variants. The final observation could be the summation of both impacts or of single one, depending on the specific case. This was further supported by our Hsp90-cochaperone interaction studies.

In these *in-vitro* experiments, we expected that the wild-type Hsp90β protein exhibits a similar behavior as the two non-phosphorylatable mutant proteins (S365A and S365N) due to the lack of post-translational modification from *E.coli* expression and purification while the phospho-mimetic variant, S365E, should display a different behavior. By reconstituting the minimal GR-activating system using purified proteins, we confirmed the enhanced activating effect that S365E, the phospho-mimetic variant, exerts on ligand binding activity of GRLBD while the wild-type joins the other two non-phosphorylatable mutant proteins in having lower activating impact. The S365E variant is also the only protein that displays impaired affinity for Aha1 and Cdc37. While both cochaperones contribute certain significant roles in activation of specific clients, the impaired affinity to both of them might help drive the cycle in another direction(s) or provide preferences for other cochaperones. More experiments such as combination of S365 phosphorylation with other modifications on Hsp90 and/or cochaperone(s) in the presence of specific client proteins would be necessary to decipher the exact role of S365 phosphorylation in the chaperone cycle.

3 MATERIALS AND METHODS

3.1 MATERIALS

3.1.1 CHEMICALS

All chemicals were analytical grade and obtained from Roche, Sigma, Merck and Roth if not otherwise stated.

3.1.2 MICROORGANISM STRAINS AND CELL LINES

E. coli strains

Name	Genotype / Description	Source
E. coli TOP10F´	*F´ g mcrA D(mrr-hsdRMS-mcrBC) f80lacZDM15 DlacX74 deoR recA1 araD139 D(ara-leu)7697 galU galK rpsL (StrR) endA1 nupG*	Lab collection
E. coli CJ236	*FΔ(HindIII)::cat* (Tra$^+$ Pil$^+$ Cm^r)/ *ung-1 relA1 dut-1 thi-1 spoT1 mcrA*	Lab collection
E. coli Rosetta (DE3)	F$^-$ *ompT hsdS*$_B$(r$_B^-$ m$_B^-$) *gal dcm* (DE3) pRARE (argU, argW, ileX, glyT, leuW, proL) (Cm^r)	Lab collection
E. coli C2925 (*dam*$^-$*dcm*$^-$)	*ara-14 leuB6 fhuA31 lacY1 tsx78 glnV44 galK2 galT22 mrcA dcm-6 hisG4 rfbD1 R(zgb210::Tn10) Tet^r endA1 rspL136(Str^r) dam13:Tn9 (Cam^r) xylA-5 mtl-1 thi-1 mcrB1 hsdR2*	New England Biolabs

S. cerevisiae strains

Name	Genotype / Description	Source
W303Σ	On the background of W303 strain with *mip1*[Σ]*ade2*	Robert Knieß
W303ΣΔPN6ΔCH2 RP	On the background of W303Σ with *hsp82::nat hsc82::hygromycin* and pRS416-pHsp82-*hsp82*	Robert Knieß
W303Σ-TS4x	On the background of W303Σ integrated with pTEF-T.Sapphire 4x from pRS304 vector	Robert Knieß
W303Σ-TS4x-GRE	On the background of W303Σ-TS4x and integrated with (pMetLR-His-GRE-Sf4xGFP) ^{2x}	Robert Knieß
W303Σ-TS4x-GRErGR	On the background of W303Σ-TS4x-GRE and integrated with pLysLR-Met-(pTEF-rGR) ^{2x}	Robert Knieß
W303Σ-TS4x-HSE	On the background of W303Σ-TS4x and integrated with (pMetLR-His-HSE-Sf4xGFP) ^{2x}	Robert Knieß
W303Σ-TS4x-PRE	On the background of W303Σ-TS4x and integrated with (pMetLR-His-PRE-Sf4xGFP) ^{2x}	Robert Knieß
W303Σ-TS4x-HapRE	On the background of W303Σ-TS4x and integrated with (pMetLR-His-HapRE-Sf4xGFP) ^{2x}	Robert Knieß

3.1.3 PLASMIDS & OLIGONUCLEOTIDES

Plasmids

Name	Description	Source
pCA528 (= pSUMO)	pET24 based with N-terminal His6-Smt3-Ulp1 site(SUMO)-tag, T7 promotor, Kan ^{R}	Dr. C. Andreasson
pSUMO-hHsp90b	His6-SUMO-hHsp90β wildtype	Dr. C. Graf
pSUMO-hHsp90b-S365A/E/N	His6-SUMO-hHsp90β S365A/E/N	This work
pRS415-pHsp82-hHsp90b-pHsc82-	pRS415 based with 2x constructs of human Hsp90β wildtype genes, each under promoter of	This work

hHsp90b (pRS415-2x hHsp90b)	the yeast homologs	
pRS415- 2x- hHsp90b S365A/E/N	Similar as above, but the corresponding phospho-mutant gene instead of wildtype	This work

Oligonucleotides

Primer name	N°	Sequence	Notes
hHsp90b-NheI-F	359	ATGgctagcCCTGAGGAAGTGCACCAT	PCR hHsp90β gene
hHsp90b-SalI-Rrc	360	CAGTGTCGACGATCTAATCGACTTCTTC CATGC	PCR hHsp90β gene
hHsp90b-S365A MluI(ap)	361	CAACTCATCACAcgcGTCCATGATGAAC	S365A mutagenesis
hHsp90b-S365A MluI	368	GTTCATCATGGACgcgTGTGATGAGTTG	S365A mutagenesis
hHsp90b-S365E BsmI(ap)	362	GTATCAACTCATCgCAttcGTCCATGATG AA	S365E mutagenesis
hHsp90b-S365E BsmI	566	TTCATCATGGACgaaTGcGATGAGTTGAT AC	S365E mutagenesis
Hsp90b gene_741+	378	CCCAAGATCGAAGATGTG	Sequencing
h90b-S365N-MfeI	431	TTCATCATGGACAatTGTGATGAGTTGA TAC	S365N mutagenesis
h90b-S365N-MfeI ap	432	GTATCAACTCATCACAatTGTCCATGATG AA	S365N mutagenesis

3.1.4 STANDARDS AND KITS

QIAPrep Spin Miniprep Kit	Qiagen
QIAGEN Plasmid Midi Kit	Qiagen
QIAquick Gel extraction Kit	Qiagen
QIAGEN PCR purification kit	Qiagen
GeneRuler™ 1kb DNA ladder	Fermentas
Protein ladder (SM0431)	Fermentas

3.1.5 ANTIBODIES, LABELS AND PROTEINS

Antibody against hHsp90	ADI-SPA-840-D (Enzo®Life Sciences)
	CIN. 10011439 (Cayman, clone K41220A)
	Self-made rabbit antibodies using purified Hsp90 proteins from E.coli
	Self-made isoform-specific antibody using 4 pairs of synthetic peptides
Hilyte488 C2 maleimide	Anaspec, Inc.
Polynucleotide kinase (and buffers)	Fermentas
Restriction enzymes (and buffers)	Fermentas or
	New England Biolabs
T4 DNA ligase (and buffers)	Fermentas
T7 DNA polymerase (and buffers)	Fermentas
Ulp1 Protease	Lab collection
Aha1	Dr. M.Boysen und Dr. S.Daturpalli
Cdc37	Dr. M.Boysen
CK2	Dr. M.Boysen
p23	Dr. C.Graf
Ydj1	Dr. A. Szlachcic

3.1.6 MEDIA

Luria – Bertani (LB) medium	10g/l tryptone
	5g/l yeast extract
	5g/l NaCl

2X YT medium 16g/l tryptone

10g/l yeast extract

5g/l NaCl

(For plates, 15g/l agar is added.)

Yeast Extract - Peptone – Dextrose (YPD) medium 10g yeast extract

20g peptone

2% glucose

(sterile separately and added later)

Minimal Synthetic Defined (SD) medium 6,7g/l Yeast Nitrogen Base

2% Glucose

(Each component is prepared in 10X and filtered sterile)

Synthetic Complete (SC) Dropout medium SD + amino acids (except for the dropped out: Leucine / Histidine / Uracil)

(Amino acid is prepared in 100X and filtered sterile)

5-FOA (5-Fluoroorotic acid) Dropout medium SC Drop-out + FOA 1% (w/v)

(filtered sterile afterwards)

For plates, appropriate amount of 3% agar (autoclaved and cooled down to 50°C) is added.

DMEM-high glucose-GlutaMAX™

G418 BC Sulfate Biochrom AG, Berlin, Germany

Fetal Calf Serum (FCS) Invitrogen, Karlsruhe, Germany

Antibiotics stocks (1000X)

Antibiotic	**Concentration**	**Solvent**
Ampicillin	100 mg/mL	distilled H_2O then sterile filter
Chloramphenicol	25 mg/mL	absolute ethanol
Kanamycin	25 mg/mL	distilled H_2O then sterile filter
Tetracyclin	25 mg/mL	absolute ethanol

3.1.7 SOFTWARES & EQUIPMENTS

Softwares

Ape (A plasmid Editor) M. Wayne Davis

Bruker Daltonics DataAnalysis 4.0	Bruker Daltonics
Biotools 3.0	Bruker Daltonics
FACS-Diva vers.6.1.3	BD-Biosciences
ImageJ	Wayne Rasband
MicroCal™ iTC200 System (control interface)	GE Healthcare
NTAnalysis	Nanotemper
Odyssey LI-COR Imaging	LI-COR Biosciences
Office 2007	Microsoft
OpenLAB CDS ChemStation Edition	Agilent technologies
Origin	OriginLab (USA)
Photoshop CS5	Adobe
Prism	Graphpad
Unicorn™ Control software	GE Healthcare

Equipments

1260 Infinity Fluorescence Detector	Agilent Technologies
Äkta HPLC Explorer	GE Healthcare
ÄktaMicro™ chromatography system	GE Healthcare
Biofuge Pico	Heraeus
Centrifuge 5424R	Eppendorf
FACS Canto-II	BD-biosystems
FLUOstarOmega	BMG Labtech
MaXis QTOF	Bruker Daltonics
MicroCal™ iTC200 System	GE Healthcare
Microfludizer EmulsiFlex-C5	Avestin
MST Monolith NT.115 (Nano-BLUE/GREEN)	NanoTemper Technologies
nanoUPLC Aquity	Waters
Odyssey LI-COR Imaging	LI-COR Biosciences
Resource-Q (6 mL)	GE Healthcare
Superdex 75 Prep Grade (16/60)	GE Healthcare
Superdex 200 Prep Grade (26/60)	GE Healthcare

Superdex 200 PC3.2 30 (analytical)	GE Healthcare
Superloop 10, 50 or 150 mL	GE Healthcare
SDS gel chamber for minigels (Mini-Protean 4)	Biorad
Thermocycler	Biometra
Thermomixer	Eppendorf
Universal 320	Hettich
UV workbench & Image Printer	IDA raytest, Mitsubishi P91
UV/VIS spectrophotometer NanoDrop ND-1000	Thermo Scientific

3.2 METHODS

3.2.1 MOLECULAR BIOLOGY TECHNIQUES

Cloning & Site-directed mutagenesis

PCR for site-directed mutagenesis

Cloning of Hsp90 single phospho-site variants was performed using wild-type Hsp90β gene on pCA528 as template. OptiTaq polymerase was used with the buffer containing $MgCl_2$ and the reaction was performed as stated below. To introduce the specific mutation, a primer carrying the corresponding modified codon was used to amplify the entire plasmid. PCR products were analyzed by a 1% agarose gel electrophoresis supplemented with 0.001% ethidiumbromide solution.

Standard PCR protocol:

Template DNA 100ng
dNTPs (10 mM) 1 µL
OptiTaq polymerase (2.5 U/µL) 1 µL
Each primer (10 pmol/µL) 1 µL
10x buffer 5 µL
Sterile H_2O up to V final = 50µl

Standard PCR program:

Step 1 melting 95 °C 2 min
Repeat step 2-4 30x
Step 2 melting 95 °C 1 min
Step 3 annealing 52-55 °C 45second
Step 4 elongation 68 °C 12 min
Step 5 pausee 4 °C (on hold)

Amplified DNA was purified with the Qiagen PCR purification kit. DNA was stored at -20 °C in TE buffer. DNA was digested, dephosphorylated and ligated using the following protocols.

Restriction digestion of DNA

Restriction enzymes (type II endonucleases) which cut dsDNA site-specifically were used for screening of introduced mutations and cloning. 0.2 -1u corresponding enzyme (NEB or Fermentas) was incubated with target DNA (1-3 µg) and the recommended buffer in a total reaction volume of 20-50µl for at least 30 minutes to 2 hours at optimum temperature. The reactions were then analyzed by agarose gel electrophoresis and in the case of cloning, desired fragments were extracted using the QIAGEN Gel extraction Kit.

DNA dephosphorylation

After digestion with restriction enzymes, the vector DNA was treated with alkaline phosphatase to prevent its religation. To this end, 2µl of alkaline phosphatase (1 U/µL) were added to the reaction mixture of a cut vector DNA and the mixture was incubated at 37 °C for 1hr.

Ligation of DNA fragments

DNA fragments were ligated as desire by formation of phosphodiester bonds between compatible ends using T4 DNA ligase. Fragments were mixed in a reaction of no more than 25µl together with T4 DNA ligase (Fermentas) and the recommended ligation buffer. The reactions were incubated either overnight at 4°C or 1.5hrs at 30°C. The optimal molar ratio of vector : insert DNA was 1:3 (sticky ends) and 1:1 (blunt ends).

Sequencing of DNA

All DNA constructs after preparation were sequenced to confirm their correct sequence. Purified plasmid DNAs were diluted to concentration of 50-100ng/µl and sent to GATC Biotech (Konstanz, Germany) for sequencing.

Determination of DNA concentration by UV/VIS spectroscopy

Concentrations of DNA solutions were determined by measuring the absorption at 260 nm using a NanoDrop®2000 spectrophotometer. The concentration was calculated according to the Beer-Lambert-Law:

$$A = C.\varepsilon_{260}.d,$$

with A being the absorption, C the concentration, $\varepsilon\lambda$ the molar extinction coefficient at the wavelength 260 nm for DNA and d the thickness of the light-path (10mm in this case).

3.2.2 MICROBIOLOGY AND CELL CULTURE METHODS

E.coli: transformation and expression

Transformation into *E.coli* chemical competent cells using $CaCl_2$-$MgCl_2$

Medium A (Standard Nutrient Agar No.1 3.7% w/v, Glucose 2% (w/v))

$CaCl_2$-$MgCl_2$ (CM) solution ($CaCl_2$ 100mM; $MgCl_2$ 100mM)

The appropriate E. coli strain was inoculated from an overnight culture in 50 mL medium A from OD600 < 0.1 to OD600 ~ 0.3-0.4 (mid-log phase) (roughly in about 1.5hr). From here on, the bacterial cells were always treated at 4°C and cold solutions. The cells were

incubated with CM solutions and pelleted by gentle centrifugation in 10min. This step was repeated for 3 times and finally, the pellets were resuspended gently in CM solution, divided in 100µl-aliquots, snap-frozen by liquid nitrogen and stored at -80°C for later use (Sambrook, J. et al., 2001).

1-3µl of plasmid DNA or the whole ligation reaction was mixed with a 100µl-aliquot of *E. coli* competent cells on ice for 5 min, then heat shocked in 2 min at 42°C followed by 5min on ice. 1 mL LB medium were added to the mixture and it was incubated at 37°C for 45min for recovery and expression of antibiotics resistance genes. Then it was spread onto LB-agar medium with corresponding antibiotics for selection.

Expression of recombinant proteins in *E.coli*

The vector pCA528-hHsp90β wild-type or its equivalent mutants was used to overexpress yeast Hsp82 protein (either wild type or mutant) in the *E. coli* BL21DE3 Rosetta strain. The culture was grown in 2 - 5l 2X YT medium supplemented with Ampicillin until OD_{600} ~1.0 at 37°C, followed by 30 minutes at 25°C for adaptation and then induced by IPTG 0.5mM for expression overnight at 25°C. Cells were harvested by centrifugation at 4500rpm (Sorvall F7 rotor) in 20 minutes at 4°C and resuspended in 100 mL lysis buffer before being lysed by a microfluidizer.

Yeast genetics techniques

Transformation into S. cerevisiae competent cells using Lithium acetate

The most commonly used yeast transformation protocol using lithium acetate is based on the fact that alkali cations such as Li^+, Na^+, K^+... are efficient in inducing competence in yeast cells (Ito, H. et al., 1983). After yeast cells are incubated in buffered lithium acetate, transforming DNA is introduced with carrier DNA. Addition of polyethylene glycol (PEG) and a heat shock at 42°C in 10 minutes trigger DNA uptake. The yeast cells are then plated on selective media at 30°C for 2-3 days for selection of successly transformed cells.

All solutions for preparing competent cells and transformation were sterile.

10X TE buffer (Tris – HCl 0.1M, EDTA 10mM pH 7.5)

10X LiAc pH 7.5 LiAC 1 M

Salmon sperm DNA (10mg/ mL)

PEG 4000 50% (w/v)

PEG/LiAC solution (freshly prepared) (PEG 40% (w/v), 1X LiAc, 1X TE)

The appropriate yeast strain was inoculated overnight at 30°C until OD600 reaches 0.3-0.5 (~10^7 cells/mL) before being harvested by centrifugation at room temperature in 5 minutes at 4,000g. After being resuspended in sterile water, the cells were centrifuged again for 5 minutes at room temperature at 5,000-6,000g. Then the yeast cells were washed in 0.5V 1X LiAc/TE solution (V: volume of cell culture). A centrifugation at room temperature in 5 minutes at 4,000 g was followed. The wash step was repeated with 0.25V 1X LiAc/TE solution. The pellet was resuspended in 1/500V TE and use immediately or stored at -80°C.

For each transformation, 10 µg carrier DNA with less than 5 µg transforming DNA were mixed in a sterile 1.5-mL microcentrifuge tube together with 50µl yeast competent cells. 0.3 mL freshly prepared PEG/LiAc solution was added and the whole mixture was incubated at 30°C at least for 30 minutes. The mixture was subsequently heat shocked for 15 minutes at

42°C and centrifuged briefly at highest speed available. The cells were resuspended in 200µL 1X LiAc/TE solution and plate on suitable selective media at 30°C in 2-3 days.

Plasmid shuffling method using 5-Fluorootic acid (5-FOA)

The method was applied as in Boeke, J. D. et al., 1987; Lundblad, V. and K. Struhl, 2002. Plasmid shuffling is a method which is particularly useful for the analysis or mutagenesis of genes that are essential for cell growth and viability. The manipulation of such essential genes is complicated by the obvious fact that cells containing mutated versions of such genes cannot be propagated. Plasmid shuffling circumvents this problem by generating a yeast strain in which the sole copy of an essential gene is present on a URA3-marked plasmid (i.e., the chromosomal copy of the essential gene is deleted). Note that the functional URA3 gene encodes for an enzyme in the uracil metabolism pathway which convert 5-FOA into the toxic form (5-fluorouracil). This strain is transformed by a second plasmid (which carries a different marker) containing a mutated version of the essential yeast gene (carried on a plasmid with a different marker), whereupon the URA3 plasmid carrying the wild-type genes is eliminated (shuffled out) by replica plating the cells on 5-FOA. This procedure efficiently generates yeast cells that contain only the plasmid with the mutated copy of the essential gene. If the mutated gene is sufficiently functional to support cell growth, the colonies can be examined under a variety of conditions (e.g., low or high temperature). Alternatively, if the mutated gene is nonfunctional, colonies will not arise on the plates containing 5-FOA.

Growth curve

The yeast strains of interest were inoculated from a single colony on plate for 1-2days at 30°C in synthetic medium (SC\Leucine). The cells were diluted to the starting OD600 of 0.1 and measured every 2 hours.

Reporter assay

The yeast strains of interested were grown to early logharithmic phase in synthetic medium at 25°C and kept diluted (OD<0.4) for at least 8h. For slow growing mutants the duration could be extended to more than 12h. Depending on the reponse element, different inducing agents were applied.

Response element	Inducing agent	Concentration / Volume of usage
HapRE (Heme Activator protein response element)	measure directly	
HSE (Heat shock element)	Heat shock at 37°C/42°C	
GRE (Glucocorticoid receptor response element)	Desoxycorticosterone (20mM)	1µl/mL → f.c. 20µM
PRE (Pheromone response element)	Alpha-factor (1mM)	3µl/mL → f.c. 3µM

An aliquot of induced culture was transferred to a FACS-tube for measuring, which was sonified shortly for 5-10 seconds and signals were recorded for around 10000-15000 events (presumably equals to number of single cells). For each induction time CST (Cytometer-Standard & Tracking) standard-beads were also recorded. The filters applied in FACS measurements were listed as following:

	Excitation	Emission

T-Sapphire	405 nm	510/50
sfGFP	488 nm	530/30
Propidium iodid	488 nm	670LP = 670-735

FACS Data processing: All data was acquired with FACS-Diva version 6.1.3 software. Compensation of spectral overlap was established with strains expressing either one of the respective proteins or none. Gating of T-Sapphire-positive events was used as vital-parameter. The selection of single-cell-gate was performed via a FSC-W/SSC-W plot. The population mean of the GFP- and the T-Sapphire-channel were taken and subtracted for autofluorescence. Then the normalization cell-fluorescence to uncompensated values of the CST-beads in the respective channel was made (3 brightest beads were chosen). The GFP-signal can be divided either by the absolute T-Sapphire-fluorescence (when different clones show similar expression and recombination events can be ruled out) or the relative values where time-point zero is set to a fluorescence of one. Since it is extremely time-consuming to build a GFP/T-Sapphire ratio based on individual cells (because of the CST-normalization), all the processing was done on the population mean. As long as there is no prominent sub-population, this is a reasonable approach.

Fitting of the data was done by a one-phase association with delay, to account for signaling tranfer from the reporters and synthesis of GFP after induction.

Cell volume measurements

For the microscopy, cells from 4 different from each of the S365-mutants were sorted on a microscope slide and stained with Solophenylflavin. Images of the maximal cell-diameter were taken and the outer cell shape was selected manually in ImageJ. From this data, diameter and volume were estimated assuming an ellipsoid cell-shape.

Cell culture

Cell culture for HELA and HepG2 cells were cultured in DMEM-high glucose-GlutaMAX™ (Gibco, Life Technologies) supplemented with 10% FCS. The cells were harvested in PBS-EDTA buffer and exchanged into Tris-based or HEPES-based Lysis buffer (Tris 25mM or HEPES 20mM pH 7.4-7.6, KCl 50mM, $MgCl_2$ 5mM, NP40 0.1%, supplemented with Phosphatase inhibitor (PhosSTOP, Roche) and/or cOmplete Protease inhibitors cocktail tablet (Roche). The cells were then lysed by passing 15-20 times over syringe with two needle sizes (21G 1½"and 27G ¾", BD-Microlane™-3) on ice (15-20 times divided in 3 parts with intervals of 3min on ice in between). The lysate was then centrifuged at 13000rpm for 15 minutes, 4°C and supernatant was collected into a new eppendorf tube. The total protein concentration was determined by a Bradford assay prior to immunoprecipitation or GA pulldown experiments.

3.2.3 BIOCHEMICAL TECHNIQUES AND DATA ANALYSIS

Electrophoresis (SDS-PolyAcrylamide Gel-Electrophoresis)

The mobility of a protein in a meshwork under an electrical field is dependent on its shape, its charge and its mass or molecular weight (MW). After being boiled in buffer containing DTT (reducing disulfide bonds) and SDS (binding to all polypeptides and creates a constant charge/mass ratio between proteins), the mobility of proteins in a meshwork of acrylamide polymer under an electric field now only depends on their MW, thus, allowing separating proteins with different MW on a polyacryamide gel containing SDS (Walker, J. M., 2002).

In this work, SDS-PAGE gels of 10% acrylamide (separating gel) were mainly used. For 2 mini gels, the components were prepared as following:

	V (µl)	
	Stacking gel (4%)	**Separating gel (10%)**
H_2O	3050	3000
0.5 M Tris-HCl pH 6.8 (stacking gel) , or	1250	0
1.5M Tris-HCl pH 8.8 (separating)	0	1875
10% (w/v) SDS	50	75
30% Acrylamide: 0.8% Bis-acrylamide (w/v)	670	2500
10% (w/v) APS	25	50
TEMED	3	5

(APS and TEMED were added just before casting the gel.)

Different protein samples were mix with 5x Sample Loading buffer and boiled for 5 minutes at 95°C, then briefly centrifuged (13,000rpm, 5 minutes) before being loaded to the rinsed wells of the gel. The whole system would start at 120V in Tris-glycine buffer until the samples enter separating gel, the voltage was then increased to 180V. The running was stopped when the bromophenol blue marker reached the end of the gel. For visualization of the protein bands, the gel was stained with Coomassie staining solution for at least 45 minutes and subsequently destained in Destaining solution until the background was transparent enough and the bands were clearly visible.

Coomassie staining solution (0.2% (w/v) Coomassive Brilliant R250, 5% (v/v) acetic acid, 50% (v/v) methanol) and filtered before use).

Destaining solution (50% (v/v) methanol, 5% (v/v) acetic acid)

Western blotting

Proteins were first separated by SDS-PAGE and subsequently electrophoretically transferred on a PDVF membrane in a Semi-Dry blotting apparatus (Biorad) at a constant current of 75 mA per mini SDS-PAGE gel for 30 minutes. After the transfer, membranes were incubated in a PBST buffer supplemented with 5% milk powder with agitation at 4 °C overnight to block free binding sites. The primary antibody was diluted in PBS-T buffer supplemented with 5% non-fat milk powder (dilution depended on the individual antibody) and incubated for overnight at 4°C or 2 hrs at room temperature. The membrane was washed

5-7x for 5 min with PBS-T buffer and incubated for 45 minutes with a secondary antibody coupled with fluorescent dye (LI-COR antibodies, normally dilution 1:20000) followed by 3-5 washing steps with PBS-T buffer, 5 min each. Detection was performed with Odysee LI-COR Imager.

Protein purification

His6x-SUMO tagged protein purification

Proteins of interest (including human Hsp90β wild-type, S365A/E/N, humanHsp90α, human Hsp70, HOP) were overexpressed from the corresponding vector as fusion proteins with His6-SUMO tag. The tag helps increase solubility of recombinant proteins and can be cleaved off by the specific protease (Ulp1) without remaining any amino acids (Malakhov, M. P. et al., 2004).

Buffer HKM **(**25 mM HEPES/KOH pH7.4, 100 mM KCl, 5mM $MgCl_2$, 10% glycerol, 3 mM β-mercaptoethanol)

Lysis buffer (Buffer HKM with 1 mM PMSF, 10 μg/mL Aprotinin, 5 μg/mL Leupeptin, 10 μg/mL Pepstatin A)

Washing Buffer (Buffer HKM)

Elution Buffer (Buffer HKM + 250 mM imidazole)

Buffer A (Buffer HKM with 100 mM KCl)

Buffer B (Buffer HKM with 1M KCl)

Storage buffer (Buffer HKM with 50 mM KCl)

The cell lysate was clarified by ultracentrifugation (40,000 rpm for 30 min at 4°C) and incubated with 3-5g Ni-IDA matrix (Protino) in 30min before being transferred to a disposable gravity column and washed with 5-10 Column volume (CV) Washing buffer. Bound proteins were eluted by 3-5 CV Elution buffer.

The Elution fractions were pooled and dialysed overnight with Ulp1 to cleave His6x-SUMO tag and eliquibrated into low salt buffer before being loaded to a 6mL-ResourceQ using an Äkta Explorer system. The proteins of interest were eluted by a gradient of 10CV from 0 to 100% buffer B. The eluted fractions were collected and analyzed on SDS-PAGE before being pooled and concentrated to lower volume. Next, the proteins were subjected to Superdex 200 16/60 Prep grade column on the Äkta system to be further polished in storage buffer. The fractions containing purified proteins were concentrated and flash-frozen in liquid nitrogen to be stored at -80°C for further use.

MBP-tagged protein purification

For GRLBD, the LBD(F602S) fragment (521-777) was cloned into a pMAL-c2E backbone vector containing an extra recognition site for PreScission protease between MBP and gene fragment. MBP-GRLBD(F602S) was expressed in BL21 star (DE3) Typically, cells were grown at 37°C until OD reaches approximately 0.7-0.8 (~ 3hrs), and then the temperature was lowered to 18°C. Cells were kept growing at 18°C for 30 min (OD ~ 1.0-1.2) then dexamethasone (Dex) was added to a final concentration of 250 μM and cells were induced overnight with 0.5 mM IPTG. Next morning, harvested cells were lysed by microfluidizer (EmulsiFlex-C5, Avestin) in MBP-lysis/Amylose column Buffer. The lysate was clarified by centrifugation and the soluble fraction was bound to pre-equilibrated Amylose resin (NEB) at 4°C under gravity flow. The column was washed with 8-10CV Amylose Wash Buffer before elution (4-5CV). The eluted fraction was subjected to size-exclusion

chromatography (Superdex S75). The fractions containing the protein of interest were pooled, divided into 2 parts and dialysed overnight into Storage Buffer with or without Dex. Purification was finished by extensive dialysis into ligand free storage buffer twice, 2hrs each on the next morning. Proteins with ligand-bound were flash-frozen in liquid nitrogen and stored at -80°C. GRLBD protein without ligand cannot be stored frozen but has to be used within the next 3 days.

Protein concentration determination by Bradford assay

The Bradford assay is a colorimetric protein assay used to determine the protein concentration. The assay is based on the observation that the absorbance maximum of the dye Coomassie Brilliant Blue G-250 shifts from 465 nm (red form) to 595 nm (blue form) upon binding of a chromophore to particularly basic and aromatic amino acids in proteins (Bradford, 1976). To this end, the commercially available solution (Dye reagent concentrate, Biorad, Cat N° 500-0006) was first diluted 1:5 with water. 999 µL of the solution was mixed with 1µL of protein solution, incubated shortly at room temperature and the absorption at 595 nm was measured. The standard curve was calculated on a BSA standard (measured for 1-10µg/µl BSA solution).

Limited proteolysis

Purifed Hsp90 proteins (wildtype: WT, S365A: SA, S365E: SE and S365N: SN) were digested individually (6µg) by Trypsin (E:S = 1:100) at 37°C. At different time points (0, 1, 5, 10, 15, 20min), 1/6 of the reaction volume was taken for SDS-PAGE. The reactions were stopped by adding Sample buffer 5x and boiled at 95°C for 3 minutes).

Size-exclusive chromatography (SEC)

The sample of interested were injected onto a Superdex 200 PC 3.2/20 analytical column using the ÄktaMicro system (GE Healthcare Life Sciences) at the flow of 0.1 µL/min. The buffer used in SEC experiments is storage buffer from protein purification (HKM with 50mM KCl) without β-mercaptoethanol and glycerol. The fractions were collected in the volume of 72µl manually or the outlet was directly connected to the 1260 Infinity Fluorescence Detector (Agilent Technologies). UV280 signal was monitored in Unicorn software (GE Healthcare Life Sciences) and fluorescent signal was recorded in the OpenLAB CDS ChemStation Edition software for LC and LC MS/MS systems (Agilent technologies).

Protein labeling

Proteins were dialyzed overnight at 4°C in Storage buffer from purification but without β-mercaptoethanol to remove β-mercaptoethanol. The cysteins in the proteins were then reduced by addition of 1 mM TCEP and incubated for 2hours at room temperature but on ice. The proteins were then labeled by 20-fold molar excess of Hilyte 488 C2 maleimide (dissolve in DMSO/DMF) while keeping the volume of DMSO less than 1% (by diluting the proteins by buffer to increase the volume if necessary). The labeling reactions were done at room temperature for 2 hours before the reaction mixture(s) were loaded on a self-packed Superdex G50 size exclusion column (pre-eliquibrated in HKM buffer) to separate free dye and labeled proteins. 10-12 fractions of approx. 100 µl were collected and checked for protein concentration by Bradford assay as well as fluorescence signal by spectro-fluorimeter. The fractions with highest concentration of protein and high fluorescence signal were kept on ice in the 4°C room and used for further experiments in the next days (maximal 1 week). The final concentration of labelled protein was determined by Bradford assay.

Microscale Thermophoresis measurement

All proteins were centrifuged using a table-top centrifugation at max speed for 15min at 4°C before the experiment. A titration series of freshly purified GRLBD was prepared in MST buffer (Tris 20mM pH 8.3, 100mM KCl, 5mM $MgCl_2$) supplemented with

freshly prepared ATP and DTT (final concentration of 2mM and 3mM, respetively), incubated at room temperature for 1hr alone or with components in the minimal GR-activating system. Then fluorescein-dexamethasone (F-dex) was added to the final concentration of 25 nM (stock solutions were dissolved in DMSO) and the whole mixture was incubated further at room temperature for 25-30 min before being measured by MST at laser power 20% or 40%. The MST instrument was Monolith NT.115 (NanoTemper Technologies). Binding curves were obtained from the thermophoresis plus temperature-jump phase, with IR laser power of 20 (which corresponds to a temperature gradient of 2°C from 25°C). Each experiment was repeated at least two times and the active fraction of GR was calculated using the quadratic equation with the constraint of a fixed Kd 150nM, ligand (L) 25 nM (Prism). To avoid day-to-day differences orignated from the labile GRLBD itself, a MST measurement of GRLBD alone was always performed and the data was normalized using this measurement. I stopped using the current purified batch of GRLBD when the active fraction calculated from this control sample was under 20%. The minimal GR-activating system consists of 2μM Hsp40 (Ydj1), 10μM Hsp70, 10μM Hsp90, 10μM HOP and 10μM p23. The fraction of active GR was calculated using Prism and the fitting used the modified quadratic equation as following:

$$y = Fo + (Fm - Fo) * \frac{\frac{f * x + L + K}{2} - sqrt\left(\frac{(f * x + L + K)^2}{4} - f * x * L\right)}{L}$$

in which:

y: thermophoretic motibility measured by fluorescence signal of F-dex unbound and bound by a given concentration of GR (x) at the IR-laser focus point (normalized to starting fluorescence)

Fo: minimum value of y → to be determined by fitting

Fm: maximum value of y → to be determined by fitting

f: ***% active x (value must be between 0& 1)*** → to be determined by fitting

x: concentration of GR (provided according to Bradford assay and dilution factor)

L: F-dex concentration (=25 nM)

K: dissociation constant (Kd = 150 nM)

A Student's t-test was performed for the MST measurements in the presence of the whole minimal GR-activating system to identify the significance of difference between the system containing Hsp90β wild-type and each of other variant proteins (one-tailed distribution, unequal variance or heteroscedastic). Each system sample included 2-4 repeats. A similar Student's t-test was also performed for the system containing Hsp90β S365E variant protein and each of the other proteins. The significance values of each pair of samples are reported in Appendix Table S2.

Isothermal Titration Calorimetry (ITC)

Affinity of Hsp90(s) and Cdc37 was determined by ITC using a MicroCal ITC200 microcalorimeter. All Hsp90 proteins were rapidly thawed and extensively dialysed at 4°C against 20 mM HEPES (pH7.4), 50 mM KCl, 5 mM $MgCl_2$ and 10% glycerol. The final protein concentration in the cell is 30-45 μM. Cdc37 was loaded in the syringe at 300-500 μM in the same buffer as Hsp90(s). Run parameters were as follows: total number of injections: 16×2.49 μl, injection duration of 4.98 s, injection spacing of 120-180 s, filter period of 5 s, cell temperature of 25°C, reference power of 11 μcal/s, initial delay of 60 s and stirring speed of 2000 rev./min. Titration raw data were fitted to a one site model using Origin software (OriginLab). Final graphs show heats from each injection against the ratio of Cdc37 as ligand

and binding partner (Hsp90 protein) in the cell (top panel) and the binding isotherm/integrated heats (bottom panel). Dissociation constant were calculated as reverse of association constant calculated by the software. SEM was calculated for 2-3 repeats.

In vitro phosphorylation with CK2

1µg purified Hsp90 protein in 50 µl final reaction volume was incubated in 20 mM Tris/HCl pH 7.8, 100 mM KCl, 5 mM MgCl2 in the presence of 0.2µg CK2 (purified protein from Dr. M. Boysen) and 1 mM ATP for 2 h at 37 °C. The samples were subjected to in-solution digestion and subsequently analysed by LC MS/MS using UPLC system and the MaXis mass spectrometer as described in MS method part. Similar Mascot database searches were performed, in which Hsp90α and Hsp90β could be detected with sequence coverage 77% and 83%, respectively. Phosphorylated peptides for the serines in the charge linker (S231/S263 of Hsp90α or S226/S255 of Hsp90β) were detected (with a few missed cleavages, too); but no other phosphorylated peptide(s) were identified.

GA pulldown experiment (adapted protocol from M. Breinig)

Usually 200 µg (could be upto 500 µg) of total cell lysate is used in GA pulldown experiments, generally in the volume of 200-500 µL. When using different samples in one GA pulldown experiment, the lysate samples were usually concentrated so that the starting volume is at least similar. 100 µL of the streptavidin magnetic beads (M-280, Invitrogen) was washed three times by 500 µL Lysis buffer before it was resuspended into 50µL Lysis buffer. 20 µL of 1M Biotinylated-GA (InVivogen) (resuspended in DMSO) were added to the beads and incubated for 2hrs at 4°C with constant rotation. The GA-coupled beads were then washed three times by 500 µL Lysis buffer before they were incubated with lysates supplemented with Protease Inhibitors and PhosSTOP (Roche) overnight at 4°C with constant rotation. A magnetic field was applied to separate the beads with supernatant to collect the flowthrough fraction. The beads were washed three times, two times by 100 µL and one by 200 µL Lysis buffer supplemented with only PhosSTOP before finally resuspended in 50µL as Bound fraction. The Bound fraction was further subjected to in-solution digestion or loaded on SDS-PAGE for in-gel digestion.

Immunoprecipitation experiment

Indirect IP was applied after unsuccessful trials with direct IP (couple antibody to beads before incubating with lysate): the antibody was successfully coupled to beads but subsequent capture of Hsp90 from lysate by this complex is low.

Hsp90 was isolated from lysate of 200 µg total protein by IP for overnight at 4 °C on a rotating wheel using 7 µg SPA840 α-specific antibody. Then 50 µL of Dynabeads® protein A (LifeTechnologies) washed and resuspended in Binding buffer (Immunoprecipitation Kit, LifeTechnologies) was added and incubated for 4 hrs at 4°C. In these incubation times, Lysis or Binding buffer was used with supplement of Proteases Inhibitors and PhosSTOP. The Dynabeads® protein A in fact is protein A coupled to magnetic beads, which allows separation of beads and supernatant under magnetic field. The mixture was washed three times with 500 µL Wash buffer and eluted with 30-50µL of Elution buffer from Immunoprecipitation Kit Protein A (Life Technologies). (I made an attempt to make the Elution buffer according to their protocol: 50mM glycine pH 2.8, but it did not work as well as commercial buffer so from then on, I always used commercial buffers for IP).

MS sample preparation

<u>Standard In-solution digestion</u>

The lysate or fraction of interest was lyophilized or Speed-Vac to dry up before resuspended in (usually) 50µL of 50mM Ammonium Bicarbonate pH 8.5 and 8M urea. DTT was added to the final concentration of 50mM and the sample was incubated in the dark for

20 min at room temperature. Fresh iodoacetamide (prepared and used within 1 week, better if only in 1 day) was supplemented to a final concentration of 10mM and incubated in the dark for 20 min at room temperature. The samples were diluted to less than 4M urea and incubated with 0.1 µg Lys-C protease overnight at 28°C. The digestion reaction was then diluted further to less than 2M Urea so that Trypsin could be applied. In some cases, if the volume is not limited by subsequent analysis, the urea concentration was diluted to less than 1M. Normally Trypsin was supplied 2-3 times, 0.1-0.5 µg each with intervals 2-4 hrs before the samples were considered ready for MS analysis. Whenever the protein content could be measured (in case of total lysate digestion for MRM-MS), an enzyme amount of Enzyme:Substrate = 1:100 was used for each addition of enzyme. Similar protocol was applied for digestion by Asp-N or GluC except Lys-C digestion step. Trypsin, Lys-C, Asp-N and Glu-C were purchased from Promega or Roche.

Filter-assisted sample preparation (FASP)

A modified In-solution digestion (FASP) protocol was also tried for MRM-MS samples. In short, proteins are denatured in SDS, reduced & alkylated where after the proteins (now unfolded) are captured on a molecular weight cut-off filter (typically 30 kDa). On the filter, detergent is washed away using 6M Urea and followed by an on-filter digestion. The generated peptides are small enough to pass through the filter and can be collected for analysis. For details, see (Wiśniewski et al. 2011).

Mass Spectrometry analysis

MS analysis by the MaXis mass spectrometer

The digestion mixtures were injected into the UPLC system and analysed with the MaXis Q-TOF. In the UPLC system the sample is pushed onto a reversed phase trap column containing Poros 10 R1 or R2 at a flow rate of 400 µl/min and subsequently washed with 0.1% formic acid for three minutes. Subsequently, the sample is eluted in a 120-min gradient from 90 % solvent A/10 % solvent B to 15% solvent A/85 % solvent B over an analytical reversed-phase column (Waters BEH C18) to separate the tryptic peptides before injected into the mass spectrometer. Hsp90 peptide spectra were acquired with a standard source (microflow), set to 4.5 kV capillary voltage, 0.8 bar nebuliser gas, 4 l/min dry gas at 190 °C and an end plate offset of -500 V. The spray was generated by the standard ESI-Sprayer supplied with the mass spectrometer. The MS/MS setting of the HyStar software was turned on during the experiment. Fragment spectra were recorded for the top five or ten MS signals. The resulting fragment spectra were processed with the Biotools 3.0 program (Bruker) and sent to the MASCOT search engine (Matrix Science) to identify proteins and peptides. Peptide lists were generated containing sequence, mass to charge ratio, charge and retention time of Hsp90 peptides. The search parameters used in Mascot search were: SwissProt database; taxonomy of *Homo sapiens*; enzyme Trypsin (or in a few cases, GluC(V8-E) or AspN) with maximum 4 missed cleavages; Fixed modifications include only oxidation for methionine; Variable modifications include Carbamidomethyl for cysteines, deamidation from asparagine to glutamine, phosphorylation for STY (serine, threonine and tyrosine); peptide tolerance 1000ppm; peptide charge 1^+, 2^+ and 3^+; MS/MS tolerance 0.05 Da and intrument ESI-QUAD-TOF. Phosphorylation site assignments were further verified by manual inspection of MS/MS spectra.

MS analysis by the Orbitrap mass spectrometer

The MS experiments were performed in collaboration with Dr. Thomas Rupert (MS facility, ZMBH). Elution or bound fractions from IP or GA-pulldown experiments were loaded onto SDS-PAGE minigels and run for short distance (approx. 1cm) before stained by colloidal Coomassie and destained by water. The gel fragment of interest or whole lane was cut out and in-gel digestion by Trypsin was performed using the Digest Pro mass

spectrometry (MS) liquid-handling system (Intavis AG). Following digestion, tryptic peptides were extracted from the gel pieces with 50% acetonitrile-0.1% trifluoroacetic acid, concentrated, and analyzed by MS. Samples were analyzed by RP-HPLC (HPLC system HP1100; Hewlett-Packard,) equipped with a µRPC C2/C18 SC 2.1/10 column (Pharmacia): eluent A, 0.05% trifluoroacetic acid; eluent B, 70% acetonitrile, 0.045% trifluoroacetic acid; gradient 90min; flow rate, 50 µl/min. Analysis was performed on line with an ion trap mass spectrometer LTQ-Orbitrap (ThermoQuest) equipped with an electrospray ion source. Each scan was acquired over the range m/z = 300-1300 in 3 s. The peptides were identified by their molecular masses calculated from the m/z peaks of the single or multiple charged ions and were confirmed by mass-spectrometric sequencing analyses. MS data were searched similarly as in MS analysis by the MaXis mass spectrometer with only exception that the Carbamidomethylation was included as fixed modification and instrument ESI-TRAP.

MRM-MS analysis

MRM-MS analyses were performed in collaboration with S.Link or L. Behrens (MS facility, ZMBH, Heidelberg) using the Qtrap 5500 MS (ABSciex) coupled with nanoUPLC Aquity (Waters). This triple quadrupole mass spectrometer with full MS^3 capabilities offers high quality, confidence and sensitivity for targeted quantification studies. The crude lysates samples either from in-solution/FASP digestion via Ziptip or in-gel digestion were applied onto the LC MS system.

4 ABBREVIATIONS

5-FOA	5-fluoroorotic acid
Å	Ångström
ADP	Adenosine diphosphate
Aha1	Activator of Hsp90 ATPase
Amp^R	Ampicilline resistance
APS	Ammonium persulfate
ATP	Adenosine triphosphate
bp	Base pair
BSA	Bovine serum albumin
Cdc37	Cell division cycle 37
Cdk	Cyclin-dependent kinase
CHIP	Carboxy terminus of Hsc70-interacting protein
Cm^R	Chloramphenicol resistance
Cyp40	Cyclophillin 40
Da	Dalton (atomic mass unit)
DMSO	Dimethylsulfoxid
DNA	Deoxyribose nucleic acid
dNTP	Deoxynucleoside triphosphate
DTT	Dithiothreitol
dTTP	2'-deoxythymidine 5'-triphosphate
dUTP	2'-deoxyuridine 5'-triphosphate
EDTA	Ethylene diamine tetraacetic acid
ES	Embryonic stem cell
ESI	Electrospray ionization
FCS	Fetal calf serum
FKBP52	FK506 (Fujimycin) binding protein 52
GA	Geldanamycin
GHKL	**G**yrase B/**H**sp90/Histidine **K**inase/Mut**L** ATPase superfamily
GR	Glucocorticoid receptor

GRLBD	Glucocorticoid receptor ligand binding domain
HEPES	4-(2-hydroxyethyl)piperazine-1-ethanesulfonic acid
HOP	Hsp70/Hsp90 organizing protein
HPLC	High performance liquid chromatography
Hsc	Heat shock cognate protein
Hsp	Heat shock protein
HtpG	High temperature protein in *E. coli*
IMAC	Immobilized metal affinity chromatography
IP	Immunoprecipitation
iPS	Induced pluripotent stem cell
IPTG	Isopropyl β-D thiogalactoside
ITC	Isothermal titration calorimetry
LC	Liquid chromatography
LiAc	Lithium acetate
MCS	Multi cloning site
MRM	Multiple reaction monitoring
MS	Mass Spectroscopy
MS/MS	tandem mass spectrometry
MST	Microscale thermophoresis
MW	Molecular weight
m/z	mass-to-charge ratio
OD	Optical density
QQQ	triple quadrupole
PAGE	Polyacrylamide gel electrophoresis
PDB	Protein databank
PEG	Polyethylene glycol
PMSF	Phenylmethanesulfonyl fluoride
PR	Progesterone receptor
RNase	RNA-hydrolyzing enzyme
SDS	Sodium dodecyl sulfate
SEM	Standard error of the mean

SILAC	Stable isotope labeling with amino acid in cell culture
SHR	Steroid hormone receptor
SUMO	Small ubiquitin-like modifier
TAE	Tris acetate ethylenediaminetetraacetate
TEMED	N, N, N', N'- tetramethylethylene diamine
TFA	Ttrifluoroacetic acid
TPR	Tetratricopeptide repeat

5 APPENDICES

FIGURE S1: MRM-MS³ IN COMBINATION WITH LIBRARY INDENTIFICATION CONFIRMS S365 PHOSPHORYLATION OF HUMAN HSP90β IN HELA LYSATE.

HELA lysate (total protein amount of 2mg) was digested by Trypsin using In-solution digestion protocol. 1/10 sample was subjected to MRM-MS³ and analyszed further by library identification. Library data were generated from synthetic phosphorylated peptides and digestion from purified proteins.

(A) Library identification of $y8^{++}$ fragment (transition 799.7/526.4). The MS3 fragmentation pattern of selected transition ($y8^{++}$) fits well to theoretical fragmentation pattern of the same transition from synthetic peptides with Fit value of 83.249.

(B) Similar to (A) except for $y6^{+}$ fragment (transition 799.7/825.6) and Fit value of 36.713.

(A)

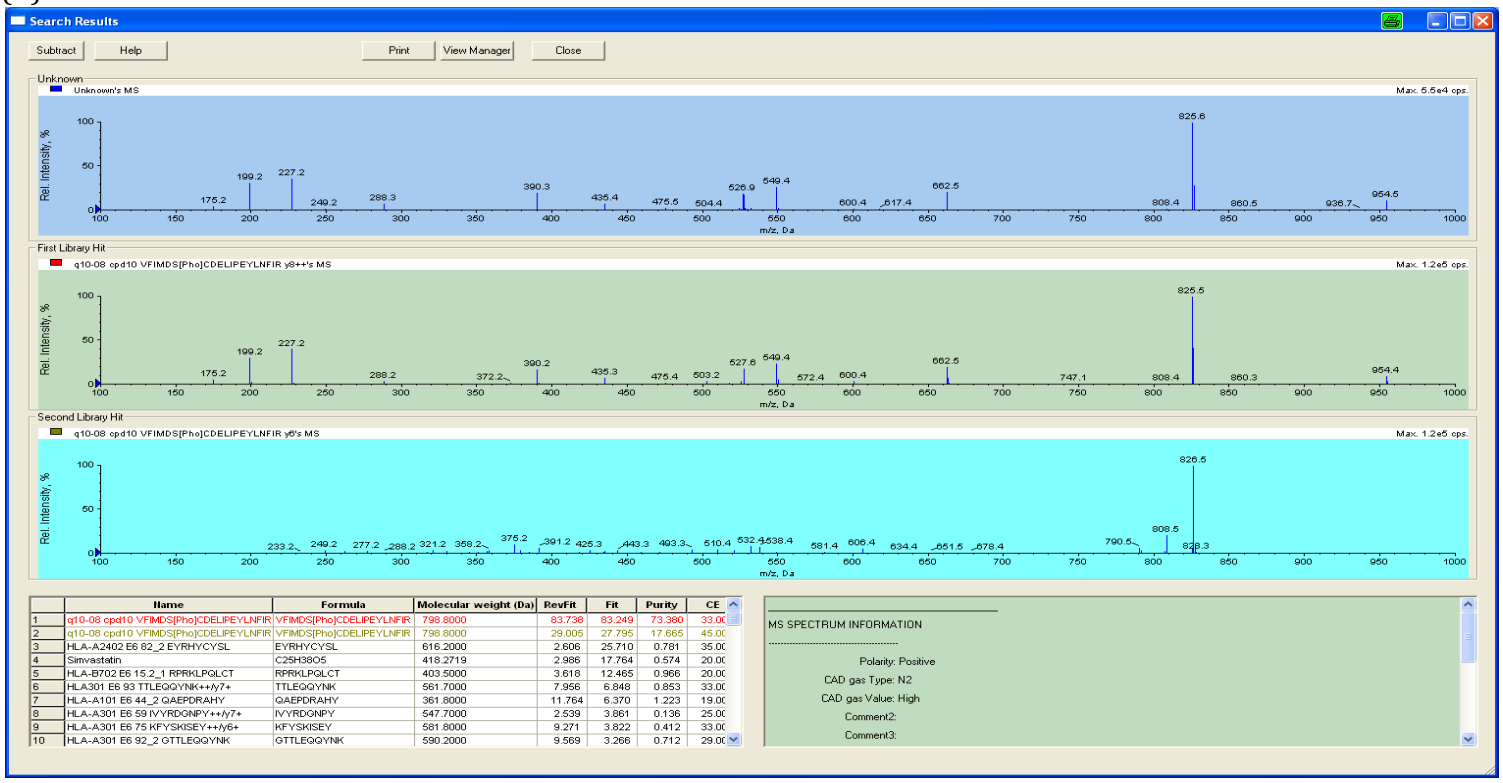

	Name	Formula	Molecular weight (Da)	RevFit	Fit	Purity	CE
1	q10-08 cpd10 VFIMDS[Pho]CDELIPEYLNFIR	VFIMDS[Pho]CDELIPEYLNFIR	798.8000	83.738	83.249	73.380	33.0
2	q10-08 cpd10 VFIMDS[Pho]CDELIPEYLNFIR	VFIMDS[Pho]CDELIPEYLNFIR	798.8000	29.005	27.795	17.665	45.0
3	HLA-A2402 E6 82_2 EYRHYCYSL	EYRHYCYSL	616.2000	2.606	25.710	0.781	35.0
4	Simvastatin	C25H38O5	418.2719	2.986	17.764	0.574	20.0
5	HLA-B702 E6 15.2_1 RPRKLPQLCT	RPRKLPQLCT	403.5000	3.618	12.465	0.966	20.0
6	HLA301 E6 93 TTLEQGYNK++/y7+	TTLEQGYNK	561.7000	7.956	6.848	0.853	33.0
7	HLA-A101 E6 44_2 QAEPDRAHY	QAEPDRAHY	361.8000	11.764	6.370	1.223	19.0
8	HLA-A301 E6 59 IVYRDGNPY++/y7+	IVYRDGNPY	547.7000	2.539	3.861	0.136	25.0
9	HLA-A301 E6 75 KFYSKISEY++/y6+	KFYSKISEY	581.8000	9.271	3.822	0.412	33.0
10	HLA-A301 E6 92_2 GTTLEQGYNK	GTTLEQGYNK	590.2000	9.569	3.266	0.712	29.0

(B)

	Name	Formula	Molecular w	RevFit	Fit	Purity
1	q10-08 cpd10 VFIMDS[Pho]CDELI	VFIMDS[Pho]CDELIPEYLNFIR	798.8000	52.259	36.713	35.197
2	HLA-B702 E7 5_1 TPTLHEYML	TPTLHEYML	551.7000	2.631	34.772	1.010
3	HLA-A101 E8 80_1 ISEYRHYCY	ISEYRHYCY	616.2000	0.316	24.048	0.094
4	10-008 6_2 TLT[Pho]VDTGIGMTK	TLT[Pho]VDTGIGMTK	714.5000	5.656	20.465	1.395
5	HLA-A2402 E6 82_2 EYRHYCYS	EYRHYCYSL	616.2000	2.666	17.434	0.778
6	q10-08 cpd10 VFIMDS[Pho]CDELI	VFIMDS[Pho]CDELIPEYLNFIR	798.8000	21.477	14.753	3.226
7	HLA-A101 PK2 IADMGHLKY+++/	IADMGHLKY	348.8000	0.220	13.243	0.029

FIGURE S2: ACTIVATION RATE CONSTANT OF GLUCOCORTICOID RESPONSE IN YEAST STRAINS CONTAINING EITHER HUMAN HSP90β AS THE SOLE SOURCE OF HSP90 PROTEIN IN THE CELLS.

GR response measured from GFP signals normalized for TEF signals were fitted to one-phase association with delay model. The data was expressed as mean ± SEM from four independent clones. Experiments were performed in collaboration with R. Knieß.

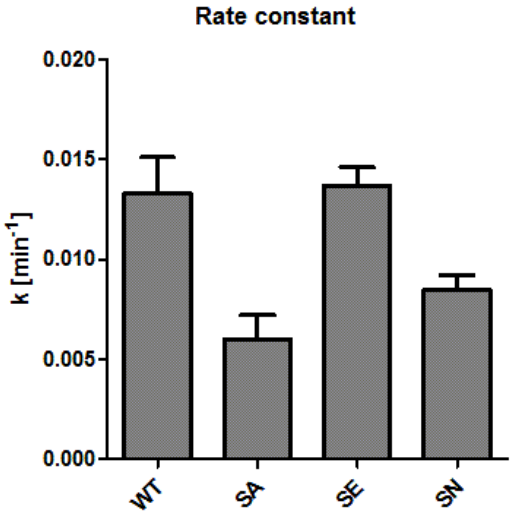

TABLE S1: LIST OF TRANSITIONS USED IN MRM-MS ANALYSIS (A) Tryptic digestion

Heat shock protein 90α

MPEETQTQDQ PMEEEEVETF AFQAEIAQLM SLIINTFYSN KEIFLRELIS NSSDALDKIR YESLTDPSKL DSGKELHINL IPNKQDRTLT IVDTGIGMTK
ADLINNLGTI AKSGTKAFME ALQAGADISM IGQFGVGFYS AYLVAEKVTV ITKHNDDEQY AWESSAGGSF TVRTDTGEPM GRGTKVILHL KEDQTEYLEE
RRIKEIVKKH SQFIGYPITL FVEKERDKEV SDDEAEEKED KEEEKEKEEK ESEDKPEIED VGSDEEEEKK DGDKKKKKKI KEKYIDQEEL NKTKPIWTRN
PDDITNEEYG EFYKSLTNDW EDHLAVKHFS VEGQLEFRAL LFVPRRAPFD LFENRKKKNN IKLYVRRVFI MDNCEELIPE YLNFIRGVVD SEDLPLNISR
EMLQQSKILK VIRKNLVKKC LELFTELAED KENYKKFYEQ FSKNIKLGIH EDSQNRKKLS ELLRYYTSAS GDEMVSLKDY CTRMKENQKH IYYITGETKD

QVANSAFVER LRKHGLEVIY MIEPIDEYCV QQLKEFEGKT LVSVTKEGLE LPEDEEEKKK QEEKKTKFEN LCKIMKDILE KKVEKVVVSN RLVTSPCCIV
TSTYGWTANM ERIMKAQALR DNSTMGYMAA KKHLEINPDH SIIETLRQKA EADKNDKSVK DLVILLYETA LLSSGFSLED PQTHANRIYR MIKLGLGIDE
DDPTADDTSA AVTEEMPPLE GDDDTSRMEE VD

Heat shock protein 90β

MPEEVHHGEE EVETFAFQAE IAQLMSLIIN TFYSNKEIFL RELISNASDA LDKIRYESLT DPSKLDSGKE LKIDIIPNPQ ERTLTLVDTG IGMTKADLIN
NLGTIAKSGT KAFMEALQAG ADISMIGQFG VGFYSAYLVA EKVVVITKHN DDEQYAWESS AGGSFTVRAD HGEPIGRGTK VILHLKEDQT EYLEERRVKE
VVKKHSQFIG YPITLYLEKE REKEISDDEA EEEKGEKEEE DKDDEEKPKI EDVGSDEEDD SGKDKKKKTK KIKEKYIDQE ELNKTKPIWT RNPDDITQEE
YGEFYKSLTN DWEDHLAVKH FSVEGQLEFR ALLFIPRRAP FDLFENKKKK NNIKLYVRRV FIMDSCDELI PEYLNFIRGV VDSEDLPLNI SREMLQQSKI
LKVIRKNIVK KCLELFSELA EDKENYKKFY EAFSKNLKLG IHEDSTNRRR LSELLRYHTS QSGDEMTSLS EYVSRMKETQ KSIYYITGES KEQVANSAFV
ERVRKRGFEV VYMTEPIDEY CVQQLKEFDG KSLVSVTKEG LELPEDEEEK KKMEESKAKF ENLCKLMKEI LDKKVEKVTI SNRLVSSPCC IVTSTYGWTA
NMERIMKAQA LRDNSTMGYM MAKKHLEINP DHPIVETLRQ KAEADKNDKA VKDLVVLLFE TALLSSGFSL EDPQTHSNRI YRMIKLGLGI DEDEVAAEEP
NAAVPDEIPP LEGDEDASRM EEVD

Transitions for tryptic peptides

Include	Precursor Mass (Da)	Fragment Mass (Da)	RT	CE	Fragment Type	Sequence	Mean Height	% CV
True	513.9227	831.46	18.7258	34	3+ / y8	YESLTDPSKLDSGK	21803	2.9448
True	513.9227	688.85	18.7258	26	3+ / y13(2+)	YESLTDPSKLDSGK	7103	3.4245
True	513.9227	624.33	18.7258	26	3+ / y12(2+)	YESLTDPSKLDSGK	30435	0.4365
True	329.7285	559.38	15.3699	20	2+ / y5	VVVITK	6308475.5	1.8521
True	329.7285	460.31	15.3699	18	2+ / y4	VVVITK	9713680	0.2168
True	329.7285	361.24	15.3699	24	2+ / y3	VVVITK	3659741	2.7824
True	345.2006	590.33	13.1884	20	2+ / y5	VTISNR	35933.5	6.7831
True	345.2006	489.28	13.1884	18	2+ / y4	VTISNR	57043	12.0638
True	345.2006	376.19	13.1884	24	2+ / y3	VTISNR	22418.5	5.5670
True	374.2341	646.41	16.1158	21	2+ / y6	TLVSVTK	2055290	1.9277
True	374.2341	533.33	16.1158	19	2+ / y5	TLVSVTK	9886684	0.2578

True	374.2341	434.26	16.1158	23	2+ / y4	TLVSVTK	4580995.5	1.7455
True	858.4787	966.04	42.9190	43	3+ / y19(2+)	TLTLVDTGIGMTKADLINNLGTIAK	176416	3.5978
True	858.4787	943.56	42.9190	43	3+ / y9	TLTLVDTGIGMTKADLINNLGTIAK	85577	5.8253
True	858.4787	915.51	42.9190	43	3+ / y18(2+)	TLTLVDTGIGMTKADLINNLGTIAK	120837.5	0.2777
True	715.3540	921.470994	32.1874	36.476	2+ / y9	TLT[Pho]LVDTGIGMTK	5268044	10.1317
True	715.3540	822.40258	32.1874	34	2+ / y8	TLT[Pho]LVDTGIGMTK	4091614.75	11.7059
True	715.3540	707.375637	32.1874	40	2+ / y7	TLT[Pho]LVDTGIGMTK	1590541.75	23.9234
True	715.3540	615.879427	32.1874	38	2+ / y12(2+)+Pho	TLT[Pho]LVDTGIGMTK	715214.75	35.8565
True	715.3540	606.327959	32.1874	38	2+ / y6	TLT[Pho]LVDTGIGMTK	1497661.25	11.6306
True	715.3540	549.306495	32.1874	40	2+ / y5	TLT[Pho]LVDTGIGMTK	434329.5	17.0759
True	683.3683	937.47	27.6036	35	2+ / y9	TLTLVDTGIGM[Oxi]TK	150881.5	5.4059
True	683.3683	838.4	27.6036	31	2+ / y8	TLTLVDTGIGM[Oxi]TK	198867	4.7773
True	683.3683	723.37	27.6036	37	2+ / y7	TLTLVDTGIGM[Oxi]TK	62356.5	0.9222
True	675.3708	921.47	31.4907	35	2+ / y9	TLTLVDTGIGMTK	4504346	2.2590
True	675.3708	822.4	31.4907	31	2+ / y8	TLTLVDTGIGMTK	4632110	3.2615
True	675.3708	707.38	31.4907	39	2+ / y7	TLTLVDTGIGMTK	1586096.5	1.9081
True	417.1995	746.4	12.4732	25	3+ / y7	TDTGEPMGRGTK	2344	3.7407
True	417.1995	517.26	12.4732	21	3+ / y10(2+)	TDTGEPMGRGTK	2581	1.4246
True	417.1995	466.73	12.4732	21	3+ / y9(2+)	TDTGEPMGRGTK	1195.5	41.1074
True	367.2263	533.33	16.5515	19	2+ / y5	SLVSVTK	10223154	100.0000
True	367.2263	434.26	16.5515	21	2+ / y4	SLVSVTK	5143038	1.0056
True	367.2263	387.22	16.5515	25	2+ / b4	SLVSVTK	605407.5	1.9285
True	583.6451	828.46	28.5267	29	3+ / b7	QDRTLTIVDTGIGMTK	587600.5	8.4563
True	583.6451	822.4	28.5267	29	3+ / y8	QDRTLTIVDTGIGMTK	745569	5.1680
True	583.6451	715.37	28.5267	31	3+ / b6	QDRTLTIVDTGIGMTK	688280	5.9958
True	964.3852	997.164077	23.2475	49	2+ / f997	NPDDITQEEY[Pho]GEFYK	165210.25	27.9054
True	964.3852	886.338262	23.2475	49	2+ / y6	NPDDITQEEY[Pho]GEFYK	737665.5	12.6858
True	643.2592	997.138547	23.2475	32	3+ / f997	NPDDITQEEY[Pho]GEFYK	329447.5	10.2253
True	643.2592	886.338262	23.2475	32	3+ / y6	NPDDITQEEY[Pho]GEFYK	1686874	12.3542
True	643.2592	457.244547	23.2475	36.163	3+ / y3	NPDDITQEEY[Pho]GEFYK	1355100.25	8.3708
True	616.6038	935.41	26.8226	31	3+ / y7	NPDDITQEEYGEFYK	33910.5	0.7899
True	616.6038	806.37	26.8226	31	3+ / y6	NPDDITQEEYGEFYK	104451.5	3.5305
True	616.6038	643.31	26.8226	31	3+ / y5	NPDDITQEEYGEFYK	121936.5	3.2282

True	957.3774	900.356	22.8620	45	2+ / y14(2+)	NPDDITNEEY[Pho]GEFYK	2304214.25	5.0651
True	957.3774	886.338262	22.8620	51	2+ / y6	NPDDITNEEY[Pho]GEFYK	933715.25	15.4447
True	957.3774	851.8296	22.8620	43	2+ / y13(2+)	NPDDITNEEY[Pho]GEFYK	189351.25	34.1573
True	957.3774	794.3161	22.8620	45	2+ / y12(2+)	NPDDITNEEY[Pho]GEFYK	56589.25	7.3709
True	917.8863	935.41	26.3149	47	2+ / y7	NPDDITN[Dea]EEYGEFYK	36016	1.2682
True	611.9319	935.41	26.3208	31	3+ / y7	NPDDITNEEYGEFYK	18936.5	4.9328
True	611.9319	806.37	26.3208	31	3+ / y6	NPDDITNEEYGEFYK	80786	0.4985
True	611.9319	643.31	26.3208	31	3+ / y5	NPDDITNEEYGEFYK	89493	1.2846
True	654.8433	978.49	17.6672	38	2+ / b8	IRYESLTDPSK	1288370.5	5.2720
True	436.8979	649.33	17.6672	24	3+ / b5	IRYESLTDPSK	595054	0.5003
True	436.8979	547.27	17.6672	24	3+ / y5	IRYESLTDPSK	718747.5	1.6229
True	594.9880	827.5	25.5201	34	3+ / y7	HLEINPDHPIVETLR	6223604.5	3.7299
True	594.9880	819.4	25.5201	34	3+ / b7	HLEINPDHPIVETLR	2619105	4.6253
True	594.9880	617.36	25.5201	36	3+ / y5	HLEINPDHPIVETLR	2924624.5	4.9990
True	446.2159	744.36	21.3400	23	2+ / y6	FYEAFSK	2680896	2.4080
True	446.2159	581.29	21.3400	23	2+ / y5	FYEAFSK	5531887	1.8987
True	446.2159	452.25	21.3400	27	2+ / y4	FYEAFSK	1358879	1.6506
True	432.2181	734.39	13.5527	22	2+ / y6	EMLQQSK	4618.5	11.8655
True	432.2181	603.35	13.5527	24	2+ / y5	EMLQQSK	72227	7.1056
True	432.2181	490.26	13.5527	20	2+ / y4	EMLQQSK	57715	4.0725
True	646.3224	936.43	19.4537	31	2+ / y9	ELISNSSDALDK	4311637.5	0.6905
True	646.3224	849.39	19.4537	31	2+ / y8	ELISNSSDALDK	1547126.5	3.4373
True	646.3224	735.35	19.4537	31	2+ / y7	ELISNSSDALDK	1553285	4.1623
True	638.3249	920.43	22.2790	31	2+ / y9	ELISNASDALDK	5285075	4.6984
True	638.3249	833.4	22.2790	31	2+ / y8	ELISNASDALDK	1999516.5	3.7138
True	638.3249	719.36	22.2790	31	2+ / y7	ELISNASDALDK	1996254.5	0.4264
True	650.6774	936.43	38.9703	33	3+ / y9	EIFLRELISNSSDALDK	738577	1.2140
True	650.6774	901.51	38.9703	37	3+ / b7	EIFLRELISNSSDALDK	402117	3.2572
True	650.6774	854.45	38.9703	35	3+ / y15(2+)	EIFLRELISNSSDALDK	853093	0.4943
True	618.3043	992.52	18.2559	30	2+ / y9	DQVANSAFVER	2233215	1.5644
True	618.3043	893.45	18.2559	30	2+ / y8	DQVANSAFVER	3739184	0.9177
True	618.3043	822.41	18.2559	34	2+ / y7	DQVANSAFVER	2210815	1.8834
True	624.7564	932.4	22.5315	30	2+ / y8	DNSTMGYMMAK	392562.5	0.4174

True	624.7564	831.36	22.5315	30	2+ / y7	DNSTMGYMMAK	759131	0.1904
True	624.7564	700.32	22.5315	30	2+ / y6	DNSTMGYMMAK	970791.5	1.9975
True	439.5372	768.41	15.4235	26	3+ / y7	DNSTMGYMAAKK	189052	0.3325
True	439.5372	544.27	15.4235	22	3+ / y10(2+)	DNSTMGYMAAKK	93771.5	4.4137
True	439.5372	450.23	15.4235	22	3+ / y8(2+)	DNSTMGYMAAKK	165596	3.6186
True	317.8262	510.19	12.6694	16	3+ / b5	ADHGEPIGR	5598	8.1599
True	317.8262	442.28	12.6694	16	3+ / y4	ADHGEPIGR	2748	27.6358
True	317.8262	345.22	12.6694	22	3+ / y3	ADHGEPIGR	6022.5	0.2949

(B)GluC digestion

Heat shock protein 90 α

MPEETQTQDQ PMEEEEVETF AFQAEIAQLM SLIINTFYSN KEIFLRELIS NSSDALDKIR YESLTDPSKL DSGKELHINL IPNKQDRTLT IVDTGIGMTK
ADLINNLGTI AKSGTKAFME ALQAGADISM IGQFGVGFYS AYLVAEKVTV ITKHNDDEQY AWESSAGGSF TVRTDTGEPM GRGTKVILHL KEDQTEYLEE
RRIKEIVKKH SQFIGYPITL FVEKERDKEV SDDEAEEKED KEEEKEKEEK ESEDKPEIED VGSDEEEEKK DGDKKKKKKI KEKYIDQEEL NKTKPIWTRN
PDDITNEEYG EFYKSLTNDW EDHLAVKHFS VEGQLEFRAL LFVPRRAPFD LFENRKKKNN IKLYVRRVFI MDNCEELIPE YLNFIRGVVD SEDLPLNISR
EMLQQSKILK VIRKNLVKKC LELFTELAED KENYKKFYEQFSKNIKLGIHE/DSQNRKKLSE/LLRYYTSASGDE/MVSLKDYCTRMKENQKH IYYITGETKD
QVANSAFVER LRKHGLEVIY MIEPIDEYCV QQLKEFEGKT LVSVTKEGLE LPEDEEEKKK QEEKKTKFEN LCKIMKDILE KKVEKVVVSN RLVTSPCCIV
TSTYGWTANM ERIMKAQALR DNSTMGYMAA KKHLEINPDH SIIETLRQKA EADKNDKSVK DLVILLYETA LLSSGFSLED PQTHANRIYR MIKLGLGIDE
DDPTADDTSA AVTEEMPPLE GDDDTSRMEE VD

Heat shock protein 90β

MPEEVHHGEE EVETFAFQAE/IAQLMSLIIN TFYSNKEIFL RELISNASDA LDKIRYE/SLT DPSKLDSGKE/LKIDIIPNPQ ERTLTLVDTG IGMTKADLIN
NLGTIAKSGT KAFMEALQAG ADISMIGQFG VGFYSAYLVA EKVVVITKHN DDEQYAWESS AGGSFTVRAD HGEPIGRGTK VILHLKEDQT EYLEERRVKE
VVKKHSQFIG YPITLYLEKE REKEISDDEA EEEKGEKEEE DKDDEEKPKI EDVGSDEEDD SGKDKKKKTK KIKEKYIDQE ELNKTKPIWT RNPDDITQEE
YGEFYKSLTN DWEDHLAVKH FSVEGQLEFR ALLFIPRRAP FDLFENKKKK NNIKLYVRRV FIMDSCDELI PEYLNFIRGVVDSE/DLPLNI SREMLQQSKI
LKVIRKNIVK KCLELFSELA EDKENYKKFY EAFSKNLKLG IHEDSTNRRR LSELLRYHTS QSGDEMTSLS EYVSRMKETQ KSIYYITGE/SKEQVANSAFV
ERVRKRGFEV VYMTEPIDEY CVQQLKEFDG KSLVSVTKEG LELPEDEEEK KKMEESKAKF ENLCKLMKEI LDKKVEKVTI SNRLVSSPCC IVTSTYGWTA

NMERIMKAQA LRDNSTMGYM MAKKHLE**INP DHPIVETLRQ KAE**ADKNDKA VKDLVVLLFE TALLSSGFSL EDPQTHSNRI YRMIKLGLGI DEDEVAAEEP NAAVPDEIPP LEGDEDASRM EEVD

Transitions for GluC Peptides

Include	Precursor Mass (Da)	Fragment Mass (Da)	RT	CE	Fragment Type	Sequence	Mean Height	% CV
True	817.0955	963.54	43.899	36	3+ / b8	YLNFIRGVVDSEDLPLNISRE	27479.25	115.9396
True	817.0955	941.54	43.899	36	3+ / y8	YLNFIRGVVDSEDLPLNISRE	30141.25	115.6112
True	817.0955	828.46	43.899	36	3+ / y7	YLNFIRGVVDSEDLPLNISRE	371090.75	115.8763
True	706.3644	963.54	37.767	30	2+ / b8	YLNFIRGVVDSE	215487	99.6151
True	706.3644	874.46	37.767	36	2+ / y8	YLNFIRGVVDSE	159430.75	102.3599
True	706.3644	761.38	37.767	33	2+ / y7	YLNFIRGVVDSE	154505.5	103.6115
True	611.3071	846.44	39.419	23	2+ / b7	VIYMIEPIDE	288676.5	79.8791
True	611.3071	749.39	39.419	23	2+ / b6	VIYMIEPIDE	983494.5	46.9956
True	611.3071	620.35	39.419	23	2+ / b5	VIYMIEPIDE	1001428.5	34.8969
True	521.2479	823.4	32.283	19	2+ / b7	VETFAFQAE	70445	18.7745
True	521.2479	695.34	32.283	19	2+ / b6	VETFAFQAE	127813.5	10.8793
True	521.2479	548.27	32.283	22	2+ / b5	VETFAFQAE	258742.75	61.7897
True	549.6138	884.45	21.319	25	3+ / b7	TQKSIYYITGESKE	111846.75	74.7358
True	549.6138	721.39	21.319	28	3+ / b6	TQKSIYYITGESKE	107368.75	88.0663
True	549.6138	650.3	21.319	25	3+ / y6	TQKSIYYITGESKE	440144.75	85.7008
True	651.8324	997.54	25.928	28	2+ / b8	TQKSIYYITGE	1014512	48.5091
True	651.8324	884.45	25.928	31	2+ / b7	TQKSIYYITGE	821513.5	77.5079
True	651.8324	721.39	25.928	28	2+ / b6	TQKSIYYITGE	503816	66.4555
True	423.2455	631.35	19.156	15	2+ / y5	TLRQKAE	2069.25	79.1982
True	423.2455	627.39	19.156	15	2+ / b5	TLRQKAE	11595.5	85.1565
True	654.8251	915.45	20.935	25	2+ / b9	TKDQVANSAFVE	434696	93.0728
True	654.8251	844.42	20.935	25	2+ / b8	TKDQVANSAFVE	72645.6667	73.0753
True	654.8251	757.38	20.935	25	2+ / b7	TKDQVANSAFVE	133695.833	39.6642
True	407.1924	666.32	29.229	17	2+ / b6	TFAFQAE	812022.75	54.9420
True	407.1924	595.29	29.229	17	2+ / b5	TFAFQAE	1255641.75	15.0244

True	407.1924	467.23	29.229	23	2+ / b4	TFAFQAE	1211806.5	48.4376
True	459.5682	588.79	17.660	18	3+ / y11(2+)	SLTDPSKLDSGKE	5283779	30.2108
True	459.5682	538.27	17.660	18	3+ / y10(2+)	SLTDPSKLDSGKE	1502967.5	14.4638
True	459.5682	480.75	17.660	18	3+ / y9(2+)	SLTDPSKLDSGKE	4647355	63.2741
True	654.8251	915.45	20.941	25	2+ / b9	SKEQVANSAFVE	522450.667	69.1306
True	654.8251	844.42	20.941	25	2+ / b8	SKEQVANSAFVE	84779.1667	58.5654
True	654.8251	757.38	20.941	25	2+ / b7	SKEQVANSAFVE	142761	35.3815
True	482.7403	718.35	23.172	17	2+ / b7	QVANSAFVE	257171	19.6262
True	482.7403	571.28	23.172	17	2+ / b6	QVANSAFVE	169617.667	87.4326
True	482.7403	500.25	23.172	17	2+ / b5	QVANSAFVE	36362.75	90.5380
True	471.9331	696.4	20.171	19	3+ / y6	QFSKNIKLGIHE	178042.5	116.9632
True	471.9331	569.83	20.171	19	3+ / y10(2+)	QFSKNIKLGIHE	327221.75	116.3572
True	471.9331	568.31	20.171	19	3+ / y5	QFSKNIKLGIHE	618638	116.6141
True	554.2666	765.38	22.422	23	3+ / y12(2+)	MVSLKDYC[CAM]TRMKE	302720.25	115.1212
True	554.2666	715.84	22.422	23	3+ / y11(2+)	MVSLKDYC[CAM]TRMKE	908051.25	114.3221
True	554.2666	615.78	22.422	23	3+ / y9(2+)	MVSLKDYC[CAM]TRMKE	455643.75	116.0373
True	687.8304	968.52	21.433	26	2+ / b8	LLRYYTSASGDE	1482509	97.8541
True	687.8304	897.48	21.433	26	2+ / b7	LLRYYTSASGDE	561357.75	100.5018
True	687.8304	810.45	21.433	26	2+ / b6	LLRYYTSASGDE	715873.25	97.4900
True	469.2283	683.4	15.421	30	3+ / b5	LLRYHTSQSGDE	771822	43.4210
True	469.2283	629.81	15.421	21	3+ / b11(2+)	LLRYHTSQSGDE	3876018.75	31.4634
True	469.2283	500.27	15.421	24	3+ / b8(2+)	LLRYHTSQSGDE	880328.25	37.8155
True	575.3001	805.9	26.829	24	3+ / y14(2+)	LISNSSDALDKIRYE	808574.25	65.7922
True	575.3001	749.36	26.829	24	3+ / y13(2+)	LISNSSDALDKIRYE	5899390	23.1308
True	575.3001	705.85	26.829	24	3+ / y12(2+)	LISNSSDALDKIRYE	839311.25	77.6107
True	569.9685	797.91	29.367	23	3+ / y14(2+)	LISNASDALDKIRYE	662215.5	69.9015
True	569.9685	741.37	29.367	23	3+ / y13(2+)	LISNASDALDKIRYE	5050484	36.0333
True	569.9685	640.83	29.367	23	3+ / y11(2+)	LISNASDALDKIRYE	845495.75	97.4065
True	462.7190	777.38	15.186	16	2+ / b6	KYIDQEE	834969.75	93.6643
True	462.7190	648.34	15.186	16	2+ / b5	KYIDQEE	725980.5	105.8815
True	462.7190	520.28	15.186	16	2+ / b4	KYIDQEE	942143.25	99.4379
True	519.2667	890.47	21.565	19	2+ / b8	INPDHSIIE	1228520.5	40.5843
True	519.2667	810.4	21.565	19	2+ / y7	INPDHSIIE	4687219	68.5244

True	519.2667	777.39	21.565	19	2+ / b7	INPDHSIIE	2665757.25	79.3017
True	517.2692	806.4	20.471	19	2+ / y7	INPDHPIVE	6750996	25.0723
True	517.2692	787.41	20.471	19	2+ / b7	INPDHPIVE	692420.25	35.6244
True	517.2692	594.32	20.471	19	2+ / y5	INPDHPIVE	623809.25	95.8938
True	715.6627	916.9007	51.900	18	3+ / y14(2+)	IAQLMSLIINT[Pho]FY[Pho]SNKE	14310.5	116.2016
True	715.6627	720.260012	51.900	44	3+ / y5	IAQLMSLIINT[Pho]FY[Pho]SNKE	4950	106.4803
True	689.0073	984.4421	52.011	40	3+ / y8+Pho	IAQLMSLIINT[Pho]FYSNKE	4115.5	86.9558
True	689.0073	870.511737	52.011	36	3+ / y7+Pho	IAQLMSLIINT[Pho]FYSNKE	13940.5	75.3087
True	689.0073	867.328426	52.004	26	3+ / y6	IAQLMSLIINTFY[Pho]SNKE	2049.5	71.7975
True	689.0073	787.362096	52.011	40	3+ / y6	IAQLMSLIINT[Pho]FYSNKE	9252.5	69.5834
True	689.0073	769.3515	52.004	29	3+ / y6+Pho	IAQLMSLIINTFY[Pho]SNKE	467.5	68.5175
True	689.0073	640.293682	52.011	46	3+ / y5	IAQLMSLIINT[Pho]FYSNKE	9729.5	74.6461
True	689.0073	477.230353	52.011	38	3+ / y4	IAQLMSLIINT[Pho]FYSNKE	24433.25	91.6941
True	662.6799	870.51	42.096	28	3+ / b8	IAQLMSLIIN[Dea]TFYSNKE	794.5	34.0871
True	662.6799	787.36	42.096	28	3+ / y6	IAQLMSLIIN[Dea]TFYSNKE	706	15.6245
True	662.3518	640.293682	42.099	28	3+ / y5	IAQLMSLIINTFYSNKE	2294.5	27.3351
True	662.3518	477.230353	42.099	28	3+ / y4	IAQLMSLIINTFYSNKE	3530	50.2386
True	354.5448	563.3	16.018	13	3+ / y5	GKTLVSVTKE	1882578.33	87.1138
True	354.5448	400.26	16.018	13	3+ / b4	GKTLVSVTKE	1367965.25	116.1309
True	354.5448	377.2	16.018	13	3+ / y3	GKTLVSVTKE	1663156	115.8978
True	651.8036	992.47	29.152	31	2+ / y8	FYKSLTNDWE	94216.25	83.7327
True	651.8036	969.47	29.152	31	2+ / b8	FYKSLTNDWE	295229.25	84.8041
True	651.8036	740.4	29.152	28	2+ / b6	FYKSLTNDWE	46955	78.2324
True	437.2380	648.34	23.339	17	3+ / b6	FDGKSLVSVTKE	1212988.5	76.4954
True	437.2380	581.83	23.339	17	3+ / b11(2+)	FDGKSLVSVTKE	1336366.25	61.0311
True	437.2380	563.3	23.339	17	3+ / y5	FDGKSLVSVTKE	3224568	72.6292
True	528.7878	828.46	28.490	25	2+ / y7	DLPLNISRE	2902130.75	71.9018
True	528.7878	731.4	28.490	34	2+ / y6	DLPLNISRE	1720832.75	66.3069
True	528.7878	618.32	28.490	34	2+ / y5	DLPLNISRE	3346665.75	56.1028
True	452.9259	643.37	22.374	24	3+ / y11(2+)	AFSKNLKLGIHE	276559.75	102.9635
True	452.9259	569.83	22.374	24	3+ / y10(2+)	AFSKNLKLGIHE	1047146.75	99.5015
True	452.9259	568.31	22.374	24	3+ / y5	AFSKNLKLGIHE	551597	107.5382

TABLE S2: SIGNIFICANCE VALUES CALCULATED FROM STUDENT'S T-TEST FOR MST MEASUREMENTS USING THE MINIMAL GR-ACTIVATING SYSTEM CONTAINING DIFFERENT HSP90 PROTEINS

0.01 < p-value <= 0.05: strong presumption against the null-hypothesis ("no difference between two groups in comparison); 0.05 < p-value: low or no presumption against the null hypothesis.

p-value	t-test vs Hsp90β S365E	t-test vs Hsp90β WT
Hsp90α	**0.0394**	0.3064
Hsp90β WT	**0.0357**	
SA	**0.0274**	0.1425
SE		**0.0357**
SN	**0.0207**	0.0511

6 REFERENCES

Abbas-Terki, T. et al., 2002. The Hsp90 co-chaperones Cdc37 and Sti1 interact physically and genetically. *Biological chemistry*, 383(9), pp.1335–42.

Abbas-Terki, T., Donzé, O. & Picard, D., 2000. The molecular chaperone Cdc37 is required for Ste11 function and pheromone-induced cell cycle arrest. *FEBS letters*, 467(1), pp.111–6.

Adinolfi, E. et al., 2003. Tyrosine phosphorylation of HSP90 within the P2X7 receptor complex negatively regulates P2X7 receptors. *The Journal of biological chemistry*, 278(39), pp.37344–37351.

Ali, M.M.U. et al., 2006. Crystal structure of an Hsp90-nucleotide-p23/Sba1 closed chaperone complex. *Nature*, 440(7087), pp.1013–7.

Bain, D.L. et al., 2007. Nuclear receptor structure: implications for function. *Annual review of physiology*, 69, pp.201–20.

Bali, P. et al., 2005. Inhibition of histone deacetylase 6 acetylates and disrupts the chaperone function of heat shock protein 90: a novel basis for antileukemia activity of histone deacetylase inhibitors. *The Journal of biological chemistry*, 280(29), pp.26729–34.

Barabutis, N. et al., 2013. LPS induces pp60c-src-mediated tyrosine phosphorylation of Hsp90 in lung vascular endothelial cells and mouse lung. *American journal of physiology. Lung cellular and molecular physiology*, 304(12), pp.L883–93.

Barati, M.T. et al., 2006. A Proteomic Screen Identified Stress-induced Chaperone as Targets of Akt Phosphorylation in mesangial cells. *J Proteome Res*, 5(7), pp.1636–1646.

Barent, R.L. et al., 1998. Analysis of FKBP51/FKBP52 chimeras and mutants for Hsp90 binding and association with progesterone receptor complexes. *Molecular endocrinology*, 12(3), pp.342–54.

Basso, A.D. et al., 2002. Akt forms an intracellular complex with heat shock protein 90 (Hsp90) and Cdc37 and is destabilized by inhibitors of Hsp90 function. *The Journal of biological chemistry*, 277(42), pp.39858–66.

Bennetzen, M. V et al., 2010. Site-specific phosphorylation dynamics of the nuclear proteome during the DNA damage response. *Molecular & cellular proteomics : MCP*, 9(6), pp.1314–23.

Biamonte, M. a et al., 2006. Orally active purine-based inhibitors of the heat shock protein 90. *Journal of medicinal chemistry*, 49(2), pp.817–28.

Bledsoe, R.K. et al., 2002. Crystal structure of the glucocorticoid receptor ligand binding domain reveals a novel mode of receptor dimerization and coactivator recognition. *Cell*, 110(1), pp.93–105.

Bohen, S.P., 1995. Hsp90 mutants disrupt glucocorticoid receptor ligand binding and destabilize aporeceptor complexes. *The Journal of biological chemistry*, 270(49), pp.29433–8.

Booher, R.N., Deshaies, R.J. & Kirschner, M.W., 1993. Properties of Saccharomyces cerevisiae wee1 and its differential regulation of p34CDC28 in response to G1 and G2 cyclins. *The EMBO journal*, 12(9), pp.3417–26.

Bose, S. et al., 1996. Chaperone Function of Hsp90-Associated Proteins. *Science*, 274(December), pp.1715–1717.

Breinig, M. et al., 2009. Targeting heat shock protein 90 with non-quinone inhibitors: a novel chemotherapeutic approach in human hepatocellular carcinoma. *Hepatology (Baltimore, Md.)*, 50(1), pp.102–12.

Bresnick, E.H. et al., 1989. Evidence that the 90-kDa heat shock protein is necessary for the steroid binding conformation of the L cell glucocorticoid receptor. *The Journal of biological chemistry*, 264(9), pp.4992–7.

Brinker, A. et al., 2002. Ligand Discrimination by TPR Domains : Relevance and selectivity of EEVD-Recognition in Hsp70.HOP.Hsp90 complexes. *JBC*, 277, pp.19265–19275.

Chadli, A. et al., 2000. Dimerization and N-terminal domain proximity underlie the function of the molecular chaperone heat shock protein 90. *Proceedings of the National Academy of Sciences of the United States of America*, 97(23), pp.12524–9.

Chang, H.C., Nathan, D.F. & Lindquist, S., 1997. In vivo analysis of the Hsp90 cochaperone Sti1 (p60). *Molecular and cellular biology*, 17(1), pp.318–25.

Chen, S. & Smith, D.F., 1998. Hop as an Adaptor in the Heat Shock Protein 70 (Hsp70) and Hsp90 Chaperone Machinery. *Journal of Biological Chemistry*, 273(52), pp.35194–35200.

Chiosis, G. & Neckers, L., 2006. Tumor selectivity of Hsp90 inhibitors: the explanation remains elusive. *ACS chemical biology*, 1(5), pp.279–84.

Cunningham, C.N., Krukenberg, K. a & Agard, D. a, 2008. Intra- and intermonomer interactions are required to synergistically facilitate ATP hydrolysis in Hsp90. *The Journal of biological chemistry*, 283(30), pp.21170–8.

Czar, M.J. et al., 1997. Geldanamycin, a heat shock protein 90-binding benzoquinone ansamycin, inhibits steroid-dependent translocation of the glucocorticoid receptor from the cytoplasm to the nucleus. *Biochemistry*, 36(25), pp.7776–85.

Davenport, E.L. et al., 2007. Heat shock protein inhibition is associated with activation of the unfolded protein response pathway in myeloma plasma cells. *Blood*, 110(7), pp.2641–9.

Davies, T.H., Ning, Y.-M. & Sánchez, E.R., 2002. A new first step in activation of steroid receptors: hormone-induced switching of FKBP51 and FKBP52 immunophilins. *The Journal of biological chemistry*, 277(7), pp.4597–600.

Degiorgis, J.A. et al., 2005. Phosphoproteomic Analysis of Synaptosomes from Human Cerebral Cortex research articles. *Journal of proteome research*, 4, pp.306–315.

Dephoure, N. et al., 2008. A quantitative atlas of mitotic phosphorylation. *Proceedings of the National Academy of Sciences of the United States of America*, 105(31), pp.10762–7.

Dezwaan, D.C. & Freeman, B.C., 2008. HSP90 The Rosetta stone for cellular protein dynamics? *Cell Cycle*, 7(8), pp.1006–1012.

Dittmar, K.D. et al., 1997. Folding of the Glucocorticoid Receptor by the Heat Shock Protein (hsp) 90-based Chaperone Machinery : The role of p23 is to stabilize receptor · hsp90 heterocomplexes formby hsp90 · p60 · hsp70. *JBC*, 272, pp.21213–220.

Dittmar, K.D. et al., 1996. Reconstitution of the Steroid Receptor hsp90 Heterocomplex Assembly System of Rabbit Reticulocyte Lysate. *Journal of Biological Chemistry*, 271(22), pp.12833–12839.

Dittmar, K.D. & Pratt, W.B., 1997. Folding of the Glucocorticoid Receptor by the Reconstituted hsp90-based Chaperone Machinery: The initial hsp90-p60-hsp70-dependent step is sufficient for creating the steroid binding conformation. *JBC*, 272(20), pp.13047–13054.

Dote, H. et al., 2006. Inhibition of hsp90 compromises the DNA damage response to radiation. *Cancer research*, 66(18), pp.9211–9220.

Dougherty, J. et al., 1987. Identification of the 90Kda substrate of rat liver type II casein kinase with the heat shock protein which binds steroid receptors. *BBA*, 927, pp.74–80.

Duval, M. et al., 2007. Src-mediated phosphorylation of Hsp90 in response to vascular endothelial growth factor (VEGF) is required for VEGF receptor-2 signaling to endothelial NO synthase. *Molecular biology of the cell*, 18(11), pp.4659–4668.

Echeverría, P.C. et al., 2009. Nuclear import of the glucocorticoid receptor-hsp90 complex through the nuclear pore complex is mediated by its interaction with Nup62 and importin beta. *Molecular and cellular biology*, 29(17), pp.4788–97.

Ecroyd, H., Jones, R.C. & Aitken, R.J., 2003. Tyrosine phosphorylation of HSP-90 during mammalian sperm capacitation. *Biology of reproduction*, 69(6), pp.1801–1807.

Eiseman, J.L. et al., 2005. Pharmacokinetics and pharmacodynamics of 17-demethoxy 17-[[(2-dimethylamino)ethyl]amino]geldanamycin (17DMAG, NSC 707545) in C.B-17 SCID mice bearing MDA-MB-231 human breast cancer xenografts. *Cancer chemotherapy and pharmacology*, 55(1), pp.21–32.

Esser, C., Scheffner, M. & Höhfeld, J., 2005. The chaperone-associated ubiquitin ligase CHIP is able to target p53 for proteasomal degradation. *The Journal of biological chemistry*, 280(29), pp.27443–8.

Felts, S.J. & Toft, D.O., 2003. P23, a Simple Protein With Complex Activities. *Cell stress & chaperones*, 8(2), pp.108–13.

Finka, A. & Goloubinoff, P., 2013. Proteomic data from human cell cultures refine mechanisms of chaperone-mediated protein homeostasis. *Cell stress & chaperones*, 18(5), pp.591–605.

Flom, G. et al., 2007. Definition of the minimal fragments of Sti1 required for dimerization, interaction with Hsp70 and Hsp90 and in vivo functions. *The Biochemical journal*, 404(1), pp.159–67.

Fontana, J., 2002. Domain Mapping Studies Reveal That the M Domain of hsp90 Serves as a Molecular Scaffold to Regulate Akt-Dependent Phosphorylation of Endothelial Nitric Oxide Synthase and NO Release. *Circulation Research*, 90(8), pp.866–873.

Forafonov, F. et al., 2008. p23/Sba1p protects against Hsp90 inhibitors independently of its intrinsic chaperone activity. *Molecular and cellular biology*, 28(10), pp.3446–56.

Franco, M.C. et al., 2013. Nitration of Hsp90 induces cell death. *Proceedings of the National Academy of Sciences of the United States of America*, 110(12), pp.E1102–11.

Freeman, B.C. et al., 2000. The p23 molecular chaperones act at a late step in intracellular receptor action to differentially affect ligand efficacies. *Genes & Development*, 14, pp.422–434.

Freeman, B.C., Toft, D.O. & Morimoto, R.I., 1996. Molecular chaperone machines: chaperone activities of the cyclophilin Cyp-40 and the steroid aporeceptor-associated protein p23. *Science (New York, N.Y.)*, 274(5293), pp.1718–20.

Frydman, J., 2001. Folding of newly translated proteins in vivo: the role of molecular chaperones. *Annual review of biochemistry*, 70, pp.603–47.

Gaiser, A.M., Kretzschmar, A. & Richter, K., 2010a. Cdc37-Hsp90 complexes are responsive to nucleotide-induced conformational changes and binding of further cofactors. *The Journal of biological chemistry*, 285(52), pp.40921–32.

Gaiser, A.M., Kretzschmar, A. & Richter, K., 2010b. Cdc37-Hsp90 complexes are responsive to nucleotide-induced conformational changes and binding of further cofactors. *The Journal of biological chemistry*, 285(52), pp.40921–32.

Galigniana, M.D. et al., 2002. Binding of hsp90-associated immunophilins to cytoplasmic dynein: direct binding and in vivo evidence that the peptidylprolyl isomerase domain is a dynein interaction domain. *Biochemistry*, 41(46), pp.13602–10.

Galigniana, M.D. et al., 2001. Evidence that the peptidylprolyl isomerase domain of the hsp90-binding immunophilin FKBP52 is involved in both dynein interaction and glucocorticoid receptor movement to the nucleus. *The Journal of biological chemistry*, 276(18), pp.14884–9.

Galigniana, M.D., 1998. Heat Shock Protein 90-Dependent (Geldanamycin-Inhibited) Movement of the Glucocorticoid Receptor through the Cytoplasm to the Nucleus Requires Intact Cytoskeleton. *Molecular Endocrinology*, 12(12), pp.1903–1913.

Galigniana, M.D. et al., 2004. Retrograde transport of the glucocorticoid receptor in neurites requires dynamic assembly of complexes with the protein chaperone hsp90 and is linked to the CHIP component of the machinery for proteasomal degradation. *Brain research. Molecular brain research*, 123(1-2), pp.27–36.

Galigniana, M.D., Erlejman, A.G. & Piwien-pilipuk, G., 2010. Role of molecular chaperones and TPR-domain proteins in the cytoplasmic transport of steroid receptors and their passage through the nuclear pore. *Nucleus*, 1(August), pp.299–308.

Gao, Y. et al., 2013. Distinct roles of molecular chaperones HSP90α and HSP90β in the biogenesis of KCNQ4 channels. *PloS one*, 8(2), p.e57282.

García-Cardeña, G. et al., 1998. Dynamic activation of endothelial nitric oxide synthase by Hsp90. *Nature*, 392(6678), pp.821–4.

Gerber, M.R. et al., 1995. Cdc37 is required for the association of Cdc28 with G1 and mitotic cyclins. *PNAS*, 92(May), pp.4651–4655.

Gnad, F. et al., 2010. Evolutionary constraints of phosphorylation in eukaryotes, prokaryotes, and mitochondria. *Molecular & cellular proteomics : MCP*, 9(12), pp.2642–53.

Gooljarsingh, L.T. et al., 2006. A biochemical rationale for the anticancer effects of Hsp90 inhibitors: slow, tight binding inhibition by geldanamycin and its analogues. *Proceedings of the National Academy of Sciences of the United States of America*, 103(20), pp.7625–30.

Graf, C. et al., 2009. Spatially and kinetically resolved changes in the conformational dynamics of the Hsp90 chaperone machine. *The EMBO journal*, 28(5), pp.602–13.

Grammatikakis, N. et al., 1999. p50(cdc37) acting in concert with Hsp90 is required for Raf-1 function. *Molecular and cellular biology*, 19(3), pp.1661–72.

Grbovic, O.M. et al., 2006. V600E B-Raf requires the Hsp90 chaperone for stability and is degraded in response to Hsp90 inhibitors. *Proceedings of the National Academy of Sciences of the United States of America*, 103(1), pp.57–62.

Hainzl, O. et al., 2009. The charged linker region is an important regulator of Hsp90 function. *The Journal of biological chemistry*, 284(34), pp.22559–67.

Han, G. et al., 2008. Large-scale phosphoproteome analysis of human liver tissue by enrichment and fractionation of phosphopeptides with strong anion exchange chromatography. *Proteomics*, 8(7), pp.1346–61.

Harrell, J.M. et al., 2004. Evidence for glucocorticoid receptor transport on microtubules by dynein. *The Journal of biological chemistry*, 279(52), pp.54647–54.

Harst, A., Lin, H. & Obermann, W.M.J., 2005. Aha1 competes with Hop, p50 and p23 for binding to the molecular chaperone Hsp90 and contributes to kinase and hormone receptor activation. *The Biochemical journal*, 387(Pt 3), pp.789–96.

Hartmann, F. et al., 1997. Effects of the tyrosine-kinase inhibitor geldanamycin on ligand-induced Her-2/neu activation, receptor expression and proliferation of Her-2-positive malignant cell lines. *International journal of cancer.*, 70(2), pp.221–9.

Harvey, S.L. & Kellogg, D.R., 2003. Conservation of mechanisms controlling entry into mitosis: budding yeast wee1 delays entry into mitosis and is required for cell size control. *Current biology : CB*, 13(4), pp.264–75.

Hawle, P. et al., 2006a. The middle domain of Hsp90 acts as a discriminator between different types of client proteins. *Molecular and cellular biology*, 26(22), pp.8385–95.

Hawle, P. et al., 2006b. The middle domain of Hsp90 acts as a discriminator between different types of client proteins. *Molecular and cellular biology*, 26(22), pp.8385–95.

He, H. et al., 2006. Identification of potent water soluble purine-scaffold inhibitors of the heat shock protein 90. *Journal of medicinal chemistry*, 49(1), pp.381–90.

Hernández, M.P., Sullivan, W.P. & Toft, D.O., 2002. The assembly and intermolecular properties of the hsp70-Hop-hsp90 molecular chaperone complex. *The Journal of biological chemistry*, 277(41), pp.38294–304.

Herskowitz, J.H. et al., 2011. Phosphoproteomic analysis reveals site-specific changes in GFAP and NDRG2 phosphorylation in frontotemporal lobar degeneration. *Journal of Proteome Research*, 9(12), pp.6368–6379.

Hessling, M., Richter, K. & Buchner, J., 2009. Dissection of the ATP-induced conformational cycle of the molecular chaperone Hsp90. , 16(3), pp.287–293.

Höhfeld, J., Cyr, D.M. & Patterson, C., 2001. From the cradle to the grave: molecular chaperones that may choose between folding and degradation. *EMBO reports*, 2(10), pp.885–90.

Holmes, J.L. et al., 2008. Silencing of HSP90 cochaperone AHA1 expression decreases client protein activation and increases cellular sensitivity to the HSP90 inhibitor 17-allylamino-17-demethoxygeldanamycin. *Cancer research*, 68(4), pp.1188–97.

Holt, S.E. et al., 1999. Functional requirement of p23 and Hsp90 in telomerase complexes. *Genes & development*, 13(7), pp.817–26.

Howard, J. et al., 1990. Mapping the HSPSO Binding Region of the Glucocorticoid Receptor. *JBC*, 265, pp.11928–35.

Hsieh, Y.-Y., Hung, P.-H. & Leu, J.-Y., 2013. Hsp90 regulates nongenetic cariation in response to environmental stress. *Molecular cell*, 50, pp.82–92.

Hsu, P.P. et al., 2011. The mTOR-regulated Phosphoproteome reveals a mechanism of mTORC1-mediated inhibition of growth factor signaling. *Science*, 332(6035), pp.1317–1322.

Hu, J., Toft, D.O. & Seeger, C., 1997. Hepadnavirus assembly and reverse transcription require a multi-component chaperone complex which is incorporated into nucleocapsids. *The EMBO journal*, 16(1), pp.59–68.

Iannotti, M., Rabideau, A. & Dougherty, J., 1988. Characterization of purified Avian 90kDa heat shock protein. *Archives*, 264(1), pp.54–60.

Iliuk, A.B. et al., 2010. In-depth analyses of kinase-dependent tyrosine phosphoproteomes based on metal ion-functionalized soluble nanopolymers. *Molecular & cellular proteomics : MCP*, 9(10), pp.2162–72.

Jakob, U. et al., 1995. Transient Interaction of Hsp90 with early unfolding Intermediates of Citrate Synthase. *JBC*, 270(March 31), pp.7288–94.

Johnson, J.L. et al., 1994. Characterization of a novel 23-kilodalton protein of unactive progesterone receptor complexes. *Molecular and cellular biology*, 14(3), pp.1956–63.

Johnson, J.L. & Brown, C., 2009. Plasticity of the Hsp90 chaperone machine in divergent eukaryotic organisms. *Cell stress & chaperones*, 14(1), pp.83–94.

Johnson, J.L., Halas, A. & Flom, G., 2007. Nucleotide-dependent interaction of Saccharomyces cerevisiae Hsp90 with the cochaperone proteins Sti1, Cpr6, and Sba1. *Molecular and cellular biology*, 27(2), pp.768–76.

Johnson, J.L. & Toft, D.O., 1995. Binding of p23 and hsp90 during assembly with the progesterone receptor. *Molecular endocrinology (Baltimore, Md.)*, 9(6), pp.670–8.

Kamal, A. et al., 2003. A high-affinity conformation of Hsp90 confers tumour selectivity on Hsp90 inhibitors. *Nature*, 425(6956), pp.407–10.

Kanelakis, K.C., Shewach, D.S. & Pratt, W.B., 2002. Nucleotide binding states of hsp70 and hsp90 during sequential steps in the process of glucocorticoid receptor.hsp90 heterocomplex assembly. *The Journal of biological chemistry*, 277(37), pp.33698–703.

Karagöz, G.E. et al., 2014. Hsp90-tau complex reveals molecular basis for specificity in chaperone action. *Cell*, 156(5), pp.963–74.

Katschinski, D.M. et al., 2002. Heat induction of the unphosphorylated form of hypoxia-inducible factor-1alpha is dependent on heat shock protein-90 activity. *The Journal of biological chemistry*, 277(11), pp.9262–7.

Kekatpure, V.D., Dannenberg, A.J. & Subbaramaiah, K., 2009. HDAC6 modulates Hsp90 chaperone activity and regulates activation of aryl hydrocarbon receptor signaling. *The Journal of biological chemistry*, 284(12), pp.7436–45.

Kelley, P.M. & Schlesinger, M.J., 1982. Antibodies to two major chicken heat shock proteins cross-react with similar proteins in widely divergent widely divergent species. *Molecular and Cellular Biology*, 2(3), pp.267–274.

Kettenbach, A.N. et al., 2013. Quantitative Phosphoproteomics identifies Subtrates and Functional Modules of Aurora and Polo-like kinase activities in mitotic cells. *Science Signal*, 4(179).

Kimura, Y. et al., 1997. Cdc37 is a molecular chaperone with specific functions in signal transduction. *Genes & Development*, 11(14), pp.1775–1785.

Kirschke, E. et al., 2014. Glucocorticoid Receptor Function Regulated by Coordinated Action of the Hsp90 and Hsp70 Chaperone Cycles. *Cell*, 157(7), pp.1685–1697.

Kjærulff, S. et al., 2005. Constitutive Activation of the Fission Yeast Pheromone-Responsive Pathway Induces Ectopic Meiosis and Reveals Ste11 as a Mitogen-Activated Protein Kinase Target Constitutive Activation of the Fission Yeast Pheromone-Responsive Pathway Induces Ectopic Meio.

Kosano, H., 1998. The Assembly of Progesterone Receptor-hsp90 Complexes Using Purified Proteins. *Journal of Biological Chemistry*, 273(49), pp.32973–32979.

Koulov, A. V et al., 2010. Biological and Structural Basis for Aha1 Regulation of Hsp90 ATPase Activity in Maintaining Proteostasis in the Human Disease Cystic Fibrosis. *Molecular biology of the Cell*, 21, pp.871–884.

Kovacs, J.J. et al., 2005. HDAC6 regulates Hsp90 acetylation and chaperone-dependent activation of glucocorticoid receptor. *Molecular cell*, 18(5), pp.601–7.

Kumar, R. & Thompson, E.B., 1999. The structure of the nuclear hormone receptors. *Steroids*, 64(5), pp.310–9.

Kuo, C.-C. et al., 2007. Involvement of heat shock protein (Hsp)90 beta but not Hsp90 alpha in antiapoptotic effect of CpG-B oligodeoxynucleotide. *Journal of immunology (Baltimore, Md. : 1950)*, 178(10), pp.6100–8.

Kurokawa, M. et al., 2008. Inhibition of apoptosome formation by suppression of Hsp90beta phosphorylation in tyrosine kinase-induced leukemias. *Molecular and cellular biology*, 28(17), pp.5494–5506.

Lan, C. et al., 2004. A novel mode of chaperone action: heme activation of Hap1 by enhanced association of Hsp90 with the repressed Hsp70-Hap1 complex. *The Journal of biological chemistry*, 279(26), pp.27607–12.

Lee, C. et al., 2012. Dynamics of the regulation of Hsp90 by the cochaperone Sti1. *The EMBO Journal*, 31(6), pp.1518–1528.

Lee, H.C., Hon, T. & Zhang, L., 2002. The molecular chaperone Hsp90 mediates heme activation of the yeast transcriptional activator Hap1. *The Journal of biological chemistry*, 277(9), pp.7430–7.

Lee, P. et al., 2004. Sti1 and Cdc37 Can Stabilize Hsp90 in Chaperone Complexes with a Protein Kinase. *Molecular Biology of the Cell*, 15(April), pp.1785–1792.

Lee, P. et al., 2002. The Cdc37 protein kinase-binding domain is sufficient for protein kinase activity and cell viability. *The Journal of cell biology*, 159(6), pp.1051–9.

Lees-Miller, S.P. & Anderson, C.W., 1989. The Human Double-stranded DNA-activated Protein Kinase phosphorylates the 90KDa Hsp (hsp90a) at two N-terminal Threonine residues. *Journal of Biological Chemistry*, 264(29), pp.17275–17280.

Lees-Miller, S.P. & Anderson, C.W., 1989. Two human 90-kDa heat shock proteins are phosphorylated in vivo at conserved serines that are phosphorylated in vitro by casein kinase II. *The Journal of biological chemistry*, 264(5), pp.2431–7.

Li, J. et al., 2013. Integration of the accelerator Aha1 in the Hsp90 co-chaperone cycle. *Nature structural & molecular biology*, 20(3), pp.326–31.

Li, J., Richter, K. & Buchner, J., 2011. Mixed Hsp90-cochaperone complexes are important for the progression of the reaction cycle. *Nature structural & molecular biology*, 18(1), pp.61–66.

Lindquist, S., Jarosz, D.F. & Taipale, M., 2010. HSP90 at the hub of protein homeostasis: emerging mechanistic insights. *Nature reviews. Molecular cell biology*, 11(7), pp.515–528.

Llauger-Bufi, L. et al., 2003. Synthesis of novel fluorescent probes for the molecular chaperone Hsp90. *Bioorganic & Medicinal Chemistry Letters*, 13(22), pp.3975–3978.

Loo, M. a et al., 1998. Perturbation of Hsp90 interaction with nascent CFTR prevents its maturation and accelerates its degradation by the proteasome. *The EMBO journal*, 17(23), pp.6879–87.

Lorenz, O.R. et al., 2014. Modulation of the hsp90 chaperone cycle by a stringent client protein. *Molecular cell*, 53(6), pp.941–53.

Lotz, G.P. et al., 2003. Aha1 binds to the middle domain of Hsp90, contributes to client protein activation, and stimulates the ATPase activity of the molecular chaperone. *The Journal of biological chemistry*, 278(19), pp.17228–35.

Louvion, J.F., Abbas-Terki, T. & Picard, D., 1998. Hsp90 is required for pheromone signaling in yeast. *Molecular biology of the cell*, 9(11), pp.3071–83.

Lu, Z. et al., 2010. Celastrol, a novel HSP90 inhibitor, depletes Bcr-Abl and induces apoptosis in imatinib-resistant chronic myelogenous leukemia cells harboring T315I mutation. *Cancer letters*, 290(2), pp.182–91.

MacLean, M. & Picard, D., 2003. Cdc37 goes beyond Hsp90 and kinases. *Cell stress & chaperones*, 8(2), pp.114–9.

Mann, M. & Jensen, O.N., 2003. Proteomic analysis of post-translational modifications. *Nature biotechnology*, 21(3), pp.255–61.

Martínez-Ruiz, A. et al., 2005. S-nitrosylation of Hsp90 promotes the inhibition of its ATPase and endothelial nitric oxide synthase regulatory activities. *Proceedings of the National Academy of Sciences of the United States of America*, 102(24), pp.8525–30.

Mayer, M.P. & Bukau, B., 1999. Molecular chaperones: the busy life of Hsp90. *Current biology : CB*, 9(9), pp.R322–5.

McCollum, A.K. et al., 2009. Cisplastin abrogates the GA-induced heat shock response. *Molecular cancer therapeutics*, 7(10), pp.3256–3264.

McGowan, C.H. & Russell, P., 1993. Human Wee1 kinase inhibits cell division by phosphorylating p34cdc2 exclusively on Tyr15. *The EMBO journal*, 12(1), pp.75–85.

McLaughlin, S.H. et al., 2006. The co-chaperone p23 arrests the Hsp90 ATPase cycle to trap client proteins. *Journal of molecular biology*, 356(3), pp.746–58.

McLaughlin, S.H., Smith, H.W. & Jackson, S.E., 2002. Stimulation of the weak ATPase activity of human hsp90 by a client protein. *Journal of molecular biology*, 315(4), pp.787–98.

McLean, P.J. et al., 2004. Geldanamycin induces Hsp70 n and prevents alpha-synuclein aggregaton and toxicity in vitro. *Biochemical and biophysical research communications*, 321, pp.665–669.

Meyer, P. et al., 2003. Structural and functional analysis of the middle segment of hsp90: implications for ATP hydrolysis and client protein and cochaperone interactions. *Molecular cell*, 11(3), pp.647–58.

Meyer, P. et al., 2004. Structural basis for recruitment of the ATPase activator Aha1 to the Hsp90 chaperone machinery. *The EMBO journal*, 23(6), pp.1402–10.

Mickler, M. et al., 2009. The large conformational changes of Hsp90 are only weakly coupled to ATP hydrolysis. *Nature structural & molecular biology*, 16(3), pp.281–6.

Milicevic, Z. et al., 2008. Molecular characterization of hsp90 isoforms in colorectal cancer cells and its association with tumour progression. *International journal of oncology*, 32(6), pp.1169–78.

Millson, S.H. et al., 2007. Expressed as the sole Hsp90 of yeast, the alpha and beta isoforms of human Hsp90 differ with regard to their capacities for activation of certain client proteins, whereas only Hsp90beta generates sensitivity to the Hsp90 inhibitor radicicol. *The FEBS journal*, 274(17), pp.4453–63.

Mimnaugh, E.G. et al., 1995. Possible Role for Serine / Threonine Phosphorylation in the Regulation of the Heteroprotein Complex between the hsp90 Stress Protein and the pp60 v- src Tyrosine Kinase *. *Journal of Biological Chemistry*, 270(48), pp.28654–28659.

Minami, Y. et al., 1994. The carboxy-terminal region of mammalian HSP90 is required for its dimerization and function in vivo. *Molecular and cellular biology*, 14(2), pp.1459–64.

Miyata, Y., 2009. CK2: the kinase controlling the Hsp90 chaperone machinery. *Cellular and molecular life sciences : CMLS*, 66(11-12), pp.1840–1849.

Miyata, Y. & Yahara, I., 1992. The 90-kDa heat shock protein, HSP90, binds and protects casein kinase II from self-aggregation and enhances its kinase activity. *The Journal of biological chemistry*, 267(10), pp.7042–7.

Mohammed, S. et al., 2008. Multiplexed proteomics mapping of yeast RNA polymerase II and III allows near-complete sequence coverage and reveals several novel phosphorylation sites. *Analytical chemistry*, 80(10), pp.3584–92.

Molina, H. et al., 2007. Global proteomic profiling of phosphopeptides using electron transfer dissociation tandem mass spectrometry. *Proceedings of the National Academy of Sciences of the United States of America*, 104(7), pp.2199–204.

Mollapour, M. et al., 2014. Asymmetric Hsp90 N domain SUMOylation recruits Aha1 and ATP-competitive inhibitors. *Molecular cell*, 53(2), pp.317–29.

Mollapour, M., Tsutsumi, S., Kim, Y.S., et al., 2011. Casein kinase 2 phosphorylation of Hsp90 threonine 22 modulates chaperone function and drug sensitivity. *Oncotarget*, 2(5), pp.407–417.

Mollapour, M., Tsutsumi, S., Truman, A.W., et al., 2011. Manuscript: Threonine 22 phosphorylation attenuates Hsp90 interaction with co-chaperone Aha1 and regulates chaperone activity. *Molecular cell*, 41(6), pp.672–681.

Mollapour, M., Tsutsumi, S., et al., 2010. *Swe1/Wee1-dependent tyrosine Phosphorylation of Hsp90 regulates chaperone function*,

Mollapour, M., Tsutsumi, S., et al., 2010. Swe1Wee1-dependent tyrosine phosphorylation of Hsp90 regulates distinct facets of chaperone function. *Molecular cell*, 37(3), pp.333–343.

Mollapour, M., Tsutsumi, et al., 2011. Threonine 22 phosphorylation attenuates Hsp90 interaction with cochaperones and affects its chaperone activity. *Molecular cell*, 41(6), pp.672–681.

Morano, K. a & Thiele, D.J., 1999. The Sch9 protein kinase regulates Hsp90 chaperone complex signal transduction activity in vivo. *The EMBO journal*, 18(21), pp.5953–62.

Morishima, Y. et al., 2008. CHIP deletion reveals functional redundancy of E3 ligases in promoting degradation of both signaling proteins and expanded glutamine proteins. *Human molecular genetics*, 17(24), pp.3942–52.

Morishima, Y. et al., 2000. Stepwise assembly of a glucocorticoid receptor.hsp90 heterocomplex resolves two sequential ATP-dependent events involving first hsp70 and then hsp90 in opening of the steroid binding pocket. *The Journal of biological chemistry*, 275(24), pp.18054–60.

Morishima, Y. et al., 2000. The Hsp Organizer Protein Hop Enhances the Rate of but Is Not Essential for Glucocorticoid Receptor Folding by the System The Hsp Organizer Protein Hop Enhances the Rate of but Is Not Essential for Glucocorticoid Receptor F. *Journal of Biological Chemistry*, 275, pp.6894–6900.

Mort-Bontemps-Soret, M., Facca, C. & Faye, G., 2002. Physical interaction of Cdc28 with Cdc37 in Saccharomyces cerevisiae. *Molecular genetics and genomics : MGG*, 267(4), pp.447–58.

Müller, L. et al., 2004. Hsp90 regulates the activity of wild type p53 under physiological and elevated temperatures. *The Journal of biological chemistry*, 279(47), pp.48846–54.

Muller, P. et al., 2012. C-terminal phosphorylation of Hsp70 and Hsp90 regulates alternate binding to co-chaperones CHIP and HOP to determine cellular protein folding/degradation balances. *Oncogene*, 32(25), pp.3101–10.

Müller, P., Ceskova, P. & Vojtesek, B., 2005. Hsp90 is essential for restoring cellular functions of temperature-sensitive p53 mutant protein but not for stabilization and activation of wild-type p53: implications for cancer therapy. *The Journal of biological chemistry*, 280(8), pp.6682–91.

Murata, S. et al., 2001. CHIP is a chaperone-dependent E3 ligase that ubiquitylates unfolded protein. *EMBO reports*, 2(12), pp.1133–8.

Murphy, P.J.M. et al., 2005. Regulation of the dynamics of hsp90 action on the glucocorticoid receptor by acetylation/deacetylation of the chaperone. *The Journal of biological chemistry*, 280(40), pp.33792–9.

Nair, S.C. et al., 1996. A pathway of multichap interactions comon to diverse regulatory proteins: estrogen receptor, Fes tyrosine kinase, heat shock transcription factor Hsf1 and the aryl hydrocarbon receptor. *Cell stress & chaperones*, 1, pp.237–250.

Nathan, D.F. & Lindquist, S., 1995. Mutational analysis of Hsp90 function: interactions with a steroid receptor and a protein kinase. *Molecular and cellular biology*, 15(7), pp.3917–25.

Nathan, D.F., Vos, M.H. & Lindquist, S., 1999. Identification of Ssf1, Cns1 and Hch1 as suppressors of a Sc Hsp90 loss-of-function mutation. *PNAS*, 96(February), pp.1409–1414.

Nathan, D.F., Vos, M.H. & Lindquist, S., 1997. In vivo functions of the Saccharomyces cerevisiae Hsp90 chaperone. *Proceedings of the National Academy of Sciences of the United States of America*, 94(24), pp.12949–56.

Nguyen, D.M. et al., 2001. Enhancement of paclitaxel-mediated cytotoxicity in lung cancer cells by 17-allylamino geldanamycin: in vitro and in vivo analysis. *The Annals of thoracic surgery*, 72(2), pp.371–8; discussion 378–9.

Nimmanapalli, R. et al., 2003. Histone Deacetylase Inhibitor LAQ824 Both Lowers Expression and Promotes Proteasomal Degradation of Bcr-Abl and Induces Apoptosis of Imatinib Mesylate-sensitive or -refractory Chronic Myelogenous Leukemia-Blast Crisis Cells Histone Deacetylase Inhibitor L.

Nimmanapalli, R., O'Bryan, E. & Bhalla, K., 2001. Geldanamycin and its analogue 17-allylamino-17-demethoxygeldanamycin lowers Bcr-Abl levels and induces apoptosis and differentiation of Bcr-Abl-positive human leukemic blasts. *Cancer research*, 61(5), pp.1799–804.

Obermann, W.M. et al., 1998. In vivo function of Hsp90 is dependent on ATP binding and ATP hydrolysis. *The Journal of cell biology*, 143(4), pp.901–10.

Ogiso, H. et al., 2004. Phosphorylation analysis of 90 kDa heat shock protein within the cytosolic arylhydrocarbon receptor complex. *Biochemistry*, 43(49), pp.15510–15519.

Old, W.M. et al., 2009. Functional proteomics identifies targets of Phosphorylation by B-Raf signaling in Melanoma. *Molecular Cell*, 34(1), pp.115–131.

Olsen, J. V et al., 2010. Quantitative phosphoproteomics reveals widespread full phosphorylation site occupancy during mitosis. *Science signaling*, 3(104), p.ra3.

Panaretou, B. et al., 2002. Activation of the ATPase activity of hsp90 by the stress-regulated cochaperone aha1. *Molecular cell*, 10(6), pp.1307–18.

Panaretou, B. et al., 1998a. ATP binding and hydrolysis are essential to the function of the Hsp90 molecular chaperone in vivo. *The EMBO journal*, 17(16), pp.4829–36.

Panaretou, B. et al., 1998b. ATP binding and hydrolysis are essential to the function of the Hsp90 molecular chaperone in vivo. *The EMBO journal*, 17(16), pp.4829–36.

Panse, V.G. et al., 2004. A proteome-wide approach identifies sumoylated substrate proteins in yeast. *The Journal of biological chemistry*, 279(40), pp.41346–51. Available at: http://www.ncbi.nlm.nih.gov/pubmed/15292183 [Accessed April 14, 2014].

Park, J. et al., 2008. Class-II HDACs play pivotal roles in hsp90-mediated proteasome degrad of VEGF receptors. *Biochemical and biophysical research communications*, 368, pp.318–322.

Pearl, L.H. & Prodromou, C., 2006. Structure and mechanism of the Hsp90 molecular chaperone machinery. *Annual review of biochemistry*, 75, pp.271–94.

Phanstiel, D.H. et al., 2012. Proteomic and phosphoproteomic comparison of human ES and iPS cells. *Nature Methods*, 8(10), pp.821–827.

Picard, D., 2002. Heat-shock protein 90 , a chaperone for folding and regulation. *Cellular and Molecular Life Sciences*, 59, pp.1640–1648.

Picard, D. et al., 1990. Reduced levels of hsp90 compromise steroid receptor action in vivo. *Nature*, 348, pp.166–168.

Piwien Pilipuk, G. et al., 2007. Evidence for NL1-independent nuclear translocation of the mineralocorticoid receptor. *Biochemistry*, 46(5), pp.1389–97.

Polier, S. et al., 2013. ATP-competitive inhibitors block protein kinase recruitment to the Hsp90-Cdc37 system. *Nature chemical biology*, 9(5), pp.307–12.

Pountney, D.L. et al., 2008. NSF, Unc-18-1, dynamin-1 and HSP90 are inclusion body components in neuronal intranuclear inclusion disease identified by anti-SUMO-1-immunocapture. *Acta neuropathologica*, 116(6), pp.603–14.

Prince, T. & Matts, R.L., 2005. Exposure of protein kinase motifs that trigger binding of Hsp90 and Cdc37. *Biochemical and biophysical research communications*, 338(3), pp.1447–54. Available at: http://www.ncbi.nlm.nih.gov/pubmed/16269130 [Accessed January 23, 2014].

Prodromou, C. et al., 1997. Identification and structural characterization of the ATP/ADP-binding site in the Hsp90 molecular chaperone. *Cell*, 90(1), pp.65–75. Available at: http://www.ncbi.nlm.nih.gov/pubmed/9230303.

Prodromou, C. et al., 1999. Regulation of Hsp90 ATPase activity by tetratricopeptide repeat (TPR)-domain co-chaperones. *The EMBO journal*, 18(3), pp.754–62.

Quanz, M. et al., 2012. Heat shock protein 90 alpha (Hsp90α) is phosphorylated in response to DNA damage and accumulates in repair foci. *The Journal of biological chemistry*, 287(12), pp.8803–15.

Queitsch, C., Sangster, T. a & Lindquist, S., 2002. Hsp90 as a capacitor of phenotypic variation. *Nature*, 417(6889), pp.618–24. Available at: http://www.ncbi.nlm.nih.gov/pubmed/12050657.

Rao, J. et al., 2001. Functional interaction of human Cdc37 with the androgen receptor but not with the glucocorticoid receptor. *The Journal of biological chemistry*, 276(8), pp.5814–20.

Rao, R. et al., 2008. HDAC6 inhibition enhances 17-AAG--mediated abrogation of hsp90 chaperone function in human leukemia cells. *Blood*, 112(5), pp.1886–93.

Ratzke, C. et al., 2010. Dynamics of heat shock protein 90 C-terminal dimerization is an important part of its conformational cycle. *Proceedings of the National Academy of Sciences of the United States of America*, 107(37), pp.16101–6.

Reed, S.I., 1980. The selection of S.cerevisiae mutants defective in the start event of cell division. *Genetics*, 95, pp.561–577.

Retzlaff, M. et al., 2010. Asymmetric activation of the hsp90 dimer by its cochaperone Aha1. *Molecular cell*, 37(3), pp.344–54.

Retzlaff, M. et al., 2009. Hsp90 is regulated by a switch point in the C-terminal domain. *EMBO reports*, 10(10), pp.1147–53.

Richter, K. et al., 2001. Coordinated ATP hydrolysis by the Hsp90 dimer. *The Journal of biological chemistry*, 276(36), pp.33689–96.

Richter, K. et al., 2006. Intrinsic inhibition of the Hsp90 ATPase activity. *The Journal of biological chemistry*, 281(16), pp.11301–11.

Richter, K. et al., 2003. Sti1 Is a Non-competitive Inhibitor of the Hsp90 ATPase : BINDING PREVENTS THE N-TERMINAL DIMERIZATION REACTION DURING THE ATPASE CYCLE. *JBC*, 278, pp.10328–10333.

Richter, K., Reinstein, J. & Buchner, J., 2002. N-terminal residues regulate the catalytic efficiency of the Hsp90 ATPase cycle. *The Journal of biological chemistry*, 277(47), pp.44905–10. Available at: http://www.ncbi.nlm.nih.gov/pubmed/12235160 [Accessed February 4, 2014].

Richter, K., Walter, S. & Buchner, J., 2004. The Co-chaperone Sba1 connects the ATPase reaction of Hsp90 to the progression of the chaperone cycle. *Journal of molecular biology*, 342(5), pp.1403–13.

Ricketson, D. et al., 2007. A conformational switch in the ligand binding domain regulates the dependence of the glucocorticoid receptor on Hsp90. *Journal of molecular biology*, 368(3), pp.729–741.

Roe, S.M. et al., 2004. The Mechanism of Hsp90 Regulation by the Protein Kinase-Specific Cochaperone p50 cdc37. *Cell*, 116, pp.87–98.

Rutherford, S.L. & Lindquist, S., 1998. Hsp90 as a capacitor for morphological evolution. *Nature*, 396(6709), pp.336–42.

Sato, S., Fujita, N. & Tsuruo, T., 2000. Modulation of Akt kinase activity by binding to Hsp90. *Proceedings of the National Academy of Sciences of the United States of America*, 97(20), pp.10832–7.

Scheufler, C. et al., 2000. Structure of TPR Domain – Peptide Complexes : Critical Elements in the Assembly of the Hsp70 – Hsp90 Multichaperone Machine. , 101, pp.199–210.

Schulte, T.W. et al., 1996. Destabilization of Raf-1 by geldanamycin leads to disruption of the Raf-1-MEK-mitogen-activated protein kinase signalling pathway . Destabilization of Raf-1 by Geldanamycin Leads to Disruption of the Raf-1 – MEK – Mitogen-Activated Protein Kinase Signalli. *Molecular and cellular biology*, 16, pp.5389–5845.

Scroggins, B.T. et al., 2007. An acetylation site in the middle domain of Hsp90 regulates chaperone function. *Molecular cell*, 25(1), pp.151–9.

Sefton, B.M., Beemon, K. & Hunter, T., 1978. Comparison of the expression of the src gene of Rous sarcoma virus in vitro and in vivo. *Journal of Virology*, 28(3), pp.957–971.

Seitz, T. et al., 2010. Enhancing the stability and solubility of the glucocorticoid receptor ligand-binding domain by high-throughput library screening. *Journal of molecular biology*, 403(4), pp.562–77.

Sepehrnia, B. et al., 1996. Heat Shock Protein 84 forms a Complex with Mutant p53 Protein predominantly within a cytoplasmic compartment of the cell. *Journal of Biological Chemistry*, 271(25), pp.15084–15090.

Shao, J. et al., 2003. Functional dissection of cdc37: characterization of domain structure and amino acid residues critical for protein kinase binding. *Biochemistry*, 42(43), pp.12577–88.

Shao, J. et al., 2001. Hsp90 regulates p50(cdc37) function during the biogenesis of the activeconformation of the heme-regulated eIF2 alpha kinase. *The Journal of biological chemistry*, 276(1), pp.206–14.

Shiromizu, T. et al., 2013. Identification of Missing Proteins in the neXtProt Database and Unregistered Phosphopeptides in the PhosphoSitePlus Database As Part of the Chromosome-Centric Human Proteome Project. *Journal of proteome research*, 12, pp.2414–2421.

Siligardi, G. et al., 2002. Regulation of Hsp90 ATPase activity by the co-chaperone Cdc37p/p50cdc37. *The Journal of biological chemistry*, 277(23), pp.20151–9.

Silva, A. et al., 2013. Involvement of yeast HSP90 isoforms in response to stress and cell death induced by acetic acid. *PloS one*, 8(8), p.e71294.

Smith, D.F., 1993. Dynamics of heat shock protein 90-progesterone receptor binding and the disactivation loop model for steroid receptor complexes. *Molecular endocrinology (Baltimore, Md.)*, 7(11), pp.1418–29.

Smith, D.F. et al., 1993. Identification of a 60-Kilodalton Stress-Related Protein , p60 , which Interacts with hsp90 and hsp70. *Molecular and cellular biology*, 13, pp.869–876.

Smith, D.F. et al., 1995. Progesterone receptor structure and function altered by geldanamycin, an hsp90-binding agent. *Molecular and cellular biology*, 15(12), pp.6804–12.

Solier, S. et al., 2012. Heat shock protein 90 (HSP90), a substrate and chaperone of DNA-PK necessary for the apoptotic response. *Proceedings of the National Academy of Sciences*, 109(32), pp.12866–12872.

Solit, D.B. et al., 2002. Advances in Brief 17-Allylamino-17-demethoxygeldanamycin Induces the Degradation of Androgen Receptor and HER-2 / neu and Inhibits the Growth of Prostate Cancer Xenografts 1. , 8(May), pp.986–993.

Song, Y. & Masison, D.C., 2006. Independent regulation of Hsp70 and Hsp90 chaperones by HOP. *JBC*, 280(40), pp.34178–34185.

Soroka, J. et al., 2012. Conformational Switching of the Molecular Chaperone Hsp90 via Regulated Phosphorylation. *Molecular Cell*, 45, pp.517–528.

Soroka, J. et al., 2013. Phospho-regulation of the Hsp90 chaperone machinery. *Molecular Cell*.

Southworth, D.R. & Agard, D. a, 2008. Species-dependent ensembles of conserved conformational states define the Hsp90 chaperone ATPase cycle. *Molecular cell*, 32(5), pp.631–40.

Stankiewicz, M. et al., 2010. CHIP participates in protein triage decisions by preferentially ubiquitinating Hsp70-bound substrates. *The FEBS journal*, 277(16), pp.3353–67.

Stepanova, L. et al., 1996. Mammalian p50Cdc37 is a protein kinase-targeting subunit of Hsp90 that binds and stabilizes Cdk4. *Genes & Development*, 10(12), pp.1491–1502.

Street, T.O., Lavery, L. a & Agard, D. a, 2011. Substrate binding drives large-scale conformational changes in the Hsp90 molecular chaperone. *Molecular cell*, 42(1), pp.96–105.

Subbarao Sreedhar, A. et al., 2004. Hsp90 isoforms: functions, expression and clinical importance. *FEBS Letters*, 562(1-3), pp.11–15.

Sullivan, W. et al., 1997. Nucleotides and Two Functional States of Nucleotides and Two Functional States of hsp90. *Protein Chemistry and Structure*.

Sun, L. et al., 2012. Characterization of the interaction of Aha1 with components of the Hsp90 chaperone machine and client proteins. *Biochimica et biophysica acta*, 1823(6), pp.1092–101.

Taipale, M. et al., 2012. Quantitative Analysis of Hsp90-client interactions reveals principles of substrate recognition. *Cell*, 150, pp.987–1001.

Terasawa, K. et al., 2006. Cdc37 Interacts with the Glycine-Rich Loop of Hsp90 Client Kinases. *Molecular and cellular biology*, 26(9), pp.3378–3389.

Tsutsumi, S. et al., 2009. Hsp90 charged-linker truncation reverses the functional consequences of weakened hydrophobic contacts in the N domain. *Nature structural & molecular biology*, 16(11), pp.1141–7.

Uehara, Y. et al., 1986. Phenotypic change from transformed to normal induced by benzoquinonoid ansamycins accompanies inactivation of p60src in rat kidney cells infected with Rous sarcoma virus. *Molecular and cellular biology*, 6, pp.2198–2206.

Unwin, R.D. et al., 2005. Multiple reaction monitoring to identify sites of protein phosphorylation with high sensitivity. *Molecular & cellular proteomics : MCP*, 4(8), pp.1134–44.

Vaughan, C.K. et al., 2009. A common conformationally coupled ATPase mechanism for yeast and human cytoplasmic HSP90s. *The FEBS journal*, 276(1), pp.199–209.

Vaughan, C.K. et al., 2006. Structure of an Hsp90-Cdc37-Cdk4 complex. *Molecular cell*, 23(5), pp.697–707.

Wandinger, S.K. et al., 2006. The phosphatase Ppt1 is a dedicated regulator of the molecular chaperone Hsp90. *The EMBO journal*, 25(2), pp.367–76.

Wandinger, S.K., Richter, K. & Buchner, J., 2008. The Hsp90 chaperone machinery. *The Journal of biological chemistry*, 283(27), pp.18473–7.

Wang, H. et al., 2002. C/EBPalpha triggers proteasome-dependent degradation of cdk4 during growth arrest. *The EMBO journal*, 21(5), pp.930–41.

Wang, X. et al., 2009. The regulatory mechanism of Hsp90alpha secretion and its function in tumor malignancy. *PNAS*, 106(50), pp.21288–21293.

Wang, X. et al., 2012. Thr90 phosphorylation of Hsp90α by protein kinase A regulates its chaperone machinery. *Biochemical Journal*, 441(1), pp.387–397.

Wang, X., Grammatikakis, N. & Hu, J., 2002. Role of p50/CDC37 in hepadnavirus assembly and replication. *The Journal of biological chemistry*, 277(27), pp.24361–7.

Weaver, A.J. et al., 2000. Crystal structure and activity of human p23, a heat shock protein 90 co-chaperone. *The Journal of biological chemistry*, 275(30), pp.23045–52.

Weber, C., Schreiber, T.B. & Daub, H., 2012. Dual phosphoproteomics and chemical proteomics analysis of erlotinib and gefitinib interference in acute myeloid leukemia cells. *Journal of proteomics*, 75(4), pp.1343–56.

Wegele, H. et al., 2003. Dissection of the contribution of individual domains to the ATPase mechanism of Hsp90. *The Journal of biological chemistry*, 278(41), pp.39303–10.

Wegele, H. et al., 2006. Substrate transfer from the chaperone Hsp70 to Hsp90. *Journal of molecular biology*, 356(3), pp.802–11.

Wegele, H., Müller, L. & Buchner, J., 2004. Hsp70 and Hsp90--a relay team for protein folding. *Reviews of physiology, biochemistry and pharmacology*, 151(January), pp.1–44.

Weikl, T. et al., 2000. C-terminal regions of Hsp90 are important for trapping the nucleotide during the ATPase cycle. *Journal of molecular biology*, 303(4), pp.583–92.

Weikl, T., Abelmann, K. & Buchner, J., 1999. An unstructured C-terminal region of the Hsp90 co-chaperone p23 is important for its chaperone function. *Journal of molecular biology*, 293(3), pp.685–91.

Welch, W.J. et al., 1983. Biochemical characterization of the mammalian stress proteins and identification of two stress proteins as glucose- and Ca2+-ionophore-regulated proteins. *JBC*, 258(11), pp.7102–11.

Whitesell, L. et al., 1992. Benzoquinonoid ansamycins possess selective tumoricidal activity unrelated to src kinase inhibition. *Cancer research*, 52(7), pp.1721–8. Available at: http://www.ncbi.nlm.nih.gov/pubmed/1551101.

Whitesell, L. et al., 1994. Inhibition of heat shock protein HSP90-pp60v-src heteroprotein complex formation by benzoquinone ansamycins: essential role for stress proteins in oncogenic transformation. *Proceedings of the National Academy of Sciences of the United States of America*, 91(18), pp.8324–8.

Whitesell, L. et al., 1998. The physical association of multiple molecular chaperone proteins with mutant p53 is altered by geldanamycin, an hsp90-binding agent. *Molecular and cellular biology*, 18(3), pp.1517–24.

Wiśniewski, J.R., Ostasiewicz, P. & Mann, M., 2011. High recovery FASP applied to the proteomic analysis of microdissected formalin fixed paraffin embedded cancer tissues retrieves known colon cancer markers. *Journal of proteome research*, 10(7), pp.3040–9.

Woo, S.H. et al., 2009. A truncated form of p23 down-regulates telomerase activity via disruption of Hsp90 function. *The Journal of biological chemistry*, 284(45), pp.30871–30880.

Xia, Q. et al., 2009. Phosphoproteomic analysis of human brain by calcium phosphate precipitation and MS. *J of Proteome Research*, 7(7), pp.2845–2851.

Xu, W. et al., 2002. Chaperone-dependent E3 ubiquitin ligase CHIP mediates a degradative pathway for c-ErbB2/Neu. *Proceedings of the National Academy of Sciences of the United States of America*, 99(20), pp.12847–52.

Xu, W. et al., 2012. Dynamic tyrosine phosphoryation modulates cycling of the Hsp90-p50Cdc37-Aha1 chaperone machinery. *Molecular cell*, 47(3), pp.434–443.

Xu, W. & Neckers, L., 2007. Targeting the molecular chaperone heat shock protein 90 provides a multifaceted effect on diverse cell signaling pathways of cancer cells. *Clinical cancer research : an official journal of the American Association for Cancer Research*, 13(6), pp.1625–9.

Xu, Y. & Lindquist, S., 1993. Heat-shock protein hsp90 governs the activity of pp60v-src kinase. *Proceedings of the National Academy of Sciences*, 90(15), pp.7074–7078.

Yang, Y. et al., 2008. Role of acetylation and extracellular location of heat shock protein 90alpha in tumor cell invasion. *Cancer research*, 68(12), pp.4833–42.

Youker, R.T. et al., 2004. Distinct Roles for the Hsp40 and Hsp90 Molecular Chaperones during Cystic Fibrosis Transmembrane Conductance Regulator Degradation in Yeast. , 15(November), pp.4787–4797.

Young, J.C., 2001. Hsp90: a specialized but essential protein-folding tool. *The Journal of Cell Biology*, 154(2), pp.267–274.

Young, J.C. et al., 2004. Pathways of chaperone-mediated protein folding in the cytosol. *Nature reviews. Molecular cell biology*, 5(10), pp.781–91.

Young, J.C. & Hartl, F.U., 2000. Polypeptide release by Hsp90 involves ATP hydrolysis and is enhanced by the co-chaperone p23. *The EMBO journal*, 19(21), pp.5930–40.

Yu, X. et al., 2002. Modulation of p53, ErbB1, B2 and Raf-1 expression in Lung Cancer Cells by Depsipeptide FR901228. *Journal of the National Cancer Institute*, 94(7), pp.504–513.

Zarzov, P., Boucherie, H. & Mann, C., 1997. A yeast heat shock transcription factor (Hsf1) mutant is defective in both Hsc82/Hsp82 synthesis and spindle pole body duplication. *Journal of cell science*, 110 (Pt 1, pp.1879–91.

Zhang, L., Hach, A. & Wang, C., 1998. Molecular mechanism governing heme signaling in yeast: a higher-order complex mediates heme regulation of the transcriptional activator HAP1. *Molecular and cellular biology*, 18(7), pp.3819–28.

Zhao, X. et al., 2011. Phosphoproteome analysis of functional mitochondria isolated from resting human muscle reveals extensive phosphorylation of inner membrane protein complexes and enzymes. *Molecular & cellular proteomics : MCP*, 10(1), p.M110.000299.

Zhao, Y.G. et al., 2001. Hsp90 phosphorylation is linked to its chaperoning function. Assembly of the reovirus cell attachment protein. *The Journal of biological chemistry*, 276(35), pp.32822–32827.

Zhou, H. et al., 2013. Toward a comprehensive characterization of a human cancer cell phosphoproteome. *Journal of proteome research*, 12(1), pp.260–71.

Zhou, Q. et al., 2008. Inhibition of histone deacetylases promotes ubiquitin-dependent proteasomal degradation of DNA methyltransferase 1 in human breast cancer cells. *Molecular cancer research : MCR*, 6(5), pp.873–83.

Zhou, W., Ryan, J.J. & Zhou, H., 2004. Global analyses of sumoylated proteins in Saccharomyces cerevisiae. Induction of protein sumoylation by cellular stresses. *The Journal of biological chemistry*, 279(31), pp.32262–8.

Zhou, Z. et al., 1993. Saccharomyces cerevisiae requires the sequential function of three protein kinases . Pheromone-Induced Signal Transduction in Saccharomyces cerevisiae Requires the Sequential Function of Three Protein Kinases. , 13(4).